Evaluating and Optimizing Distributed Energy Resources

Utkarsha Agwan

Electrical Engineering and Computer Sciences
University of California, Berkeley

August 9, 2023

Evaluating and Optimizing Distributed Energy Resources

By

Utkarsha Agwan

A dissertation submitted in partial satisfaction of the

requirements for the degree of

Doctor of Philosophy

in

Engineering - Electrical Engineering and Computer Sciences

in the

Graduate Division

of the

University of California, Berkeley

Committee in charge:

Professor Costas J. Spanos, Co-chair
Professor Kameshwar Poolla, Co-chair
Professor Duncan Callaway

Summer 2023

Evaluating and Optimizing Distributed Energy Resources

Abstract

Evaluating and Optimizing Distributed Energy Resources

by

Utkarsha Agwan

Doctor of Philosophy in Engineering - Electrical Engineering and Computer Sciences

University of California, Berkeley

Professor Costas J. Spanos, Co-chair

Professor Kameshwar Poolla, Co-chair

Climate change is one of the most urgent problems faced by humanity, and rising sea levels, extreme weather events and desertification pose a severe threat to human life as we know it. Greenhouse gas emissions resulting from human activities have caused long-term global warming, and are primarily caused by the burning of fossil fuels to generate energy, e.g., for electricity, heat or transport. It is essential that we move to cleaner sources of energy across the board to prevent further greenhouse gas emissions, and this move is driven by three main trends.

First, the rise of distributed energy resources through rooftop solar, backup batteries and electric vehicles has led to the creation of a new class of consumers which have electricity production capability. These resources tend to be variable, and are owned and operated independently. Second, the move to variable clean energy production will lead to power system operators having an increased need for demand side flexibility in order to accommodate the supply-side variability. Flexible consumers can bid in their flexibility into markets for profit, or use it to reduce their emissions impact. Third, the increasing share of electric vehicles will led to an intersection of the transportation and power networks, where electric vehicles will be able to use their batteries as 'mobile' storage in the power network.

This dissertation addresses some key challenges associated with each of these trends, and proposes solutions for them.

To my family

Contents

List of Figures

List of Tables

Acknowledgments

I owe a debt of gratitude to my advisors, Prof. Costas J. Spanos and Prof. Kameshwar Poolla. I started working with Costas fresh out of undergrad, and my meetings with him used to be the most energizing and motivating part of my week. He taught me to think about the practical implications of problems I worked on, and always made sure that I was grounded in reality. Thank you, Costas, for making sure I set the 'right' parameters for success in my PhD. Kameshwar took me under his wing at the end of my second year, and among other things, taught me how to get to the core of a problem, how to ground it in math, and how to write. Kameshwar, your constant belief in my abilities was the biggest encouragement you could have given me, and I am grateful for your friendship. Costas and Kameshwar were a well matched advisor pair – alongside being long standing friends and collaborators, they had different approaches to the problems I was working on, and I learned a lot just from observing the two of them discuss our research problems. They were united by their desire to see me succeed, and were unfailingly generous with their time and mentorship – I consider myself exceedingly fortunate to have acquired such an amazing set of advisors.

Kameshwar also introduced me to Junjie (now Prof. Junjie Qin), who did the hard work of hand-holding me through the mathematical formulation of our mobile storage work. He would patiently answer every question I had, was always available at the drop of a hat for discussions, and I would not have earned this degree without the hard work that Junjie put into training me. It was through Junjie and Kameshwar that I met Prof. Pravin Varaiya, who was a source of good cheer and deep questions. His varied interests, both in research and outside, sparked some great conversations during our walks in Tilden, and I was blessed to get the opportunity to interact with him during my time at Berkeley.

It takes a village to raise a child, and it took a department (and more) to get me my PhD. I had the privilege of having Prof. Duncan Callaway on my dissertation committee, who was generous with his time and advice. Attending EMAC meetings was a great source of inspiration and learning, and the folks in Duncan's group helped shape my work. Prof. Bin Yu was the chair of my qualifying exam committee, and taught me how to evaluate the choices I made while working with data – thank you for teaching an amazing statistics course. I am also grateful to the EECS staff – Pat Hernan, Shirley Salanio, and everyone who helped me cheerfully and promptly. My lab mates and friends – Lucas Spangher, Jaimie Swartz, Hari Prasanna Das, Wendy Lin, Akhil Shetty, Jared Porter, Alex Devonport, Ioannis Konstantakopoulos, Yu Yang, Matti Aro, Chitra Nambiar, Austin Jang, Tarang Srivastava, and Will Arnold inspired and taught me, and were a source of support throughout. I have been fortunate to work with some amazing Berkeley undergrads – Samuel Bobick, Srinath Rangan, Sushant Vema, and Isabella Siu, whose work ethic and relentless optimism enabled me to work on interesting problems. I learnt a lot about teaching from my GSI mentors – Prof. Gireeja Ranade and Prof. Murat Arcak, who were distinguished by how much they cared about their students (and GSIs). They were invariably optimistic, and always willing to help me out – thank you for being great teachers and mentors. I was privileged to be a part of many great communities during my time at Berkeley – Berkeley Energy & Resources

Chapter 1

Introduction

Climate change is an existential threat to life as we know it, and remains one of the most pressing problems faced by humanity today. The increase in the Earth's temperature due to greenhouse gas emissions related to human activities has caused multiple changes in the climate, all of which pose an imminent risk to human life. Rising sea levels have the potential to displace millions of people worldwide, particularly those living in coastal and low-lying island regions. Extreme weather events such as hurricanes, heatwaves and droughts are projected to occur with increasing frequency and intensity. Large swathes of land are expected to become uninhabitable deserts. These changes will have an immense impact on humanity, and can be attributed to long-term global warming caused by greenhouse gas (GHG) emissions resulting from human activity. GHG emissions can be broken down by economic sector as shown in Fig. 1.1.

More than half of these greenhouse gas emissions result from the burning of conventional fossil fuels for the production of electricity in the power sector, and for energy in internal combustion engines in the transportation sector. A reduction in emissions tied to these two sectors can be achieved through:

1. Energy efficiency measures: technological progress and regulations have made most energy consumption more efficient over the years;

2. Clean electricity: using energy sources which do not result in emissions, such as solar or wind production; and

3. Electrification: shifting energy consumption from fossil fuels in industrial and transportation sectors to clean electricity.

Technological progress and high volume production have driven down the cost of clean energy generation dramatically, to the point where the levelized cost of energy from solar and wind is cheaper than alternatives. There are three main factors that affect the transition to a lower-emissions grid, and we will now discuss each of them.
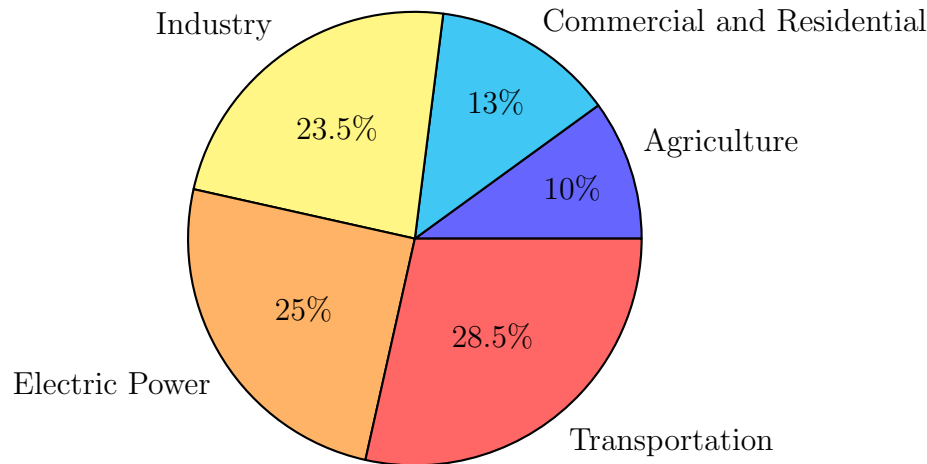
Figure 1.1: Share of greenhouse gas (GHG) emissions by economic sector in the US in 2021 [3]. The majority of GHG emissions from each sector (except agriculture) result from the burning of fossil fuels to produce energy, e.g., fossil fuels burned for heat & lighting in the commercial, residential and industrial sector, and for electricity in the electric power sector.

The rise of distributed energy resources (DERs)

Market forces have led to a steady decline in the cost of solar, wind, lithium-ion batteries and electric vehicles. These trends are aided by policies such as the Inflation Reduction Act (IRA) which facilitate significant investments in clean energy resources, tax and rebate programs across the world which incentivize solar and storage, and incentives for electric vehicles both by the federal government and by individual states in the US. The declining supply-side cost trends have been accompanied and driven by a steady rise in demand-side adoption - more and more people are getting solar for their rooftops, purchasing electric vehicles and heat pumps, and installing backup batteries. Commercial consumers are also increasingly capitalizing on their rooftop space for onsite generation. This has led to a new and growing category of resources, called distributed energy resources (DERs). These are characterized by being connected to the distribution network in the power grid, and being distributed geographically. This is in contrast to the traditional model of the power grid where centralized generation was used to supply distributed consumers, with a unidirectional power flow. The rise of DERs means that resources on the distribution network are increasingly feeding power back into the grid, and there are two characteristics that make this a notable trend:

1. Renewable distributed energy resources tend to be variable, i.e., they are *intermittent*, *uncertain* and *uncontrollable*.

2. Many renewable resources are distributed geographically, and are owned and operated

independently.

These new resources are also known as *prosumers*, i.e., con*sumers* which have electricity *pro*duction capability.

The need for demand side flexibility

Clean energy generation sources tend to be inherently uncertain and uncontrollable. For example, the power production from a wind farm depends on uncertain weather variables such as wind speed, and can not be increased on command. Power system operators are increasingly turning to demand-side resources to accommodate this variability in power production, both due to the potential for low-cost flexibility, and due to regulatory mandates.

Load flexibility is a broad term that can refer to any action taken by a consumer to modulate their energy consumption based on external incentives such as payments, penalties for peak loads, or dynamic rate structures. Utilities and system operators have historically used demand side flexibility for peak grid events, such as when a generator unexpectedly fails, or during seasonal peak loads when the system demand exceeds the peak generation capacity. An example of this is the September 2022 heat wave in California, when the power system operator sent out urgent notifications to consumers across the state asking them to reduce their energy consumption in order to avoid blackouts. There are existing programs run by utilities (e.g., PG&E's Automated Demand Response Program) and system operators (e.g., CAISO Demand Response Auction Mechanism) to facilitate the participation of flexible loads. In particular, FERC Order 2222 has mandated that wholesale power markets across the US facilitate the participation of demand-side flexible loads.

As we move to an increasingly decarbonized grid, the production side will have increasingly variable output. In that situation, it is important for demand side flexibility to accommodate the increasing variability on the supply side. The advent of newly electrified loads such as electric vehicles and heat pumps means that an increasing number of consumers will be able to change their consumption schedules, either to provide valuable services to the power grid, or to reduce their carbon footprint.

The intersection of the transportation and power network

An increasingly decarbonized power grid will also require a large amount of storage, both seasonal and short term. There are a variety of new and existing technologies to fulfill this need, and examples include pumped hydro storage, flow batteries, thermal batteries and lithium ion (Li-ion) batteries. According to the McKinsey report on the state of Li-ion battery production, the vast majority of Li-ion batteries being produced in the world are going into the mobility sector instead of into the stationary storage sector [18]. This means that most of the Li-ion battery capacity in the world will be embedded inside cars, buses and trucks, and it is essential that the power network tap into this new resource. Electric vehicles will constitute a huge new load for the power grid, with some estimates saying that

the US power system will need to increase the electricity generation capacity by 50% by 2050 in order to meet the increased demand due to electrification of transportation [50]. Utilities are already facing challenges in building the infrastructure needed to support EV charging.

Alongside being a load for the power network, electric vehicle batteries can also be harnessed as mobile storage for the power grid. This constitutes an intersection of the transportation and the power network, where electric vehicles will not only move around passengers and freight, but can also move energy across both space and time.

Thesis outline

This thesis is divided into three parts, and in each part I will go over some challenges associated with each of these trends. The first part focuses on demand side flexibility (Ch. 2, Ch. 3) - how to optimize it, form aggregations, and the potential for impact on emissions. The second part focuses on the intersection of the transportation and power networks, and how EV batteries can act as mobile storage in the power network (Ch. 4, Ch. 5). The third part considers prosumers, how optimal aggregations can be set up and how reinforcement learning can be used for pricing within these aggregations (Ch. 6, Ch. 7).

1. Part 1: Demand Side Flexibility

   - In Chapter 2, I will discuss how the rise of clean energy resources creates the need for demand side flexibility, and how this flexible load can be optimized. This work was published in [11].

   - In Chapter 3, I will discuss the potential impact of demand side flexibility on CO_2 emissions. This work was published in [5].

2. Part 2: Electrified Transportation and the Power Network

   - In Chapter 4, I will discuss the value of mobile batteries for the power system operator, based on work presented in [8].

   - In Chapter 5, I will discuss the payoffs for EV owners when they participate in a mobile storage sharing scheme and their equilibrium behavior, based on work presented in [7].

3. Part 3: Aggregations of Energy Prosumers

   - In Chapter 6, I will discuss the rise of prosumers, and how prosumer aggregations can be set up optimally, based on work presented in [6].

   - In Chapter 7, I will present an RL controller which can be used to set prices for a prosumer aggregation, based on work presented in [10].

Part I

Demand Side Flexibility

Chapter 2

Optimizing Demand Response Participation for Flexible Consumers

2.1   Introduction to Demand Response

Demand response (DR) programs are tools to modulate the demand for electricity in a wide variety of situations. For example, at certain times such as mid afternoons on hot summer days, the procurement of additional electricity to meet demand peaks is expensive. At these times, it is more cost effective for the utility to cajole a reduction in demand through financial incentives than to procure an increase of supply to maintain power balance [61]. Another scenario is a grid with significant renewable generation assets. Here DR promises to be a superior balancing resource when compared with conventional gas turbines in the metrics of cost and emissions. In a similar vein, FERC Order 745 mandates that DR assets be compensated for load reduction on par with generation [24].

Participation in DR programs requires assets to accurately estimate their curtailable load and decide on the curtailment they will provide based on their expected net profit. The curtailable load is random and depends on the operating status of the asset at the time of the DR event. This makes it difficult for the asset to determine the optimal load reduction that it can deliver reliably. Asset aggregations can benefit participants by spreading the risk of default on the promised curtailment, and forming aggregations optimally can offer a significant marginal benefit to the aggregation participants.

Demand response programs

There are two flavors of DR programs: *direct load control*, where utilities can modulate loads at will subject to certain contractual limits, and *indirect load control*, where agents are incentivized to yield their discretionary electricity consumption [61]. This work focuses on the latter.

We explore the situation where the utility enters into bilateral contracts with a collection of agents. These agents might be buildings with flexible electricity demand, or aggregators

that manage a collection of DR assets. An agent which enters into a contract of size C kWh receives a payment of $\pi_r C$ from the utility for their obligated reduction in demand, where π_r is the incentive rate set by the utility. In the event the agent is unable to deliver the contractual demand reduction C, it pays a penalty proportional to the shortfall. There are often contractual riders that limit the frequency with which DR assets are called on in response to a DR event. The results in this chapter were published in [11], [12].

Notation

C	Size of contract signed by the asset (kWh)
q	Curtailment capability (random variable) (kWh)
$f(q)$	Probability density function of q
$F(q)$	Cumulative distribution function of q
π_e	Retail tariff paid by the building for energy consumed $(\$/kWh)$
p	*Ex-ante* probability of DR event (h^{-1})
π_r	Incentive paid by utility to participate in DR program, per unit of curtailment contracted $(\$/kWh)$
π_p	Penalty imposed on shortfall in curtailment during a demand response event $(\$/kWh)$

2.2 Problem Formulation

Consider a forward window for the delivery of demand response services, e.g., Tuesday 3-4 pm next week. The retail price of electricity during this window is π_e. Let p denote the probability of a DR event in this window which can be estimated *ex ante* using historical data and exogenous forecasts of temperature and demand, and utilities often publish this information on public-facing dashboards [23]. An agent with DR assets (ex: a building with flexible load) can provide demand reduction during this window. The agent's available demand reduction q in this forward window is a random variable with density function $f(\cdot)$ and cumulative distribution function $F(\cdot)$. This reduction q depends on realizations of underlying random processes such as temperature, total load, occupancy and other variables which determine the functions $f(\cdot), F(\cdot)$. The agent promises to reduce its demand by C kWh to the utility codified through a bilateral contract which may have additional riders, and the utility pays the agent $\pi_r C$ in advance for this promise. The reward price π_r can depend on the delivery window, and is set by the utility and published *ex ante*. Because the available demand reduction q is a random variable, the agent may not be able to meet its demand reduction promise of C kWh. The utility imposes an *ex post* penalty $\pi_p(C-q)^+$ on the shortfall $(C-q)^+ = \max(0, C-q)$, to be paid by the agent.

Agent decisions

During the DR event, the agent has no incentive to curtail its demand beyond the contracted value C, as it receives no additional payment for doing so. The realized curtailment is

$$x = \min(C, q), \tag{2.1}$$

where q is the agent's available demand reduction capability over the DR window. The profit of the DR agent is a random variable, and depends on whether a DR event occurs. If a DR event is called, the realized profit is

$$\pi_{\mathrm{r}}C - \pi_{\mathrm{p}}(C - x) + \pi_{\mathrm{e}}x, \tag{2.2}$$

and the realized profit in the absence of a DR event is

$$\pi_{\mathrm{r}}C. \tag{2.3}$$

Note that the agent receives a payment for its contract C irrespective of whether or not a DR event occurs. The three components of the agent profit are a payment $\pi_{\mathrm{r}}C$ for the contract, a penalty $\pi_{\mathrm{p}}(C - x)$ on the shortfall, and a surplus $\pi_{\mathrm{e}}x$ from avoided electricity use. The agent's profit is a random variable, and it will seek to maximize its expected profit

$$J^{\mathrm{a}} = \pi_{\mathrm{r}}C - p\pi_{\mathrm{p}}\int_0^C (C - q)f(q)dx + p\pi_{\mathrm{e}}\left[\int_0^C qf(q)dq + \int_C^\infty Cf(q)dq\right]. \tag{2.4}$$

In reducing their electricity consumption during a DR event, the agent will suffer some loss of utility. For example, the occupants of a building that reduces its electricity consumption from baseline may suffer the inconvenience of elevated temperatures. Building managers may not be able to assign a monetary value to this loss of utility. A simple approach is to regard the agent's available demand reduction as yielding their discretionary electricity consumption. We can therefore simply bound the contract size by C^{max} to reflect the maximum available discretionary electricity consumption, i.e.

$$q \leq C \leq C^{\mathrm{max}}. \tag{2.5}$$

Another approach is to explicitly introduce a disutility term. Agents will cede some of their baseline consumption only if the marginal disutility is lower than the marginal profit. While these can be readily incorporated into our formulation, we will not do so to keep our exposition simple.

Agents providing DR may be risk averse. For example, flexible buildings may wish to maximize their expected profit while bounding their worst case loss. Risk aversion can be handled through metrics such as CVaR, which is a quantification of the tail risk.

$$\mathrm{CVaR} = \pi_{\mathrm{r}}C + \frac{p}{1 - \hat{c}}\int_0^{F^{-1}(1-\hat{c})} \left[\pi_{\mathrm{e}}q - \pi_{\mathrm{p}}(C - q)\right]f(q)dq \tag{2.6}$$

The risk averse agent will then optimize a combination of its expected profit and the risk assessment measure, weighted by a risk aversion factor α as:

$$\max_{C} \; J^{\mathrm{a}} + \alpha \mathrm{CVaR}(C)$$
$$\text{s.t. } C \leq C^{\mathrm{max}} \tag{2.7}$$

Demand response contracts

Utilities are mandated to reliably procure electricity to meet the random needs of their customers, and they conduct demand forecasts to drive their purchase decisions in the day-ahead market. They subsequently purchase additional electricity in the real time market for a fine balance of supply and demand, at prices that may vary widely. Utilities absorb the price volatility in these two settlement markets, and resell procured electricity to their customers at a retail tariff π_{e} which may be fixed or have time of use structure. At times when the aggregate demand is high such that it strains the generation resources, the price of electricity will be large enough that it will be in the utility's financial interest to displace additional procurement with demand reduction through DR programs [61]. The utility might seek demand reduction for other reasons, such as environmental concerns around scheduling high emissions peaker plants, available capacity, and transmission constraints. There are two reasons why a utility could choose an incentive based program instead of a real time DR market:

1. *Price risk.* FERC regulations dictate that DR assets be compensated for their curtailment on par with market rates. Contracts insulate the utility from high real time prices by committing DR assets to *ex ante* compensation.

2. *Quantity risk.* The curtailment realized from DR assets is uncertain. Contract mechanisms can reduce this uncertainty through a well designed penalty structure. This is more effective than relying on very accurate curtailment forecasts which is necessary in organized markets.

2.3 Optimal Agent Decisions

Recall that the expected profit of the DR agent is given in (2.4), and the agent's CVaR risk aversion metric is given in (2.6). We consider optimal agent decisions in a single DR window. Assume $\pi_{\mathrm{r}} - p\pi_{\mathrm{p}} < 0$.

Result 1. *Optimal Contract and Profitability*

1. *The optimal contract size that maximizes the agent's risk averse expected profit (see Equation 2.7) is given by*

$$C^* = F^{-1} \left[\frac{\pi_r + p\pi_e + \alpha(\pi_r - p\pi_p)}{p(\pi_p + \pi_e)} \right] \tag{2.8}$$

2. *The corresponding expected profit is*

$$J^{a*} = p(\pi_p + \pi_e) \int_0^{C^*} q f(q) dq - \alpha(\pi_r - p\pi_p)C^* \tag{2.9}$$

3. *Risk aversion, i.e. increasing α decreases the expected profit and the optimal contract size, but reduces worst case losses.*

Proof. The agent's optimization objective (2.7) is concave in the contract size C, which can be proven with the second derivative test. Then the optimal contract C^* can be calculated from the zero of the second derivative of the objective and clipping it to $[0, C^{\max}]$. The expression for profit can be calculated by substituting C^* in (2.4). $\square$

The value of this result hinges on being able to calculate the quantile in (2.8). While the distribution of curtailment capability at any time may not be readily available, it can be estimated using a combination of historical data, operational information and forecasts of causal variables like weather. The expected profitability of participating in the DR program without any underlying curtailment capability, i.e., without any physical asset is $(\pi_r - p\pi_p)$. The utility will set reward and penalty such that $\pi_r - p\pi_p < 0$; otherwise, it will encourage unwanted behavior, such as bidding without any DR asset capability.

The optimal contract C^* and corresponding profit depend intimately on the distribution of curtailment capability $f(\cdot)$. The standard deviation σ of the curtailment distribution is a measure of the uncertainty in its estimation. A smaller σ signifies a tighter estimate of future capability, and reduces the risk of shortfall. Under a mild symmetry assumption on f, we have

Result 2. *Effect of Uncertainty in Future DR Capability*

1. *Contract: Suppose f is symmetric about the mean μ, with standard deviation σ, then*

$$C^* = \mu + \gamma\sigma \tag{2.10}$$

where γ is a function of $p, \pi_r, \pi_p, \pi_e, \alpha$ derived from the expression for optimal contract (2.8). If $\gamma < 0$, i.e. contract is lower than μ, then decreasing σ leads to a higher contract. If $\gamma > 0$, decreasing σ leads to lower contract. A decrease in σ pushes the contract size closer to μ.

2. *Profit: The coefficient of σ is negative up until a certain positive γ value, i.e. until $\gamma = \hat{\gamma}$, and positive after that. For $\gamma < \hat{\gamma}$, an increase in uncertainty (i.e., increase in σ) causes a decrease in expected profit.*

The symmetry assumption is reasonable, particularly where the curtailment capability has a 'base' value with some error due to operational variability. This is consistent with outputs from a linear regression based prediction model, which assumes that errors are normally distributed.

Result 2 could be useful in evaluating the benefits of lowering uncertainty. For example: paying for more accurate weather forecasts, or paying to install submetering equipment in buildings could add value by leading to tighter estimations of future DR capability. Knowing the value of reduced uncertainty (i.e., lower σ) in terms of increased DR profit can help in making a decision on the cost-benefit tradeoff. Also, as the DR event window approaches, the estimation of DR capability might improve (e.g. predicting DR capability one month in advance vs. a few hours in advance). Our results will be useful for these near-term predictions as well, which might have lower uncertainty.

2.4 Optimizing Demand Response Aggregations

DR assets can be aggregated to provide DR as a single entity, sharing the burden of curtailing load and reducing their individual risk. We will not explore how DR assets can be induced to form such aggregations; instead, we focus on optimal decisions of the aggregation as a joint entity.

For the results presented in this section, we make the following assumption: DR agent curtailments are similarly distributed (i.e. from the same family of probability distributions), but with different mean and variance parameters μ, σ. Further, the sum of agent curtailments is distributed similarly as well (ex: normal distribution), and the distribution $f_k(\cdot)$ of the curtailment capability of asset k is completely characterized by its mean and variance. From Result 2, the optimal contract for asset k is

$$C_k^* = \mu_k + \gamma \sigma_k \tag{2.11}$$

where γ is completely determined by utility and DR program rates. The aggregate DR asset curtailment capability is

$$q_{\text{ag}} = \sum_k q_k \tag{2.12}$$

The optimal contract for the aggregation differs from the sum of contracts for the individual participants due to the different variance.

$$
\begin{aligned}
C_{\text{ag}}^* = \mu_{\text{ag}} + \gamma \sigma_{\text{ag}} = \sum_k \mu_k + \gamma \sigma_{\text{ag}} \\
\sum_k C_k^* = \sum_k \mu_k + \gamma \sum_k \sigma_k
\end{aligned}
\tag{2.13}
$$

Result 3. *Aggregation Contract Size and Profitability*

   1. The optimal contract for the aggregation is

$$C_{ag}^* = F_{ag}^{-1} \left[\frac{\pi_r + p\pi_e + \alpha_{ag}(\pi_r - p\pi_p)}{p(\pi_p + \pi_e)} \right] \tag{2.14}$$

where α_{ag} *is the risk aversion factor for the aggregation, and* $F_{ag}(\cdot)$ *is the cumulative density function for the aggregation's curtailment capability* q_{ag}.

2. *The relation between the aggregation's contract size and the aggregate contract of individual participants is*

$$C_{ag}^* : \begin{cases} < \sum_b C_b^* & \text{if } \gamma > 0 \\ > \sum_b C_b^* & \text{if } \gamma < 0 \end{cases} \tag{2.15}$$

3. *At the optimal contract, total increase in profit for an aggregation of assets with common* α *is*

$$\Delta J^a = -\alpha(\pi_r - p\pi_p)(C_{ag} - \sum_k C_k)$$
$$+ p(\pi_p + \pi_e) \left[\int_0^{C_{ag}} q f(q) dq - \sum_k \int_0^{C_k} q_k f_k(q_k) dq_k \right] \tag{2.16}$$

We examine the profit differential for assets whose curtailments are normally distributed, i.e. $q_k \sim \mathcal{N}(\mu_k, \sigma_k)$; $C_k^* = \mu_k + \gamma\sigma_k$. For a normal distribution, the quantile function is given by

$$F^{-1}(p) = \mu + \sigma[\sqrt{2}\mathrm{erf}^{-1}(2p-1)] = \mu + \sigma\gamma$$

which gives us the expression

$$\Delta J^{\mathrm{a}} = -p(\pi_{\mathrm{p}} + \pi_{\mathrm{e}})(N_k - 1)\frac{1}{2}\left[\mathrm{erf}\left(\frac{\gamma}{\sqrt{2}}\right) + 1\right]$$
$$+ \left(\sum_k \sigma_k - \sigma_{\mathrm{ag}}\right)\left\{ p(\pi_{\mathrm{p}} + \pi_{\mathrm{e}})\frac{e^{-\frac{\gamma^2}{2}}}{\sqrt{2\pi}} + \alpha(\pi_{\mathrm{r}} - p\pi_{\mathrm{p}})\gamma \right\} \tag{2.17}$$

We define an optimal aggregation as one which maximizes the increase in *social welfare*, i.e., leads to the greatest increase in profit for its participants. In the expression for profit increase (2.17), we can see that the mean of the distributions of curtailment capability does not affect the marginal benefit, rather the variability does. If the random variables q_k (the DR capability) of two assets are highly correlated, they will have a lower marginal benefit in aggregating as compared to two uncorrelated assets. The intuition is that uncorrelated variability de-risks the contract commitment and reduces the total variability of the sum of curtailment capacities.

Definition 1. *Complementarity Test*
To evaluate DR assets $k \in \mathcal{N}$ *that aim to form an aggregation, the metric*

$$\Delta\sigma = \sum_{k \in \mathcal{N}} \sigma_k - \sigma_{ag} \tag{2.18}$$

*is an indicator of the marginal increase in profitability upon aggregation. Here σ_k is the
standard deviation of the distribution of curtailment capability for asset k, and σ_{ag} is the
standard deviation of the distribution of the sum of curtailment capabilities for all assets
$k \in \mathcal{N}$.*

Note that σ_{ag} is lower than the sum of individual σ_k, as it exploits the low correlations
across different assets. The lower the correlation of two assets, the higher this difference, (and
consequently the marginal increase in profit) will be. This test can be useful for third-party
DR aggregators that want to optimally package or aggregate assets while signing curtailment
contracts. While it may seem that the information needed to calculate this metric is difficult
to obtain, it might be readily available to entities such as smart thermostat aggregators or
battery management companies.

2.5   Discussion

In this chapter, we presented a framework for optimizing DR asset participation in incen-
tive based demand response programs. We modeled the DR capability of assets as a random
variable, and developed analytical expressions for optimal contract size and profit for a profit
maximizing asset. We also explored the effect of variability in capability estimates and risk
aversion on both contract size and profit. We then explored the marginal benefit of aggre-
gation for such assets, and devised a test for asset complementarity under the assumption
that DR curtailment follows a normal distribution.

The usefulness of our work hinges on the ability to estimate probability distributions
for DR capability. Our complementarity test depends on the goodness-of-fit of a normal
distribution to the observed data-driven distribution, which may not always be an accurate
distribution model for different DR assets. However, there are a few reasons that a normal
distribution could be a good fit. In the case of an aggregation, if the flexibilities of the
constituent assets are independently and identically distributed, the flexibility of the aggre-
gation as a whole will be approximately normally distributed per the central limit theorem.
Even for an individual asset, if the uncertainty in flexibility is due to a linear combination
of random causal factors, the asset's flexibility will be approximately normally distributed.
Constructing probabilistic forecasts for flexible load capacity is an active area of research, and
these forecasts are essential to appropriately model and account for the inherent uncertainty
in demand response.

Chapter 3

Emissions Impact of Flexible Loads

In Chapter 2, we explored how flexible consumers can optimize their participation in programs designed to compensate them monetarily for their flexibility. However, there are consumers who may wish to use their load flexibility to reduce their emissions impact. The analysis in this chapter was published in [5].

3.1   Problem Formulation

Climate-conscious consumers can reduce their carbon footprint by implementing load reduction and load shift measures to minimize the emissions caused by their energy consumption. Retail consumers are usually served by utilities who procure energy from various sources while minimizing cost. The emissions impact of reduced energy consumption is through the *marginal* resource, which is often the most expensive generation source [74].

The marginal emissions intensity of energy generation can be defined as the carbon emissions (lbs. CO_2) produced per unit of energy generated (measured in MWh). It varies significantly across time of day and year, which then affects the emissions impact of reduced energy consumption [82]. Researchers have studied the aggregate impact of repeated load shift measures using marginal emissions intensity data [17], and found that load flexibility can help reduce emissions significantly.

However, load shift/shed measures are expensive- they cause discomfort to building occupants, and require either manual intervention or investment in automated equipment. For loads which can not be shifted or shed repeatedly, we need to prioritize interventions which can achieve the highest emissions reduction by understanding the time-varying nature of marginal emissions intensity.

In order to prioritize load shift/shed interventions, it is necessary to evaluate whether *a few time periods in the year have an outsize potential to reduce emissions.*

3.2   Methods

We use data on the emissions intensity of electricity consumption from WattTime [75], and data on electricity consumption of residential consumers using simulated end-use load profiles from a study by NREL [27].

Marginal emissions intensity

Marginal emissions intensity is characterized by the Marginal Operating Emissions Rate (MOER), and is measured in lbs. of CO_2 emitted per MWh of energy generated. We use the WattTime API [75] to access historical MOER for the Northern Californian grid for 2018-2021, reported at 5-min intervals and calculated using empirical modeling of the power system. MOER values typically range between $800 - 1200$ lbs. CO_2 per MWh.

The MOER also exhibits spikes, and shifting and shedding load around these times can be particularly effective for reducing emissions. A quantity of interest for us is the *MOER differential*, i.e., the maximum MOER decrease possible within ± 1 hour of the time period under consideration, which can be interpreted as the emissions reduction possible if one unit of energy consumption can be shifted to any time up to one hour before or after the time period under consideration.

We analyze time periods when either the MOER or MOER differential is particularly high, in order to increase the effectiveness of load shed or shift actions. We rank time periods based on these parameters, and pick the top 1000 (approximately 1%) 5-minute periods to study. This translates to studying the impact of load shift or load shed for the most impactful 1% of the year.

Energy consumption data

We use residential electricity consumption data from simulated end-use load profiles generated in the ResStock analysis tool by NREL [27]. We constrain our analysis to Alameda County in California, and use data simulated using the actual meteorological measurements in 2018. Table 3.1 illustrates the average 15 minute energy consumption for major end-use loads for winter and non-winter months. Plug loads are the largest end-use category, and seasonal variations in temperature cause the shift in heating and cooling loads.

Time	Plug Loads	Lighting	Refrigerator	Heating	Cooling	Misc
Non-Winter Months	36.7	14.2	10.8	3.2	7.1	22.8
Winter Months	41.6	17.5	8.6	14.3	1.9	24.8

Table 3.1: Average 15-min load (MWh) for residential end-uses in Alameda County, 2018. Winter months include January, February, November, and December.

3.3 Findings

We analyze four years (2018 - 2021) of MOER data, and find similar seasonal and daily variations across years, with the exception of higher MOER peaks in 2021. High MOER values occur largely in the winter, and high MOER differential values occur throughout the year, but typically in the afternoon. Consistent patterns in MOER and MOER differentials suggest that planned load shift and load shed actions could reliably reduce emissions. We find that plug loads and heating are the biggest end-use loads active during peak MOER periods, which makes them good candidates for load shed actions. Plug loads and refrigeration are the biggest shiftable end-use loads active during peak MOER differential periods, and will be good candidates for load shift. Some plug loads can be shifted, e.g., dishwashers and washing machines, while others such as desk lamps and computers are not shiftable.

MOER exhibits seasonality, with wide intra-day variation

MOER has a consistent seasonal pattern across seasons, with the lowest MOER in the summer months. There can be high intra-day MOER variation, and the spread of MOER values includes a cluster around 0 lbs. CO_2/MWh as seen in Figure 3.1, caused by the marginal resource being a zero-carbon resource. This is caused by high solar penetration on the Californian grid, which can result in solar being curtailed, making it the marginal resource.
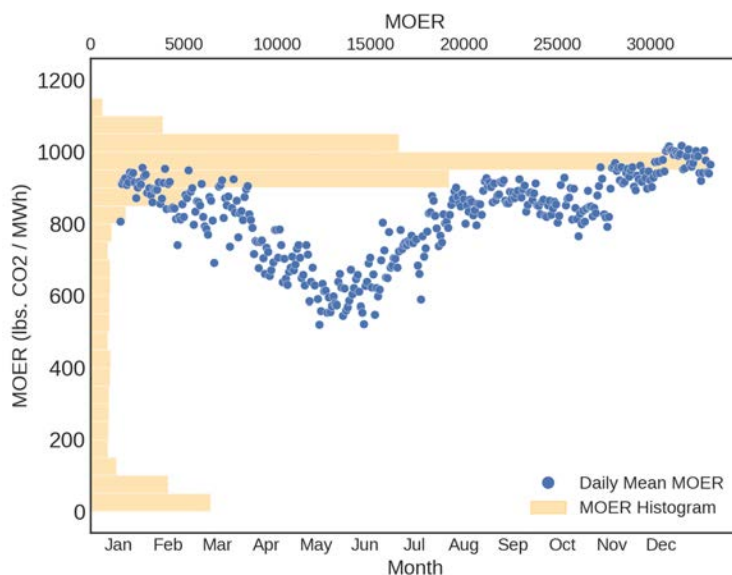
Figure 3.1: Scatter plot of mean MOER by day across 2018, overlaid on a histogram showing the spread of all MOER values in 2018 measured at 5-minute intervals

Winter months have the highest marginal emissions

We analyze peak MOER periods, i.e., the 1000 time periods (top $\sim 1\%$ MOER of 5-minute time periods in a year) with the highest MOER values over 2018. Figure 3.2 illustrates the MOER over the course of 2018, alongside a count of the number of peak MOER periods in each month. The winter and spring months (December through April) account for most of them, which has implications for load shed: shedding loads during the winter months can have the highest impact on emissions.
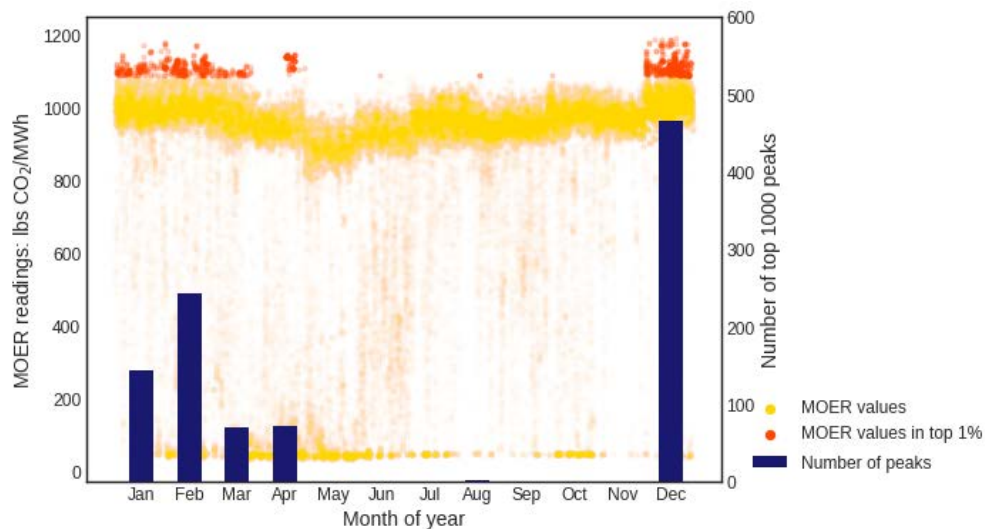
Figure 3.2: Scatter plot of MOER values across 2018 highlighting the peak MOER periods, overlaid by a bar plot indicating the number of peak MOER periods in each month.

Some time periods have a sharp drop-off in marginal emissions intensity within an hour

The *MOER differential* characterizes the emissions reduction possible if one unit of energy consumption can be shifted, i.e., consumed at another time up to one hour before or after its original consumption time. Figure 3.3 illustrates how prioritizing load shift actions at peak MOER differential times will have a much higher impact on emissions than at other time periods. MOER differentials exhibit a trend by time of day, and most of the high MOER differential time periods lie between 6 am - 6 pm. This has implications for load shift: shifting loads that are active during this window will lead to the highest emissions reductions. The short drop-off period in MOER indicates that it is critical to accurately forecast MOER, since even a small window of error could result in shifting load to a high MOER period.
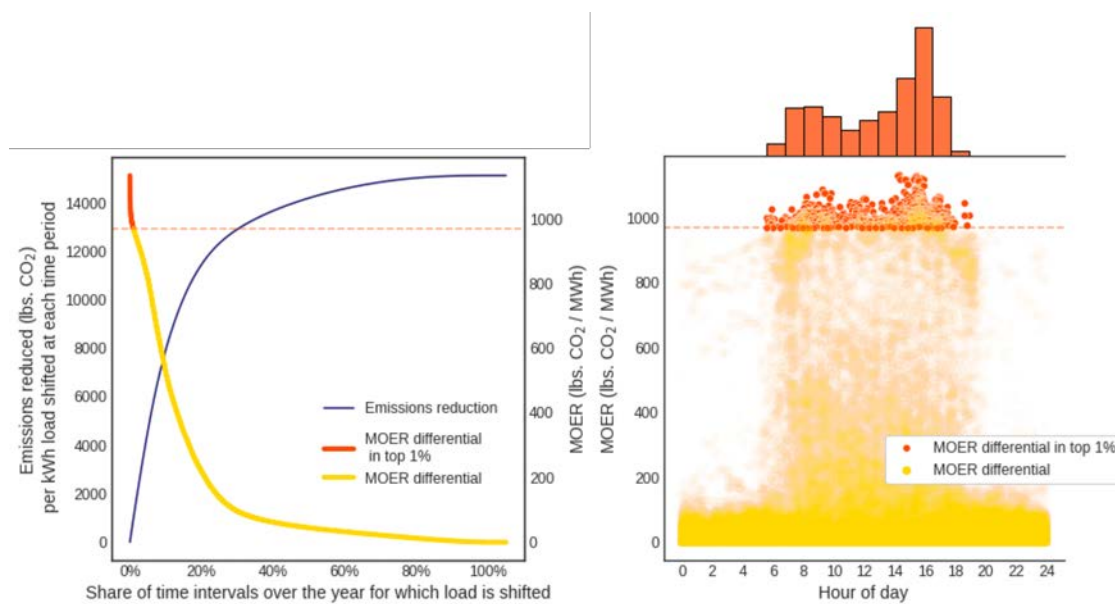
Figure 3.3: On the left, the spread of MOER differentials over the course of 2018 arranged in descending order, overlaid by a plot of potential emissions reduction if load is shifted for an increasing share of time periods over the year. On the right, the MOER differential values by hour of day, with the top 1% highlighted in orange.

End-use loads that are active during high emissions periods

The largest end-use loads active during peak MOER periods (ref. Table 3.2) are plug loads and heating, which makes them a good target for load shed measures. Of the shiftable end-use loads, the largest ones active during peak MOER differential periods are plug loads and refrigeration (ref. Table 3.2), which makes them a good target for load shift measures. Since load only needs to be shifted over a few time periods, fast discharge batteries can be good candidates to enable this load shift.

Time	Plug Loads	Lights	Refrig.	Heating	Cooling	Misc
Top 1000 MOER Values	38.6	12.9	8.5	16.0	1.1	18.3
Top 1000 MOER Differential	42.2	21.9	10.1	5.5	5.2	23.8
Yearly Average	38.3	15.3	10.1	6.8	5.4	23.6

Table 3.2: Average 15-min consumption (MWh) for different residential end use loads during peak MOER and MOER differential periods, compared to the yearly average in 2018 in Alameda County

3.4 Discussion

Our analysis shows that in order to reduce CO_2 emissions associated with energy consumption, there are time periods in the year when it is particularly effective to modify consumption. It is important to note that this analysis is specialized to the Northern Californian grid, and that results may vary based on the particular geography and resource mix under consideration.

The true value of these time periods can be estimated by simulating load shift and load shed using flexible load estimates. A possible source of loaf flexibility estimates is the California Demand Response Potential Study [29], which details load shift and shed capacity by end-use. These estimates can be paired with energy consumption data to get a sense of emissions reductions possible at scale.

In order to capitalize on these high impact time periods, it is important to have accurate forecasts of emissions intensity, as well as communications and control infrastructure that can enable consumers to act on this information.

Part II

Electrified Transportation and the Power Network

Chapter 4

Marginal Value of Mobile Storage in the Power Network

In the previous two chapters, we studied how flexible consumers can optimize their participation in demand response contracts, and the potential impact of flexible energy consumption on emissions. With increasing electrification of transportation, the batteries in electric vehicles can fulfill an important function as mobile storage for the power grid. In this chapter, we discuss the value of this mobile storage resource for the power system. The results in this chapter were published in [8].

4.1 Introduction

The share of variable renewable energy resources in the power grid is accelerating worldwide, and we will require a large amount of energy storage to be connected to the grid to balance the variability of these resources. This is driven by profound technological and economic trends including the dramatic reduction in cost of battery systems and the advance of power electronics for programmable inverters. Meanwhile, mandates and goals for storage deployment have been proposed in many states including California and Massachusetts. As a result, new storage capacity is being connected to the grid at a record pace [76]. On the other hand, transportation electrification and more generally the trend to "electrify everything"[65] are expected to significantly increase the peak load for power systems. When the peak load is constrained by transmission or distribution capacity, the conventional wisdom is to install more wires or reinforce existing ones [28]. However, such wire-based solutions have high capital costs, are usually time-consuming to implement, and can face public opposition [47]. Therefore, non-wire alternatives that can avoid or delay the need for capacity expansion are highly valued by system operators and utility companies.

Mobile energy storage can simultaneously serve the role of energy storage and wires as it can help balance the supply and demand in both time and space. There are many forms of mobile energy storage. Truck-mounted mobile energy storage units have been tested by

Con Edison [79] for utility-scale applications. Electric vehicles and electric trucks together with bidirectional chargers can be used as mobile energy storage [64]. Internet data centers whose load can be shifted across space (among data centers located at different geographical areas) and time [43] behave as a form of virtual mobile storage. Understanding the value of mobile storage, particularly with respect to the value of stationary storage and wires is an essential first step in assessing the potential of this technology for future power systems.

Contribution and chapter organization

In this chapter, we analyze the value of mobile storage from the point of view of a power system operator through a stylized formulation for joint operation of the power network and a fleet of mobile storage units. It is known that the clearing price of electricity in wholesale markets depends on location, and these prices are called locational marginal prices (LMPs). Given the relocation pattern of mobile storage, we show that the marginal value of mobile storage can be computed analytically using LMPs. Using this analytical expression, we compare the marginal value of mobile storage with that of corresponding stationary storage and wires. Examples/conditions where the marginal value of mobile storage is strictly higher, lower, or equal to the sum of the marginal values of stationary storage and wires are presented, which offer insights on when mobile storage is preferred over stationary storage. We then propose efficient algorithms for the optimal storage relocation problem based on analytical expressions for the marginal value of mobile storage.

This chapter is organized as follows: Section 6.2 describes our model for the power network, mobile storage and transport. Section 4.3 introduces the problem of multi-period economic dispatch with storage, and formulates the optimal relocation problem for mobile storage. Section 4.4 studies the rapid mobile storage case, where storage can relocate and charge rapidly. Section 4.5 treats the general mobile storage case. Section 4.7 concludes the chapter.

Related literature

Several papers address the question of quantifying the marginal value of stationary storage. Bose and Bitar [15] develop an expression for locational marginal value of storage in a stochastic setting, i.e. when the system operator has to meet uncertain demand by dispatching generation and storage, and the marginal value is determined to be a function of the expected LMPs. Qin et al. [52] derive an expression for the marginal locational value of stationary storage in terms of locational marginal prices (LMPs) determined by the economic dispatch problem, and propose a discrete optimization framework for optimal siting from the system operator perspective. Bitar et al. [14] explore the economic value of storage colocated with a wind producer. Each of these papers adds a level of complexity to the problem of valuing stationary storage, but considers an ideal storage model with no power constraints. Our results in Section 4.5 generalize the storage model by incorporating power constraints.

In contrast to stationary storage, mobile storage can add extra value by relocating across the power network. There is a growing literature that addresses this. Qin et al.[54] propose using EV batteries to reduce demand charges, and justify this value proposition through a numerical case study. Rossi et al. [57] model the coupling between transportation and power networks for on-demand transport services, and develop a joint optimization problem for the combined network. The economic value of truck mounted mobile storage is evaluated using numerical simulations in [31].

4.2 Modeling Grid, Storage, and Transportation

Notation

For any natural number n, let $[n] := \{1, \ldots, n\}$. We use $\mathbf{1}$ to denote all-one vectors of appropriate dimensions, $\mathbf{e}_i \in \mathbb{R}^n$ to denote the i-th elementary vector whose i-th element is one and all other elements are zeros. For any time dependent vector $\mathbf{x}(t) \in \mathbb{R}^n$ with $t \in [T]$ and $T \in \mathbb{N}$, we use $\mathbf{x}_i \in \mathbb{R}^T$ to denote $[x_i(1), \ldots, x_i(T)]^\top$.

Power network

We consider the operation of a power network with n buses and m lines over a finite horizon of length T. For each time slot $t \in [T]$, we denote the power generation and inelastic load over different buses in the power network by $\mathbf{g}(t) \in \mathbb{R}^n$ and $\boldsymbol{\ell}(t) \in \mathbb{R}^n$, respectively. The generation cost function for generator at bus i is denoted by $C_i(\cdot)$ and so the total generation cost in time period t is

$$C(\mathbf{g}(t)) = \sum_{i=1}^n C_i(g_i(t)), \quad t \in [T]. \tag{4.1}$$

For simplicity, we assume $C_i(\cdot)$ is convex quadratic. This assumption can be relaxed with other conditions that ensure differentiability of the optimal value function.

Denote the net power injection vector in time period t by $\mathbf{p}(t) \in \mathbb{R}^n$. The net power injection vector needs to satisfy the linearized AC power flow constraints:

$$\mathbf{1}^\top \mathbf{p}(t) = 0, \quad t \in [T], \tag{4.2a}$$

$$H\mathbf{p}(t) \leq \bar{\mathbf{f}}, \quad t \in [T], \tag{4.2b}$$

where $\mathbf{1}$ denotes the all-one vector, $H \in \mathbb{R}^{2m \times n}$ refers to the shift-factor matrix of the power network, and $\bar{\mathbf{f}} \in \mathbb{R}^{2m}$ models the thermal constraints of the lines (cf. [52] for a derivation of this version of the linearized AC power constraints).

Mobile energy storage

Consider a fleet of K mobile energy storage units. We denote the charging and discharging operation of storage unit k in time period t by $u_k(t)$, with the convention that $u_k(t) > 0$

models charging and $u_k(t) < 0$ models discharging. We assume that each storage unit is fully discharged at the beginning of the decision horizon, so the state of charge (SoC) of storage k at the beginning of time period $t + 1$ is

$$\sum_{\tau=1}^{t} u_k(\tau), \quad k \in [K], \quad t \in [T]. \tag{4.3}$$

The SoC of each storage unit must satisfy the energy capacity constraint. In particular, denote the energy capacity of storage k by $\bar{s}_k$. Then we have

$$0 \leq \sum_{\tau=1}^{t} u_k(\tau) \leq \bar{s}_k, \quad k \in [K], \quad t \in [T]. \tag{4.4}$$

Denote the vector of charging and discharging operation of storage k by $\mathbf{u}_k \in \mathbb{R}^T$. Then constraint (4.4) can be written as

$$\mathbf{0} \leq L\mathbf{u}_k \leq \bar{s}_k \mathbf{1}, \quad k \in [K], \tag{4.5}$$

where L is a lower triangular matrix defined as

$$L_{ij} = \begin{cases} 1, & \text{if } i \geq j, \\ 0, & \text{otherwise.} \end{cases} \tag{4.6}$$

In addition to the energy capacity constraint, storage units often have a power capacity rating which limits the amount of energy that can be charged or discharged for each unit of time. Denote the power rating of storage k by $\bar{u}_k$. In general, when we vary the energy capacity of a storage units (e.g. by adding more battery packs), the power rating will also vary. Thus we write $\bar{u}_k = \bar{u}_k(\bar{s}_k)$ when we want to highlight this dependence, where $\bar{u}_k(\cdot)$ is continuously differentiable.

The energy transfer into/out of a storage unit in a time period also depends on the time that is available for storage operation. Denote the length of each time period in our discrete time model by Δ. Since it takes time for mobile storage units to move between different buses in the power network, the time that is available for storage k to charge or discharge in time period t, denoted by $\Delta_k^{\mathrm{S}}(t)$, satisfies $0 \leq \Delta_k^{\mathrm{S}}(t) \leq \Delta$. As a result, the power capacity leads to the following constraint

$$-\Delta_k^{\mathrm{S}}(t)\bar{u}_k \leq u_k(t) \leq \Delta_k^{\mathrm{S}}(t)\bar{u}_k, \quad k \in [K], \quad t \in [T]. \tag{4.7}$$

Denote the bus at which storage k is located at the beginning of time period t by $i_k(t)$, and define matrix $E(t) \in \mathbb{R}^{n \times K}$ as

$$E(t) = \begin{bmatrix} \mathbf{e}_{i_1(t)} & \cdots & \mathbf{e}_{i_K(t)} \end{bmatrix}, \quad t \in [T], \tag{4.8}$$

where $\mathbf{e}_i$ is the i-th elementary vector with a one at the i-th element and zeros elsewhere. Note that the sequence $\{i_k(t)\}_{t \in [T]}$ characterizes the relocation process (i.e., the trajectory) of storage k, while $E(t)$ provides a snapshot of the locations of all mobile storage units in the power network in time period t. For convenience, we denote the collections of trajectories and snapshots by

$$\mathfrak{I} = \{\mathfrak{I}_k\}_{t \in [T]} := \{i_k(t)\}_{k \in [K], t \in [T]}, \quad \mathfrak{E} := \{E(t)\}_{t \in [T]}, \tag{4.9}$$

respectively, where we use $\mathfrak{I}_k$ to denote the trajectory of mobile storage k. Since (4.8) defines a one-to-one mapping between $\mathfrak{I}$ and $\mathfrak{E}$, we will use them interchangeably.

Transportation model

The system operator can determine whether to relocate storage k in each time period. If storage k is relocated in time period t, a portion of time period t is used to move the storage from one bus to another. Let $D \in \mathbb{R}^{n \times n}$ be a matrix whose (i, j)-th element is the travel time from bus i to bus j. We assume that the length of the time intervals Δ is selected so that $D_{i,j} \leq \Delta$ for all i, j. Denote the time needed for moving storage k in time period t by $\Delta_k^{\mathrm{M}}(t)$. Since storage k is moved from bus $i_k(t)$ to bus $i_k(t+1)$ in time t, we have

$$\Delta_k^{\mathrm{M}}(t) = \mathbf{e}_{i_k(t)}^{\top} D \mathbf{e}_{i_k(t+1)}, \quad k \in [K], \quad t \in [T]. \tag{4.10}$$

Thus the time left for storage to charge or discharge in time period t is

$$\Delta_k^{\mathrm{S}}(t) = \Delta - \Delta_k^{\mathrm{M}}(t), \quad k \in [K], \quad t \in [T]. \tag{4.11}$$

We adopt the convention that if a storage k is moved in time period t, it will first use $\Delta_k^{\mathrm{S}}(t)$ time to charge/discharge at bus $i_k(t)$ and then use $\Delta_k^{\mathrm{M}}(t)$ time to relocate to bus $i_k(t+1)$.

Transporting energy storage between buses is costly. For example, truck mounted mobile storage consumes fuel to travel between buses. Denote the relocation cost per unit of travel time by κ. Then the total cost for relocation is

$$J^{\mathrm{R}}(\mathfrak{I}) := J_k^{\mathrm{R}}(\mathfrak{I}_k) := \kappa \sum_{k=1}^{K} \sum_{t=1}^{T} \mathbf{e}_{i_k(t)}^{\top} D \mathbf{e}_{i_k(t+1)}, \tag{4.12}$$

where $J_k^{\mathrm{R}}(\mathfrak{I}_k)$ is the relocation cost for the k-th mobile storage unit.

4.3   Optimal Dispatch and Relocation

In a centralized optimization setting, the system operator controls both the power grid and the mobile storage fleet. Given the locations of the mobile storage units $\mathfrak{E}$, the operation of

the grid and the charging/discharging of the storage units can be formulated as the following optimization problem:

$$\min_{\mathbf{p},\mathbf{u}} \quad \sum_{t=1}^{T} C_t(\mathbf{p}(t)) \tag{4.13a}$$

$$\text{s.t.} \quad \mathbf{1}^{\top}(\mathbf{p}(t) - \mathbf{d}(t) - E(t)\mathbf{u}(t)) = 0, \qquad\qquad t \in [T], \tag{4.13b}$$

$$H(\mathbf{p}(t) - \mathbf{d}(t) - E(t)\mathbf{u}(t)) \leq \bar{\mathbf{f}}, \qquad\qquad t \in [T], \tag{4.13c}$$

$$\mathbf{0} \leq L\mathbf{u}_k \leq \bar{s}_k \mathbf{1}, \qquad\qquad k \in [K], \tag{4.13d}$$

$$-\bar{u}_k(\bar{s}_k)\boldsymbol{\Delta}_k^{\text{S}} \leq \mathbf{u}_k \leq \bar{u}_k(\bar{s}_k)\boldsymbol{\Delta}_k^{\text{S}}, \qquad\qquad k \in [K]. \tag{4.13e}$$

where $\{\boldsymbol{\Delta}_k^{\text{S}}\}_{k\in[K]}$ is calculated via (4.10) and (4.11), and the locations of mobile storage units summarized by $E(t)$ are given. We refer to this problem as *multi-period economic dispatch problem with storage* (MPED-S). The optimal value of this problem characterizes the total generation cost of meeting the loads when generators and storage charging/discharging are optimized. Denote the optimal value as a function of the storage locations and storage capacities by $J^{\text{ED}}(\mathfrak{E},\bar{\mathbf{s}})$.

Note that it is possible to incorporate *stationary* storage into our model by disallowing relocation of a subset of mobile storage units. In other words, if storage unit $\widetilde{k}$ is a stationary storage, we require $i_{\widetilde{k}}(t)$ or the $\widetilde{k}$-th row of matrix $E(t)$ to stay constant over time. Alternatively, stationary storage can be modeled using a separate set of variables and constraints in the MPED-S problem (cf. [52]).

The problem of optimizing the movements of the mobile storage fleet is then

$$\min_{\mathfrak{I}} \quad J^{\text{ED}}(\mathfrak{E}(\mathfrak{I}),\bar{\mathbf{s}}) + J^{\text{R}}(\mathfrak{I}), \tag{4.14}$$

where the initial locations of the mobile storage units $\{i_k(1)\}_{k\in[K]}$ are given, and the decision variable $\mathfrak{I} := \{i_k(t)\}_{k\in[K],t\in[T]}$ is optimized such that each $i_k(t) \in \mathcal{I}_k^{\text{S}} \subseteq [n]$ and $\mathcal{I}_k^{\text{S}}$ is the set of buses with which mobile storage unit k can be connected.

Note that unlike the multi-period economic dispatch problem (4.13) which is a convex program, the optimal storage relocation problem (4.14) is a combinatorial optimization problem.

4.4 Rapid Mobile Storage

We first consider storage that can both charge/discharge and move instantaneously: it does not require any time to move between buses, and the power limit for charging and discharging is large enough that the power constraints (4.13e) are never binding. This analysis serves two purposes: (a) it provides a theoretical account of the problem focusing on the *relocation* aspect while omitting the complexity associated with travel times (which is addressed in Section 4.5), and (b) it offers a good model for *virtual mobile storage*, including storage

capabilities offered by flexible loads that are geographically shiftable such as a collection of
Internet data centers.

Given the locations of the mobile storage units $\mathfrak{E}$, the MPED-S problem is given by (4.13)
without the power constraint (4.13e):

$$\min_{\mathbf{p},\mathbf{u}} \quad \sum_{t=1}^{T} C_t(\mathbf{p}(t)) \tag{4.15a}$$

$$\text{s.t.} \quad \mathbf{1}^\top(\mathbf{p}(t) - \mathbf{d}(t) - E(t)\mathbf{u}(t)) = 0, \qquad t \in [T], \tag{4.15b}$$

$$H(\mathbf{p}(t) - \mathbf{d}(t) - E(t)\mathbf{u}(t)) \leq \overline{\mathbf{f}}, \qquad t \in [T], \tag{4.15c}$$

$$\mathbf{0} \leq L\mathbf{u}_k \leq \overline{s}_k\mathbf{1}, \qquad k \in [K]. \tag{4.15d}$$

While we do not model travel times for storage relocation for power constraints in this case,
we can still capture the cost of moving storage from one bus to another. In particular, we use
κD_{ij} to model the cost of relocating from bus i to bus j. For the example of Internet data
centers, this cost may model the loss of quality of service from moving energy consuming
data-processing loads from one data center to another. With relocation cost defined as
(4.12), the optimal relocation problem still takes the form of (4.14).

Marginal value of rapid mobile storage

Tackling the optimal relocation problem requires a good understanding of the optimal value
of MPED-S problem (4.15), which in turn depends on the spatial and temporal distribution
of storage capacities. One way to characterize such dependence is through analyzing the
marginal value of mobile storage with fixed relocation pattern $\mathfrak{E}$.

Definition 2 (Marginal value of mobile storage). *Given storage relocation pattern $\mathfrak{E}$, the
marginal value of mobile storage k is defined as*

$$\mathsf{MV}_k^{\mathrm{ms}}(\mathfrak{E},\overline{\mathbf{s}}) = -\frac{\partial J^{\mathrm{ED}}(\mathfrak{E},\overline{\mathbf{s}})}{\partial \overline{s}_k}, \quad k \in [K]. \tag{4.16}$$

The quantity $\mathsf{MV}_k^{\mathrm{ms}}(\mathfrak{E},\overline{\mathbf{s}})$ characterizes the reduction in the operation cost of the grid
when we marginally increase the storage capacity of mobile storage k, given the relocation
pattern $\mathfrak{E}$. As the objective function of (4.15) is convex quadratic, it is easy to check that
the partial derivatives in (4.16) indeed exist.

It turns out that we can obtain an explicit and intuitive characterization of $\mathsf{MV}_k^{\mathrm{ms}}(\mathfrak{E},\overline{\mathbf{s}})$ via
the dual variables of (4.15). Denote the (optimal) dual variables associated with constraints
(4.15b), (4.15c), and (4.15d) by $\gamma(t) \in \mathbb{R}$, $\boldsymbol{\beta}(t) \in \mathbb{R}^{2m}$, and $(\boldsymbol{\nu}_k, \boldsymbol{\mu}_k) \in \mathbb{R}^T \times \mathbb{R}^T$, respectively,
where $\boldsymbol{\nu}_k$ is associated with the lower bound in (4.15d) and $\boldsymbol{\mu}_k$ is associated with the upper
bound. We can also calculate the *locational marginal prices* (LMPs), denoted by $\lambda_i(t)$, for
each bus i and time period t using these dual variables (cf. [52]):

$$\boldsymbol{\lambda}(t) = \gamma(t)\mathbf{1} - H^\top\boldsymbol{\beta}(t), \quad t \in [T]. \tag{4.17}$$

Notice that the dual variables and LMPs depend implicitly on the relocation pattern $\mathfrak{E}$ and storage capacities $\bar{\mathbf{s}}$.

Theorem 4 (Marginal value of mobile storage). *The marginal value of mobile storage k with relocation pattern $\mathfrak{E}$ is*

$$MV_k^{\mathrm{ms}}(\mathfrak{E}, \bar{\mathbf{s}}) = \mathbf{1}^\top \boldsymbol{\mu}_k = \sum_{t=1}^{T} \left(\lambda_{i_k(t+1)}(t+1) - \lambda_{i_k(t)}(t) \right)_+, \tag{4.18}$$

where $\boldsymbol{\lambda}(T+1) := \mathbf{0}$.

Proof. From the Lagrangian of the economic dispatch problem in (4.15), we get that

$$\mathsf{MV}_k^{\mathrm{ms}}(\mathfrak{E}, \bar{\mathbf{s}}) = \mathbf{1}^\top \boldsymbol{\mu}_k.$$

Further, from the stationarity KKT condition with respect to $u_k(t)$, we get

$$L_t^\top (\boldsymbol{\mu}_k - \boldsymbol{\nu}_k) = -\gamma(t) + E_k(t)^\top H^\top \boldsymbol{\beta}(t),$$

where $L_t^\top$ is the tth column of $L^\top$, and $E_k(t)$ is the kth column of $E(t)$. At any time, only one of the pair of constraints in (4.15d) will be binding. Hence, either $\mu_k(t) = 0$ or $\nu_k(t) = 0$. Using the definition of $\boldsymbol{\lambda}(t)$ from (4.17), we get the expression in (4.18). □

We can see that the marginal value of mobile storage can be directly obtained by summing up the dual variables associated with the upper bound in storage capacity constraints (4.15d). Indeed, the dual variable $\boldsymbol{\mu}_k$ upper bounds the improvement in the objective function (generation costs) per unit relaxation of the constraint, i.e. per unit increase in the storage capacity. Finally, the marginal value of mobile storage k can be calculated from the sum of (non-negative) increases in LMPs along the relocation path of the mobile storage unit.

Comparison to stationary storage and wires

Theorem 4 not only provides a way to relate the marginal value of a mobile storage unit to its relocation path, but also offers insights for understanding the value of mobile storage through well-understood quantities in electricity markets. In particular, we can compare the marginal value of a mobile storage to the marginal value of wires and stationary energy storage. To this end, we denote the marginal value of the capacity associated with e-th line capacity constraint by $\mathsf{MV}_e^{\mathrm{w}}$, and denote the marginal value of *stationary energy storage* located at bus i by $\mathsf{MV}_i^{\mathrm{ss}}$. These quantities are related to the dual variables as follows [52, 68]:

$$\mathsf{MV}_e^{\mathrm{w}} = \sum_{t=1}^{T} \beta_e(t), \quad \mathsf{MV}_i^{\mathrm{ss}} = \sum_{t=1}^{T} \left(\lambda_i(t+1) - \lambda_i(t) \right)_+. \tag{4.19}$$

For convenience, we also define the marginal values for each time period as

$$\mathsf{MV}_e^{\mathrm{w}}(t) = \beta_e(t), \quad \mathsf{MV}_i^{\mathrm{ss}}(t) = \big(\lambda_i(t+1) - \lambda_i(t)\big)_+, \tag{4.20}$$

$$\mathsf{MV}_k^{\mathrm{ms}}(t) = \mu_k(t) = \big(\lambda_{i_k(t+1)}(t+1) - \lambda_{i_k(t)}(t)\big)_+, \tag{4.21}$$

for each $t \in [T]$, $e \in [2m]$, $i \in [n]$ and $k \in [K]$, where we have omitted the dependence on $\mathfrak{E}$ and $\bar{\mathbf{s}}$ as they are fixed in this subsection.

We provide three illustrative examples highlighting the role of mobile storage with different power network topologies and congestion patterns.

Example 1: mobile storage = storage + wire

Consider a two-bus network operated across two time periods. This is illustrated in Fig. 4.1 using a time-extended graph of the network. Here each node in time period t represents a bus in the power network, black solid lines represent electric wires, the blue solid line and the blue dashed line represent the "power flow links" created by a mobile storage unit moving from bus 1 to bus 2 and a stationary storage unit located at bus 2, respectively.
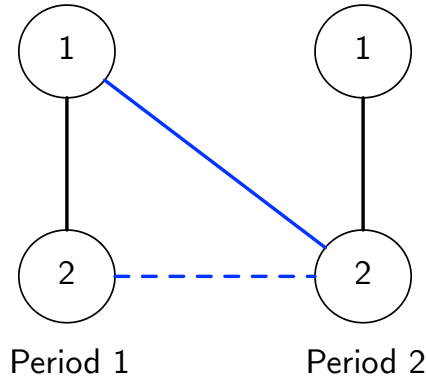
Figure 4.1: Time-extended graph for Example 1: mobile storage = storage + wire

Suppose for this network we have $\lambda_2(2) > \lambda_2(1) > \lambda_1(1)$. Then we can obtain (see e.g. [68] for the relation between LMPs and dual variables associated with transmission constraints for a radial network) that $\mathsf{MV}^{\mathrm{w}}(1) = \lambda_2(1) - \lambda_1(1)$, $\mathsf{MV}^{\mathrm{ss}}(1) = \lambda_2(2) - \lambda_2(1)$, and $\mathsf{MV}^{\mathrm{ms}}(1) = \lambda_2(2) - \lambda_1(1)$, where we have omitted the subscripts for the marginal values as they are clear from the context. As a result,

$$\mathsf{MV}^{\mathrm{ms}}(1) = \mathsf{MV}^{\mathrm{w}}(1) + \mathsf{MV}^{\mathrm{ss}}(1), \tag{4.22}$$

in this case. This is intuitive as both flow paths $(i = 1, t = 1) \to (i = 2, t = 2)$ and $(i = 1, t = 1) \to (i = 2, t = 1) \to (i = 2, t = 2)$ enable sending energy from $(i = 1, t = 1)$ to $(i = 2, t = 2)$.

In fact, we can show this holds for any radial network:

Lemma 5 (Radial network). *For a mobile storage unit moving from bus i to bus j in time period t, its marginal value for time period t is the same as the sum of marginal values of wires on the path from bus i to bus j on the power network for period t and the marginal value of a stationary storage unit located at bus j for period t.*

Proof. For a two node network with a single edge, we can obtain from (4.17) that $\lambda_2 - \lambda_1 = \beta_e$ at any time. A radial network has a single unique path between any two nodes, and the difference in LMPs of any two nodes can be decomposed similarly as a sum of β_e along the edges in the path. □

Example 2: mobile storage > storage + wire

Now we consider the operation of a three bus network across 2 periods as depicted in Fig. 4.2. The mobile storage unit moves from bus 3 to bus 1. Suppose that $\lambda_1(2) > \lambda_1(1) > \lambda_3(1)$, and the line $3 \to 1$ and another line in the loop (i.e., $3 \to 2$ or $2 \to 1$ in power network) are congested in period 1. In this case, we have $\beta_{3\to1}(1) < \lambda_1(1) - \lambda_1(3)$, where $\beta_{3\to1}(1)$ is the dual variable associated with the line capacity constraint for the flow from bus 3 to bus 1 in time period 1. Appendix A provides the data for a problem instance where this holds.
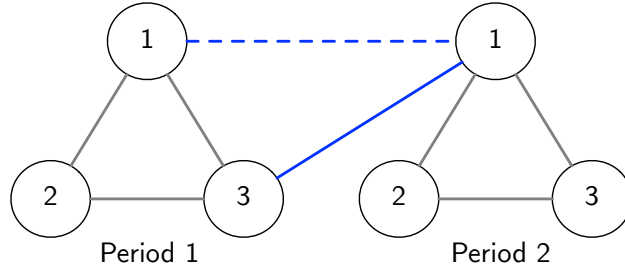
Figure 4.2: Time-extended graph for Example 2 and 3: mobile storage $\neq$ storage + wire

In this case, we have $\mathsf{MV}^{\mathrm{ms}}(1) = \lambda_1(2) - \lambda_3(1)$, $\mathsf{MV}^{\mathrm{ss}}(1) = \lambda_1(2) - \lambda_1(1)$, and $\mathsf{MV}^{\mathrm{w}}(1) = \beta_{3\to1}(1) < \lambda_1(1) - \lambda_1(3)$. Therefore, it is clear that

$$\mathsf{MV}^{\mathrm{ms}}(1) > \mathsf{MV}^{\mathrm{w}}(1) + \mathsf{MV}^{\mathrm{ss}}(1), \tag{4.23}$$

where $\mathsf{MV}^{\mathrm{w}}(1)$ denotes the marginal value of the line connecting bus 3 and bus 1 in time period 1. The gap stems from the fact that the flow paths $(i = 3, t = 1) \to (i = 1, t = 2)$ and $(i = 3, t = 1) \to (i = 1, t = 1) \to (i = 1, t = 2)$ are not equivalent. This is because for a power network with loops the flow on a line in the loop cannot be freely determined due to Kirchhoff's voltage law. When another line in the loop is also congested, increasing the capacity of link $3 \to 1$ in the power network by one unit does not mean that we can

increase the flow on the link by one unit due to the binding capacity constraint of the other
congested line. This effect is referred to as *loop externality* [78].

Example 3: mobile storage < storage + wire

Consider the same network and storage configuration in Example 2 (Fig. 4.2). Now we
require that $\lambda_1(2) > \lambda_1(1) > \lambda_2(1) > \lambda_3(1)$, and the line $3 \rightarrow 1$ is the only line congested in
period 1. In this case, increasing the capacity of line $3 \rightarrow 1$ can increase not only the flow
on the link $3 \rightarrow 1$, but also allow the flow along the links $3 \rightarrow 2 \rightarrow 1$ to be increased. As a
result, we can have $\beta_{3\rightarrow1} > \lambda_1(1) - \lambda_3(1)$. It follows that in this case, we have

$$\mathsf{MV}^{\mathrm{ms}}(1) < \mathsf{MV}^{\mathrm{w}}(1) + \mathsf{MV}^{\mathrm{ss}}(1), \tag{4.24}$$

where $\mathsf{MV}^{\mathrm{w}}(1)$ denotes the marginal value of the line connecting bus 3 and bus 1 in time
period 1. Appendix A provides a numerical example where this holds.

Optimal relocation of small mobile storage

Solving the optimal relocation problem for rapid mobile storage using brute-force methods
is computationally intractable because the computation time scales with the problem size as
$O(n^{KT})$. However, in practice, we can simplify the optimal relocation problem for a mobile
storage fleet because we expect that the storage capacities of such fleets will be relatively
small in the near future. This is motivated by the fact that the total storage capacity is
still a tiny fraction of the total power load. To get a sense, the estimated total capacity of
storage deployed in 2020 is about 0.296% of the estimated load in the same year [76]. We
formalize this concept in the following assumption:

Assumption 3 (Small storage)**.** *We assume that the storage capacities $\bar{\mathbf{s}}$ are small so that*
$\arg\min_{\mathfrak{J}}\{J^{\mathrm{ED}}(\mathfrak{E}(\mathfrak{J}), \bar{\mathbf{s}}) + J^{\mathrm{R}}(\mathfrak{J})\} = \arg\min_{\mathfrak{J}}\{\widehat{J}^{\mathrm{ED}}(\mathfrak{E}(\mathfrak{J}), \bar{\mathbf{s}}) + J^{\mathrm{R}}(\mathfrak{J})\},$ *where $\widehat{J}^{\mathrm{ED}}(\mathfrak{E}, \bar{\mathbf{s}})$ is the*
first order Taylor approximation of $J^{\mathrm{ED}}(\mathfrak{E}, \bar{\mathbf{s}})$:

$$\widehat{J}^{\mathrm{ED}}(\mathfrak{E}, \bar{\mathbf{s}}) = J^{\mathrm{ED}}(\mathfrak{E}, \mathbf{0}) - \sum_{k=1}^{K} MV_k^{\mathrm{ms}}(\mathfrak{E}, \mathbf{0})\bar{s}_k. \tag{4.25}$$

Note that Assumption 1 does not rule out the possibility that there is a significant amount
of *stationary storage* connected to the system. These stationary storage units can be modeled
using a separate set of variables and constraints in the MPED-S problem.

Under the small storage assumption, the optimal relocation problem for the fleet de-
couples. In other words, solving the optimal relocation problem for a fleet is equivalent to
solving K optimal relocation problems for individual units:

$$\max_{\mathfrak{J}_k} \quad \mathsf{MV}_k^{\mathrm{ms}}(\mathfrak{E}, \mathbf{0})\bar{s}_k - J_k^{\mathrm{R}}(\mathfrak{J}_k), \quad k \in [K], \tag{4.26}$$

where the initial locations of the mobile storage units $\{i_k(1)\}_{k\in[K]}$ are given, and the decision variable $\mathfrak{I}_k = \{i_k(t)\}_{t\in[T]}$ is optimized such that each $i_k(t) \in \mathcal{I}_k^{\mathrm{S}} \subseteq [n]$ and $\mathcal{I}_k^{\mathrm{S}}$ is the set of buses with which mobile storage unit k can be connected. The optimal trajectory for different storage units may be different because they have different storage capacities and initial locations.

The optimal relocation problem (4.26) can be converted into a shortest path problem and thus solved efficiently in polynomial time ($O(n^2T)$) with a range of algorithms including the Bellman-Ford algorithm and linear programming. Indeed, we can construct a time-extended graph $G(\mathcal{V}, \mathcal{E})$. The set of nodes $\mathcal{V}$ includes T copies of all the nodes in the power network $[n]$, and a dummy sink node. The set of edges $\mathcal{E}$ includes *directed* edges from every node i in t-th copy to every node j in the $(t+1)$-th copy, with edge weight

$$w_{ij}(t) = \kappa D_{ij} - \bar{s}_k(\lambda_j(t+1) - \lambda_i(t))_+, \quad t \in [T-1], \tag{4.27}$$

and *directed* edges from every node in the T-th copy to the dummy sink node, with edge weight 0. Here the LMPs are calculated using dual variables for (4.15) with $\bar{\mathbf{s}} = \mathbf{0}$. By solving the shortest path problem from source node $i_k(1)$ to the dummy sink node in the time extended graph, we can identify the optimal trajectory $\{i_k(t)\}_{t\in[T]}$ for storage k.

Fig. 4.3 provides an example of the graph on which we are solving the shortest path problem for determining the optimal relocation of mobile storage k.
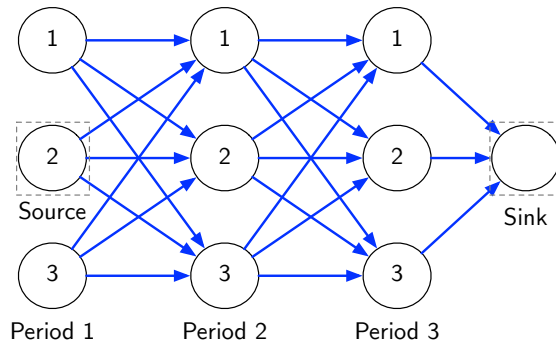
Figure 4.3: Example of the time extended graph on which the shortest path problem is defined. In this example, $n = 3$, $T = 3$, and the initial location for storage k is $i_k(1) = 2$.

4.5   General Mobile Storage

In practice, the time needed for relocating mobile storage units is not negligible, and both energy limits and power limits should be considered for mobile storage operation. In this case, we need to solve the general version of the MPED-S problem (4.13) and the optimal relocation problem (4.14).

Marginal value of mobile storage

As in Section 4.4, we quantify the marginal value of mobile storage for a fixed relocation pattern $\mathfrak{E}$. Denote the (optimal) dual variables associated with constraints (4.13b) and (4.13c) by $\gamma(t) \in \mathbb{R}$ and $\boldsymbol{\beta}(t) \in \mathbb{R}^{2m}$. $\boldsymbol{\nu}_k$ and $\boldsymbol{\mu}_k$ are associated with the lower bound and upper bound in (4.13d), and $\boldsymbol{\omega}_k$ and $\boldsymbol{\phi}_k$ are associated with the lower bound and upper bound in (4.13e), respectively. We define the LMPs $\boldsymbol{\lambda}(t)$ as in (4.17).

When the power limits depend on the energy limits (i.e., $\bar{u}_k$ is a function of $\bar{s}_k$), it is necessary for us to keep track of which constraints (energy or power) are binding at each time step. For simplicity, we introduce the following standard assumption for the MPED-S problem under consideration.

Assumption 4 (LICQ). *Given any relocation pattern $\mathfrak{E}$, the constraints binding at the solution of the MPED-S problem* (4.13) *are linearly independent.*

When optimizing the movement of mobile storage in a power network, we may be able to forecast the LMPs ahead of time. These prices will not be affected by the movement of mobile storage under the small storage assumption (Assumption 3). Meanwhile, we can identify the set of binding storage constraints for each storage k using a simpler optimization involving LMPs and the parameters for the storage unit.

Lemma 6. *Suppose that for each storage k, the price arbitrage problem given by*

$$\max_{\mathbf{u}_k} \ -\sum_{t=1}^{T} \lambda_{i_k(t)}(t)u_k(t) \tag{4.28}$$
$$s.t. \ \mathbf{0} \leq L\mathbf{u}_k \leq \bar{s}_k \mathbf{1}; \ -\overline{u}_k(\bar{s}_k)\boldsymbol{\Delta}_k^{\mathrm{S}} \leq \mathbf{u}_k \leq \overline{u}_k(\bar{s}_k)\boldsymbol{\Delta}_k^{\mathrm{S}}.$$

has a unique solution. Then the optimal operation $\mathbf{u}_k$ for storage k in a solution of the MPED-S problem (4.13) *is the same as the solution of the price arbitrage problem* (4.28).

Corollary 7. *Since the optimal operation of storage k in the MPED-S problem* (4.13) *coincides with the solution of the price arbitrage problem* (4.28), *they will lead to the same collection of binding constraints for storage k.*

Under Assumption 4, the binding constraints in (4.28) can then be used to partition $[T]$ into two disjoint sets:

$$\mathcal{T}_k^{\mathrm{e}}(\mathfrak{E}) = \{t_r^{\mathrm{e}}\}_{r \in [T_k^{\mathrm{e}}]}, \quad \mathcal{T}_k^{\mathrm{p}}(\mathfrak{E}) = \{t_s^{\mathrm{p}}\}_{s \in [T_k^{\mathrm{p}}]}$$

where $\mathcal{T}_k^{\mathrm{e}}(\mathfrak{E})$ and $\mathcal{T}_k^{\mathrm{p}}(\mathfrak{E})$ represent the times when energy capacity and power capacity constraints are binding, and T_k^{e} and T_k^{p} are the number of time periods within $\mathcal{T}_k^{\mathrm{e}}(\mathfrak{E}), \mathcal{T}_k^{\mathrm{p}}(\mathfrak{E})$, respectively. Henceforth we omit the dependence on $\mathfrak{E}$ and k to simplify the notation. Let $\sigma : \mathcal{T}^{\mathrm{p}} \mapsto \mathcal{T}^{\mathrm{e}}$ denote the mapping from each power capacity constrained time to the next energy capacity constrained time, i.e., $\sigma(t^{\mathrm{p}}) = \inf_\tau \{\tau \in \mathcal{T}^{\mathrm{e}} : \tau > t^{\mathrm{p}}\}$. Fig. 4.4 provides an
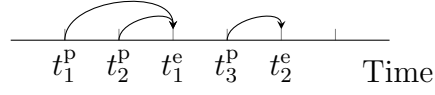
Figure 4.4: σ operator

illustration of σ. The σ mapping is defined for all $t^{\mathrm{p}} \in \mathcal{T}^{\mathrm{p}}$ when $T \in \mathcal{T}^{\mathrm{e}}$. This is the case when we have nonnegative LMPs since the optimal state of charge (SoC) in the terminal time period T will be empty.

Theorem 8 (Marginal value of mobile storage). *The marginal value of mobile storage k with relocation $\mathfrak{E}$ is*

$$MV_k^{\mathrm{ms}}(\mathfrak{E}, \bar{\mathbf{s}}) = \mathbf{1}^\top \boldsymbol{\mu}_k + \bar{u}_k'(\bar{s}_k)(\boldsymbol{\Delta}_k^{\mathrm{S}})^\top(\boldsymbol{\omega}_k + \boldsymbol{\phi}_k), \tag{4.29}$$

where for each $t_r^{\mathrm{e}} \in \mathcal{T}^{\mathrm{e}}$,

$$\mu_k(t_r^{\mathrm{e}}) = \left(\lambda_{i_k(t_{r+1}^{\mathrm{e}})}(t_{r+1}^{\mathrm{e}}) - \lambda_{i_k(t_r^{\mathrm{e}})}(t_r^{\mathrm{e}})\right)_+, \tag{4.30}$$

$$\omega_k(t_r^{\mathrm{e}}) + \phi_k(t_r^{\mathrm{e}}) = 0, \tag{4.31}$$

for each $t_s^{\mathrm{p}} \in \mathcal{T}^{\mathrm{p}}$,

$$\mu_k(t_s^{\mathrm{p}}) = 0, \tag{4.32}$$

$$\omega_k(t_s^{\mathrm{p}}) + \phi_k(t_s^{\mathrm{p}}) = \left|\lambda_{i_k(\sigma(t_s^{\mathrm{p}}))}(\sigma(t_s^{\mathrm{p}})) - \lambda_{i_k(t_s^{\mathrm{p}})}(t_s^{\mathrm{p}})\right|, \tag{4.33}$$

and we define $t_{T^{\mathrm{e}}+1}^{\mathrm{e}} := T + 1$ and $\boldsymbol{\lambda}(T + 1) := 0$.

Similar to the rapid storage case (4.18), the marginal value of mobile storage is nonnegative, i.e., increasing the storage capacity $\bar{s}_k$ will weakly decrease the optimal cost for the dispatch problem. The marginal value is obtained by summing the dual variable associated with the upper bound in the storage capacity constraint (4.13d), and the dual variables associated with the power constraints (4.13e) weighted by the time available to charge $\boldsymbol{\Delta}_k^{\mathrm{S}}$ and the dependence of power capacity on storage capacity $\bar{u}_k'(\bar{s}_k)$. The dual variable $\boldsymbol{\omega}_k$ characterizes the value of increasing the discharging power capacity, and the dual variable $\boldsymbol{\phi}_k$ characterizes the value of increasing the charging power capacity. Comparing the marginal value expression in (4.29) to that of rapid mobile storage (4.18), we observe that the new expression uses LMP increases across consecutive energy capacity-constrained time periods as well as LMP differences across power constrained and energy constrained time periods. The price arbitrage across $t_r^{\mathrm{e}} \in \mathcal{T}^{\mathrm{e}}$ is not a complete measure of the marginal value, as charge/discharge also occurs at intermediate time steps ($t_r^{\mathrm{p}} \in \mathcal{T}^{\mathrm{p}}$).

Corollary 9. *In the case that power constraints have no dependence on $\bar{s}_k$, i.e. $\bar{u}'_k(\bar{s}_k) = 0$, the marginal value is*

$$MV_k^{\mathrm{ms}}(\mathfrak{E}, \bar{\mathbf{s}}) = \mathbf{1}^\top \boldsymbol{\mu}_k \tag{4.34}$$

with $\mu_k(t)$ defined as in Theorem 8.

This is similar to the case in Theorem 4, as any increase in storage capacity will not alleviate power constraints. However, the expression for $\boldsymbol{\mu}_k$ here is different from that in Theorem 4 due to the storage power constraints. Stationary storage can also be viewed as a special case of mobile storage where the battery is located at a single bus at all times.

Corollary 10 (Marginal value of stationary storage). *The marginal value of stationary storage k located at bus i, i.e., $i_k(t) = i$ for all t, is*

$$MV_k^{\mathrm{ss}}(\bar{\mathbf{s}}) = \mathbf{1}^\top \boldsymbol{\mu}_k + \bar{u}'_k(\bar{s}_k)\Delta\mathbf{1}^\top(\boldsymbol{\omega}_k + \boldsymbol{\phi}_k) \tag{4.35}$$

where for each $t_r^{\mathrm{e}} \in \mathcal{T}^{\mathrm{e}}$,

$$\mu_k(t_r^{\mathrm{e}}) = \left(\lambda_i(t_{r+1}^{\mathrm{e}}) - \lambda_i(t_r^{\mathrm{e}})\right)_+, \ \ \omega_k(t_r^{\mathrm{e}}) + \phi_k(t_r^{\mathrm{e}}) = 0, \tag{4.36}$$

for each $t_s^{\mathrm{p}} \in \mathcal{T}^{\mathrm{p}}$,

$$\mu_k(t_s^{\mathrm{p}}) = 0, \ \ \omega_k(t_s^{\mathrm{p}}) + \phi_k(t_s^{\mathrm{p}}) = \left|\lambda_i(\sigma(t_s^{\mathrm{p}})) - \lambda_i(t_s^{\mathrm{p}})\right|, \tag{4.37}$$

and we define $t_{T^{\mathrm{e}}+1}^{\mathrm{e}} := T + 1$ and $\boldsymbol{\lambda}(T + 1) := 0$.

This result generalizes existing results on the locational marginal value of stationary storage [15, 52] by incorporating storage power constraints.

Comparison to stationary storage and wires

Since the rapid mobile storage model discussed in Section 4.4 is a special case of the general mobile storage model, the examples discussed in Section 4.4 remain valid for the general mobile storage model. However, Lemma 5 does not generalize to the general mobile storage case as the storage power constraints and time taken to travel can impact the marginal value of mobile storage. Intuitively, with a nonzero travel time, the time available for mobile storage to charge/discharge is strictly less than that for stationary storage. As a result, in scenarios where the storage power constraints are binding and the reduced charging/discharging time matters, the marginal value of mobile storage can be strictly less than the sum of marginal values of the corresponding stationary storage unit and wires even if the network does not have loops.

Optimal relocation of small mobile storage

Under Assumption 3, the optimal relocation problem for the mobile storage fleet decouples as in the case of rapid mobile storage, and we can use LMPs for $\bar{\mathbf{s}} = \mathbf{0}$ in the marginal value calculation. However, the marginal value of general mobile storage depends on the order of binding constraints. When the constraint binding pattern $(\mathcal{T}^{\mathrm{e}}, \mathcal{T}^{\mathrm{p}})$ is given, we can identify the optimal relocation associated with $(\mathcal{T}^{\mathrm{e}}, \mathcal{T}^{\mathrm{p}})$ by solving a shortest path problem referred to as $\mathsf{SP\text{-}E}(\mathcal{T}^{\mathrm{e}}, \mathcal{T}^{\mathrm{p}})$ over all energy constrained time periods. We construct a time-extended graph $G(\mathcal{V}, \mathcal{E})$ where the set of nodes $\mathcal{V}$ includes T^{e} copies of all the nodes in the power network $[n]$, and a dummy sink node. The set of edges $\mathcal{E}$ includes *directed* edges from every node i in the copy corresponding to t_r^{e} to every node j in the copy corresponding to t_{r+1}^{e}, with an edge weight

$$w_{ij}(t_r^{\mathrm{e}}) = \begin{cases} -\bar{s}_k \left(\lambda_j(t_{r+1}^{\mathrm{e}}) - \lambda_i(t_r^{\mathrm{e}})\right)_+ + \kappa D_{ij}, & \text{if } t_{r+1}^{\mathrm{e}} = t_r^{\mathrm{e}} + 1, \\ -\bar{s}_k \left(\lambda_j(t_{r+1}^{\mathrm{e}}) - \lambda_i(t_r^{\mathrm{e}})\right)_+ + J_{ij}^{\mathsf{SP\text{-}P}}(t_r^{\mathrm{e}}), & \text{otherwise,} \end{cases}$$

and *directed* edges from every node in the T^{e}-th copy to the dummy sink node, with edge weight 0. If $t_{r+1}^{\mathrm{e}} \neq t_r^{\mathrm{e}} + 1$, there are power constrained time periods between t_r^{e} and t_{r+1}^{e}, and the edge weight will depend on the cost of traveling along an optimal path for all intermediate power constrained time periods $t_s^{\mathrm{p}} \in \{t_r^{\mathrm{e}} + 1, \ldots, t_{r+1}^{\mathrm{e}} - 1\}$ denoted by $J_{ij}^{\mathsf{SP\text{-}P}}(t_r^{\mathrm{e}})$.

Calculating $J_{ij}^{\mathsf{SP\text{-}P}}(t_r^{\mathrm{e}})$

The optimal path for the power constrained time periods between t_r^{e} and t_{r+1}^{e} can be found by formulating a shortest path problem referred to as $\mathsf{SP\text{-}P}_{ij}(t_r^{\mathrm{e}})$. For each $i, j \in [n]$, $t_r^{\mathrm{e}} \in \mathcal{T}^{\mathrm{e}}$, we construct a shortest path problem on a time-extended graph $\widetilde{G}(\widetilde{\mathcal{V}}, \widetilde{\mathcal{E}})$ where we omit the dependence on i, j and t_r^{e} to simplify notation. The set of nodes $\widetilde{\mathcal{V}}$ include a source node (representing node i in time t_r^{e}), a sink node (representing node j in time t_{r+1}^{e}), and a copy of all the nodes in the power network $[n]$ for each $t_s^{\mathrm{p}} \in \{t_r^{\mathrm{e}} + 1, \ldots, t_{r+1}^{\mathrm{e}} - 1\}$. The set of edges $\widetilde{\mathcal{E}}$ includes *(a)* a directed edge from the source node i to every node $\widetilde{j} \in [n]$ in the first copy (which corresponds to $t_s^{\mathrm{p}} = t_r^{\mathrm{e}} + 1$), with weight $w_{i\widetilde{j}} = \kappa D_{i\widetilde{j}}$, *(b)* if $|\{t_r^{\mathrm{e}} + 1, \ldots, t_{r+1}^{\mathrm{e}} - 1\}| > 1$, a directed edge from every node $\widetilde{i} \in [n]$ in the copy corresponding to each $t_s^{\mathrm{p}} \in \{t_r^{\mathrm{e}} + 1, \ldots, t_{r+1}^{\mathrm{e}} - 2\}$ to every node $\widetilde{j} \in [n]$ in the copy corresponding to t_{s+1}^{p}, with weight

$$w_{\widetilde{i}\widetilde{j}}(t_s^{\mathrm{p}}) = \kappa D_{\widetilde{i}\widetilde{j}} - \bar{s}_k \bar{u}_k'(\bar{s}_k) \Delta_{\widetilde{i}\widetilde{j}}^{\mathrm{S}} |\lambda_j(t_{r+1}^{\mathrm{e}}) - \lambda_{\widetilde{i}}(t_s^{\mathrm{p}})|, \tag{4.38}$$

and *(c)* a directed edge from each node $\widetilde{i} \in [n]$ in the last copy (corresponding to $t_s^{\mathrm{p}} = t_{r+1}^{\mathrm{e}} - 1$) to the sink node j, with weight defined in (4.38). We overload the notation Δ_{ij}^{S} to represent the time available for battery operation if it travels from node i to j in that time period. $J_{ij}^{\mathsf{SP\text{-}P}}(t_r^{\mathrm{e}})$ is the cost of traveling along the shortest path in this extended graph.

Solving SP-E$(\mathcal{T}^{\mathrm{e}}, \mathcal{T}^{\mathrm{p}})$

In order to solve SP-E$(\mathcal{T}^{\mathrm{e}}, \mathcal{T}^{\mathrm{p}})$, we first solve $J_{ij}^{\mathsf{SP-P}}(t_r^{\mathrm{e}})$ for each $i, j \in [n]$, $t_r^{\mathrm{e}} \in \mathcal{T}^{\mathrm{e}}$ and determine the edge weights of the time-extended graph $G(\mathcal{V}, \mathcal{E})$. We then solve the shortest path problem SP-E$(\mathcal{T}^{\mathrm{e}}, \mathcal{T}^{\mathrm{p}})$ using the edge weights determined by (4.38).

Identifying optimal relocation $\mathfrak{E}$

First, from the solution of SP-E$(\mathcal{T}^{\mathrm{e}}, \mathcal{T}^{\mathrm{p}})$, we obtain the sequence of nodes where mobile storage is located at each time in $\mathcal{T}^{\mathrm{e}}$. We use this to obtain the nodes (i, j) at which the mobile storage is located for each pair of non-consecutive energy constrained time periods ($t_r^{\mathrm{e}}, t_{r+1}^{\mathrm{e}}$ such that $t_{r+1}^{\mathrm{e}} \neq t_r^{\mathrm{e}}+1$), and the solution to SP-P$_{ij}(t_r^{\mathrm{e}})$ provides the relocation pattern for the storage during the power constrained time periods between t_r^{e} and t_{r+1}^{e}. Piecing together the locations of the storage in energy constrained times and power constrained times results in the optimal relocation pattern $\mathfrak{E}(\mathcal{T}^{\mathrm{e}}, \mathcal{T}^{\mathrm{p}})$ given $(\mathcal{T}^{\mathrm{e}}, \mathcal{T}^{\mathrm{p}})$.

In practice, we do not know the constraint binding patterns $(\mathcal{T}^{\mathrm{e}}, \mathcal{T}^{\mathrm{p}})$ without knowing the optimal relocation, as moving along different relocation paths will change the optimal storage operation. One approach is to enumerate all possible constraint binding patterns $(\mathcal{T}^{\mathrm{e}}, \mathcal{T}^{\mathrm{p}})$ and solve SP-E$(\mathcal{T}^{\mathrm{e}}, \mathcal{T}^{\mathrm{p}})$ for each constraint binding pattern. This will result in an optimal relocation pattern $\mathfrak{E}(\mathcal{T}^{\mathrm{e}}, \mathcal{T}^{\mathrm{p}})$, whose consistency with the assumed constraint binding pattern needs to be checked by computing the actual constraint binding pattern under this relocation pattern and comparing with the assumed $(\mathcal{T}^{\mathrm{e}}, \mathcal{T}^{\mathrm{p}})$. If they are the same, this relocation pattern is an admissible solution. After going through all $O(2^T)$ possibilities, we can find the optimal relocation pattern by finding the admissible solution with the lowest cost. Since for small storage either energy or power constraint is binding at every time step, this amounts to solving the shortest path problem described above $O(2^T)$ times. As our model focuses on daily operation with every time period long enough for mobile storage to relocate, T is usually relatively small (e.g., $T = 12$ for 2 hour time periods). Algorithm 1 summarizes the steps to generate an optimal relocation path for general mobile storage.

Algorithm 1: Optimal relocation for general mobile storage

> **for** each possible $(\mathcal{T}^{\mathrm{e}}, \mathcal{T}^{\mathrm{p}})$ **do**
>> **for** $t_r^{\mathrm{e}} \in \mathcal{T}^{\mathrm{e}}$, $i, j \in [n]$ **do**
>>> Compute $J_{ij}^{\mathsf{SP-P}}(t_r^{\mathrm{e}})$ by solving SP-P$_{ij}(t_r^{\mathrm{e}})$;
>>> Compute weights in SP-E$(\mathcal{T}^{\mathrm{e}}, \mathcal{T}^{\mathrm{p}})$ with (4.38);
>>
>> **end**
>> Compute $\mathfrak{E}(\mathcal{T}^{\mathrm{e}}, \mathcal{T}^{\mathrm{p}})$ by solving SP-E$(\mathcal{T}^{\mathrm{e}}, \mathcal{T}^{\mathrm{p}})$; **if** $\mathfrak{E}(\mathcal{T}^{\mathrm{e}}, \mathcal{T}^{\mathrm{p}})$ is admissible **then**
>>> Store $\mathfrak{E}(\mathcal{T}^{\mathrm{e}}, \mathcal{T}^{\mathrm{p}})$
>>
>> **end**
>
> **end**
> **return** $\mathfrak{E}^{\star}$ with the minimum cost among all the stored $\mathfrak{E}(\mathcal{T}^{\mathrm{e}}, \mathcal{T}^{\mathrm{p}})$
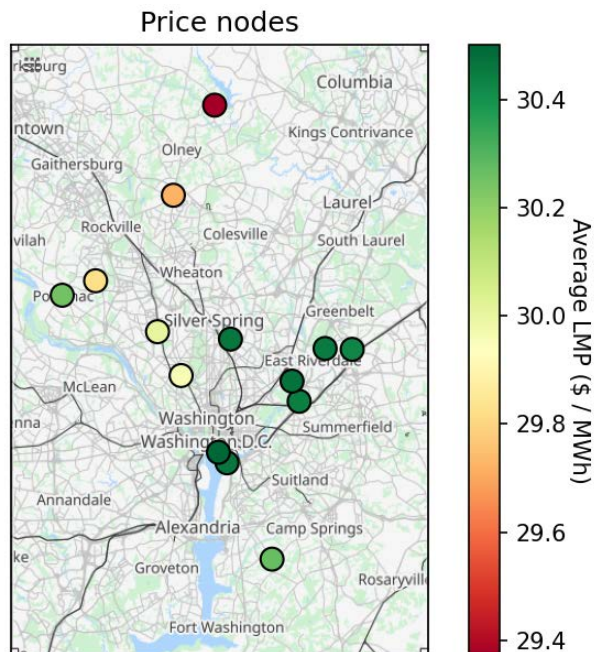
Figure 4.5: Average LMP of the selected nodes in May 2021

4.6 Illustrations

We consider a subset of price nodes in Maryland within PJM territory, shown in Fig. 4.5, which are intended to be representative of LMP zones. The LMPs for nodes are obtained from the PJM DataMiner [1] for the month of May 2021. LMP node names are used to identify locations on a map, and we model the entirety of an LMP zone as a single interconnection point. The travel time between nodes is modeled using the straight line distance and a speed of 50 miles per hour, and travel cost is taken to be 4 cents/mile from the US DoE estimate [2] for passenger EVs, and 16 cents/mile for an electric truck. We consider a time horizon of 24 hours, with a time step of 1 hour. We model two mobile storage units: a Tesla Model 3 with a 50 kWh battery and a maximum power throughput of 11 kW (level 2 AC charging power), and a Tesla Semi with a 500kWh battery and maximum power throughput of 100 kW. The selected nodes exhibit spatial price differences, illustrated by variation in the average LMP in Fig. 4.5. They also exhibit temporal price variation, i.e., the LMP at a single node varies over the course of the day. In Fig. 4.6 we show the spread of prices over two days in the month of May. At each hour, the LMPs across all nodes are used to make a boxplot to illustrate how the LMPs are spread out. A longer boxplot height indicates that there is high spatial variance in LMP at that hour, which is the case on 4 May 2021 at 4 pm. A shorter boxplot indicates that the LMP across nodes is largely similar, which is the case on 8 May 2021. The spatial variation in prices can change significantly from one day
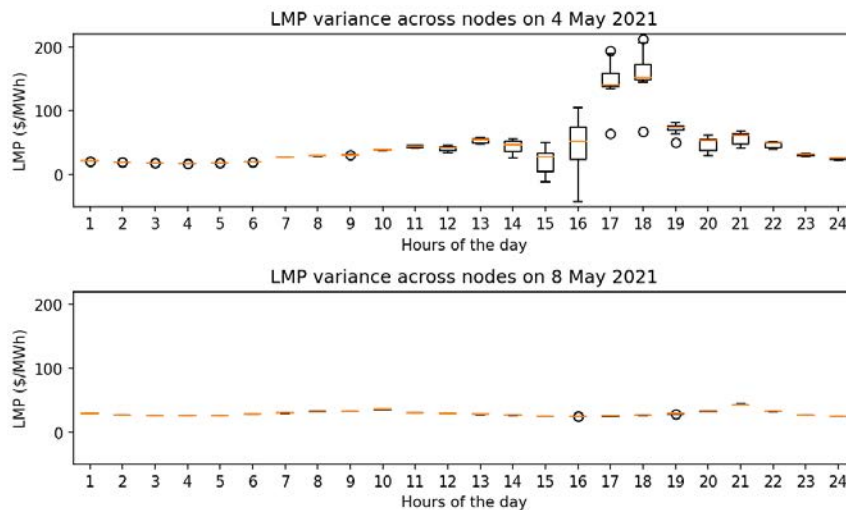
Figure 4.6: Range of LMPs across nodes on two dates

to the next, depending on the grid constraints in force on either day. A mobile storage unit, e.g., an EV can capitalize on these differences as discussed previously. We use Algorithm 1 to optimize the movement and operation of an EV over the price nodes in Fig. 4.5 on 4 May 2021, a day of high spatial LMP variation.

We start by modeling a Tesla Model 3, which is initially charged to 40%, and starts the day at the LANHAM node. Fig. 4.7 illustrates the movement of the EV over the course of 4 May 2021. The arrows indicate the optimized movement of the EV over time, and the circles indicate the change in state-of-charge (SoC) at each node with a radius proportional to the magnitude of the net energy charge or discharge at that node. Red circles indicate discharging and green circles indicate charging. The EV starts at 40% charge from a node in the bottom-right corner of the figure, and continues to move across nodes over the course of the day, ending the day at a node in the top-left corner with 0% charge. The value gained from arbitrage is $7.12, and the travel costs work out to $0.78, making the net profit $6.34 for 4 May 2021. Most of the value is captured by discharging at BELLSMIL node at 5 pm and 6 pm. This indicates that there are a few high-value hours when we can prioritize dispatch.

We now consider a Tesla Semi that moves across the power network to maximize its price arbitrage value. A Tesla Semi has a significantly higher battery capacity, and can consequently generate more value. The optimal movement for a truck starting at 40% capacity is illustrated in Fig. 4.8, and the value gained from arbitrage is 69.8$. The travel costs work out to 3.23$ over the course of the day. The net profit from operating this EV on 4 May 2021 is 66.56$, and most of the value is generated by discharging during 5-7 pm, i.e., there are a few high-value hours when we can prioritize dispatch.

While putting these numerical results in perspective, we need to consider that all days
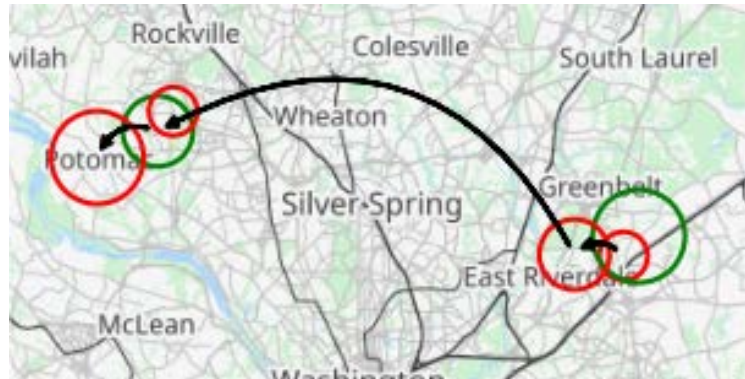
Figure 4.7: Movement of an EV over the course of 4 May 2021 with charging/discharging operations
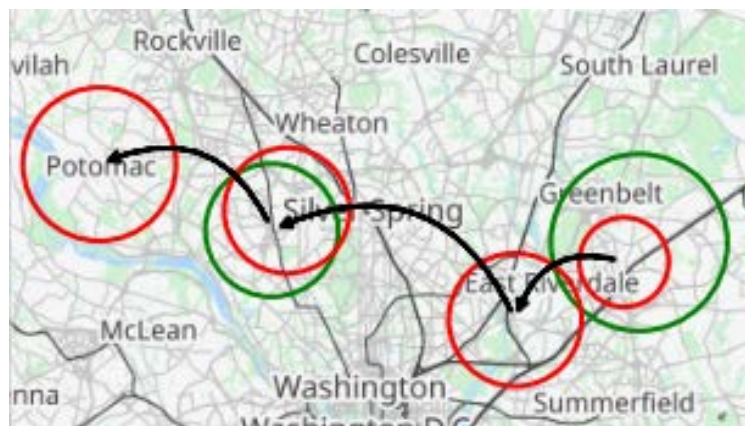
Figure 4.8: Movement of a Tesla Semi truck over the course of 4 May 2021 with charging/discharging operations.

will not look the same for an EV conducting price arbitrage. We chose a date which had high inter-node price variability which led to higher revenue from spatial price arbitrage. We also modeled an EV that could be controlled completely, i.e., could be moved around and charged/discharged at will. In reality, operators will likely not be able to control EV movement without giving monetary incentives, and may have to work with existing EV movement patterns (e.g., people driving their EVs to work and back). They will also not be able to charge/discharge the full battery capacity, and will have to reserve a portion of the battery to move the EV itself. Charging and discharging the battery will accelerate its degradation, and there will be associated costs that the operator will have to incur.

At the same time, there are a number of ways that mobile storage could provide value to

the grid while also garnering enough compensation to incentivize the driver. As discussed,
most of the day's value is captured in a few hours, and mobile storage operators could be
strategically incentivized to capture arbitrage value in those few hours. There are also a few
high value nodes within the network which have a larger difference in LMPs across the day
as compared to other nodes. If mobile storage is initially located near those nodes, it will be
able to generate more value. EV batteries can also potentially provide high value services,
such as peak shaving for commercial buildings [54] or ancillary services. The optimal service
and market model through which mobile storage participates in the power network will de-
pend on the availability of bidirectional charging infrastructure and the market participation
programs in place.

These simulations are an important step in modeling the *value* of mobile storage. How-
ever, they represent only one side of the picture, and in order to fully evaluate this new
resource we also need to model the *cost* of mobile storage. For example, the cost of travel is
not just the cost of the electrical energy needed to move the vehicle, but also the amortized
cost of the full vehicle, which is why the IRS allows 65.5 cents/mile as a business expense
[70]. The cost of travel will also include wages for the driver, which will vary by region. The
effective cost of the mobile storage resource will also vary by the technology being consid-
ered - Li-ion batteries in electric vehicles vs. moving electricity consumption in data centers
across locations. Developing cost models for mobile storage is a critical task that we leave
for future work.

4.7   Discussion

This chapter formalizes the marginal value of mobile storage from a system operator's per-
spective and develops analytical expressions for two storage models: a simplified rapid storage
model and a general storage model that incorporates travel time and power constraints. We
developed illustrative examples to demonstrate the value of mobile storage as compared to
stationary storage and wires. Efficient algorithms to compute the optimal relocation path
are then proposed based on analytical expressions for the marginal value of mobile storage.

In practice, the mobile storage resource will likely be owned and operated independently,
e.g., by EV owners. It is important to consider their response to the incentives provided
(i.e., to being compensated at wholesale market prices), and to characterize their equilibrium
operation. We discuss the EV operator perspective in Chapter 5.

Chapter 5

Electric Vehicle Battery Sharing Game: Mobile Storage Service Provision in Power Networks

In the previous chapter, we developed analytical expressions for the marginal value of *rapid* and *general* mobile storage from a system operator's perspective, and devised algorithms to optimally relocate mobile storage. In this chapter, we examine the mobile storage sharing game, where an EV operator can choose to use their EV battery to participate as mobile storage in the power system. The work in this chapter was presented in [7].

5.1 Introduction

Transportation causes 29% of global CO_2 emissions[69], and electrifying transport is an important step in any climate change mitigation plan. Some transportation sectors such as long-haul trucking, shipping and aviation are difficult to electrify due to the requirement for larger batteries with higher energy density, critical battery safety concerns, and the need for high-power charging. In contrast, the passenger vehicle sector has seen rapid electrification in the last 10 years with 9% of global car sales being electric vehicles (EVs) in 2021 [34]. EVs are equipped with batteries which can also be used to function as *mobile energy storage* in the power network with the help of bidirectional chargers, by charging at the origin of a route and discharging at the destination, thus moving energy across both space and time. Such mobile energy storage in the form of EV batteries can help avoid time consuming and expensive transmission line upgrades, and also serve as energy storage on the grid [8].

In contrast with utility scale battery projects that can be dispatched by the power system operator, EVs are owned and operated by individual drivers. EV drivers will make independent decisions on whether to provide mobile storage service based on their individual costs and the value they create, which will be determined by the operation of the power network and on how much mobile storage capacity is available in the grid. They may have different

motivations: some EV drivers may function as *commuters*, i.e. travel along fixed routes, and some EV drivers could be available *on-demand* to travel along specific routes to provide mobile storage service. A fundamental question arises: *will the market equilibrium lead to a socially desirable level of mobile storage capacity?*

This chapter examines this question in three contexts: (a) when there are a number of commuter EVs traveling along fixed routes in the power network which can provide mobile storage service along those routes, (b) when there are a number of on-demand EV drivers which can provide mobile storage service along any route, and (c) when there is a mix of commuter EVs and on-demand EVs in the network. The mobile storage service is provided in a wholesale market, and a transmission-constrained two-period economic dispatch problem is solved to determine the operation of the grid and mobile storage. This also determines the locational marginal prices, which are used to compensate mobile storage service providers. We make the following research contributions: (a) we develop novel game theoretic models in the context of sharing EV batteries as mobile energy storage, which incorporate both operation constraints of the power network and incentives for the EV drivers; (b) we explicitly characterize the Nash Equilibrium (NE) of the proposed EV battery sharing games together with several benchmarks, and establish that NE support social welfare for all our settings.

Our work is built upon two lines of recent research. The first is game theoretic analysis of storage sharing. Among many papers in this area, the closest related works include: [37], which studies the storage sharing and investment decisions of a collection of firms without considering network constraints, and [53], which analyzes the distributed storage investment game in power networks. [16] formulates a cooperative game for sharing energy storage within a residential microgrid, [80] formulates a Stackelberg game to model the sharing of cloud energy storage, and [81] studies a two-stage problem of a central storage owner sharing virtualized sections of the storage capacity with multiple users. The second line of research is the growing literature on utilizing EVs as mobile energy storage to provide grid services. See [54] for the cost-benefit analysis of the business model of sharing EVs to help commercial and industrial electricity users to reduce demand charges, [8] for the joint optimization of power network and a fleet of mobile storage units, and [31] for a simulation study of the value of truck based mobile storage units in the California power grid.

5.2   Model

Consider a setting where EVs can provide mobile storage service in the power network. The power network model is the same as in Chapter 4.

EVs as mobile storage

An EV can function as a mobile storage unit by charging at one bus, moving to another bus and then discharging. In a power network with n buses, there are a total of n^2 routes that the EV can take, which include the "route" where the EV stays at the same location.

Consider an aggregate mobile storage capacity $S_{i,j}$ moving from bus i at $t = 1$ to bus j at $t = 2$, which comprises of all of the EVs moving along that route and providing mobile energy storage service. The charging/discharging operation vector along route $i \to j$ is given by $\mathbf{u}_{i,j} \in \mathbb{R}^2$, where positive values of $u_{i,j}^{(t)}$ indicate charging and negative values indicate discharging. We assume that each EV starts with an empty battery at $t = 1$, which means that the aggregate state-of-charge at the end of time period $t \in \mathcal{T}$ is given by $\sum_{\tau=1}^{t} u_{i,j}^{(\tau)}$, which is the sum of charging/discharging operations until that time. The state of charge must satisfy the energy capacity constraint of the aggregate storage capacity, i.e.

$$0 \leq \sum_{\tau=1}^{t} u_{i,j}^{(\tau)} \leq S_{i,j}, \quad t \in \mathcal{T}. \tag{5.1}$$

Alternatively, we can write the constraint as

$$\mathbf{0} \leq L\mathbf{u}_{i,j} \leq S_{i,j}\mathbf{1}, \tag{5.2}$$

where $L \in \mathbb{R}^{2 \times 2}$ is a lower triangular matrix with $L_{t,t'} = 1$ for all $t \geq t'$. The vector of mobile storage capacities on all routes in the network is given by $\mathbf{S} \in \mathbb{R}^{n^2}$, and has an element $S_{i,j}$ corresponding to each route in the network. The power injection at each bus is the sum of generation and aggregate storage operation minus the demand, i.e.

$$p_i^{(1)} = g_i^{(1)} - d_i^{(1)} - \sum_{j=1}^{n} u_{i,j}^{(1)}, p_i^{(2)} = g_i^{(2)} - d_i^{(2)} - \sum_{i=1}^{n} u_{i,j}^{(2)}. \tag{5.3}$$

In the first time period, the storage operation $u_{i,j}^{(1)}$ occurs at the route origin, i.e. bus i, while in the second time period the operation $u_{i,j}^{(2)}$ occurs at the route destination, i.e. bus j. This explains the asymmetrical definition of power injection.

The LMP at a load bus determines the payment made by loads, and the LMP at a generation bus is the price at which generators are compensated. Mobile storage must pay for the electricity it consumes through charging at the LMP, and is also compensated at the LMP for discharging. The LMP depends on the mobile storage capacity available, i.e. it is a function of $\mathbf{S}$ which is the vector of mobile storage capacities along each route in the network. We denote the LMPs by $\boldsymbol{\lambda}^{(t)}(\mathbf{S})$ to emphasize this dependence, but omit it in places for notational convenience.

Commuter EV drivers with fixed routes

Consider an EV driven by a commuter who regularly moves along one of the n^2 possible routes in the network. *The route choice for individual drivers in this case is exogenous.* The EV driver has the choice to use the EV battery as mobile storage along that route by charging at the origin and discharging at the destination. Each EV constitutes an infinitesimally small amount of storage traveling along a route, and we model the individual EVs as a continuum

indexed by $k \in \mathcal{K}_{i,j} = [0,1]$. In providing this service, the EV driver buys electric energy at the locational marginal price (LMP) at the origin in the off-peak period, and sells that energy at the destination LMP in the peak period, thus capitalizing on the spatial-temporal LMP difference along the route. The value gained by an EV driver moving along the route $i \to j$ by providing mobile storage service per unit of storage capacity is

$$\lambda_j^{(2)}(\mathbf{S}) - \lambda_i^{(1)}(\mathbf{S}), \tag{5.4}$$

where $\lambda_j^{(2)}(\mathbf{S})$ is the LMP at the destination node at time 2 and $\lambda_i^{(1)}(\mathbf{S})$ is the LMP at the origin node at time 1.

In order to provide this service, the driver has to cycle through the EV battery capacity, thus causing some battery degradation. We model this battery degradation as a cost κ of providing the service, which is incurred by the EV driver and is uniform across EV drivers. Further, the driver may have to park at a specialized charging station or wait longer than originally planned, and undergo some amount of inconvenience. For a driver $k \in \mathcal{K}_{i,j}$ traveling along the route $i \to j$, we model this inconvenience as a cost θ_k. The collection of drivers $\mathcal{K}_{i,j}$ have a range of inconvenience costs, which can be modeled as a continuous range of θ_k values. Since the commuter EV moves along the route in any case, the travel cost does not factor into the decision to provide mobile storage service.

Each EV driver makes a decision on whether to provide the mobile storage service by comparing the value, i.e. the LMP difference in (5.4), with the sum of battery degradation and inconvenience costs. We model this decision with a binary variable s_k, which is 1 when the driver k provides mobile storage service, and 0 when she does not. The payoff for driver $k \in \mathcal{K}_{i,j}$ is

$$\pi_k(s_k, \mathbf{S}) = \left[\lambda_j^{(2)}(\mathbf{S}) - \lambda_i^{(1)}(\mathbf{S}) - \theta_k - \kappa \right] s_k \tag{5.5}$$

per unit of storage capacity. The only difference in payoffs for drivers on the same route $i \to j$ is the inconvenience cost, which is different for each driver. Thus we can denote the decision to provide mobile storage service for each driver as a route-specific function $\sigma_{i,j} : \mathbb{R} \to \{0,1\}$ of the inconvenience cost, i.e.,

$$s_k = \sigma_{i,j}(\theta_k), \quad k \in \mathcal{K}_{i,j}, \quad i,j \in \mathcal{N}. \tag{5.6}$$

The proportion of EVs that provide service is given by

$$S_{i,j} = \mathbb{E}\sigma_{i,j}(\theta_k) = \int_{k \in \mathcal{K}_{i,j}} \sigma_{i,j}(\theta_k) \, \mathrm{d} \, F_{i,j}(\theta_k) \quad \leq 1, \tag{5.7}$$

where $F_{i,j}(\cdot)$ is the cumulative distribution of inconvenience costs of the drivers on route $i \to j$.

We can re-scale the actual storage capacity (in kWh), and generation across the network such that the total mobile storage capacity available on each route ($\int_{k \in \mathcal{K}_{i,j}} dF(\theta_k)$) is normalized to 1. For routes with a lower number of EVs, we can add 'dummy' EVs with infinite inconvenience cost to obtain the same nominal number of EVs along each route. Non-linear coefficients of generation and load will need to be scaled appropriately.

On-demand EV drivers with flexible routes

Consider an EV which is signed up with a transportation network company (TNC) and can be requisitioned to provide mobile storage service along any of the n^2 possible routes in the network. Each EV driver has the choice to use the EV battery as mobile energy storage by charging and then discharging along any of the possible routes, or to not provide the service at all. In a large fleet of EVs, each EV is an infinitesimally small amount of storage and we model the individual EVs as a continuum indexed by $\ell \in \mathcal{L} = [0, 1]$.

The value for the EV driver moving along $i \to j$ is the same as that for an EV driver with a fixed route, given in (5.4), and is dependent on the amount of mobile storage capacity in the network. However, the EV driver has to travel along $i \to j$ to provide this service, which she would not have otherwise since the sole purpose of the trip is providing mobile storage service. By providing this service, the EV battery will undergo some amount of degradation. The travel and battery degradation costs are modeled as a non-negative route-specific cost $\kappa_{i,j}$, and are the same for each EV traveling on this route. Further, the EV driver has to spend time and effort in traveling and providing mobile storage service and will need to be compensated for the inconvenience caused. This inconvenience can be modeled as a non-negative cost θ_ℓ which is specific to driver ℓ but is route-independent.

Each EV driver compares the value and cost of providing mobile storage service to make their decision. An EV driver signed up with a TNC has n^2+1 possible choices: providing the service at any of the n^2 routes, or not providing the service at all. We denote the decision to provide service on route $i \to j$ with $s_{\ell; i,j} \in \{0, 1\}$, and note that $\sum_{i,j} s_{\ell; i,j} \leq 1$. The payoff for the on demand EV driver $\ell \in \mathcal{L}$ is

$$\pi_\ell(\mathbf{s}_\ell, \mathbf{S}) = \sum_{i,j} \left(\lambda_j^{(2)}(\mathbf{S}) - \lambda_i^{(1)}(\mathbf{S}) - \theta_\ell - \kappa_{i,j} \right) s_{\ell; i,j} \tag{5.8}$$

per unit of storage capacity, where $\mathbf{s}_\ell = \{s_{\ell; i,j}\}_{i,j \in \mathcal{N}} \in \mathbb{R}^{n^2}$. The only difference in payoffs for different EVs is their inconvenience cost, which in turn determines their route choice. We can then denote the optimal service provision choice by $\mathbf{s}_\ell = \delta(\theta_\ell), \ell \in \mathcal{L}$, where $\delta : \mathbb{R} \mapsto \{0, 1\}^{n_2}$. We also define $s_\ell = \mathbf{1}^\top \mathbf{s}_\ell = \sum_{i,j} s_{\ell; i,j} \in \{0, 1\}$ which denotes whether the EV provides service along any route in the network. If $s_\ell = 0$, EV ℓ does not provide service along any route. We define $S_{i,j}$ as the amount of mobile storage available on $i \to j$. We have

$$S_{i,j} = \int_{\ell \in \mathcal{L}} \delta(\theta_\ell)_{i,j} \, \mathrm{d}\, F(\theta_\ell) \leq 1, \tag{5.9}$$

where $\delta(\theta_\ell)_{i,j} = s_{\ell; i,j}$ is the decision to provide service on route $i \to j$, and $F(\cdot)$ is the cumulative distribution of the inconvenience costs of the on-demand EVs. Note that $\sum_{i,j} S_{i,j} \leq 1$ as well.

Solution concepts

Both commuter and on-demand EVs can be operated by a variety of centralized operators and decentralized agents with different objectives. We begin by considering two benchmark

solution concepts:

1. *Myopic EV drivers:* EVs act in a decentralized manner and maximize their own individual payoffs without considering the effect of mobile storage service on the LMPs. They optimize their operation under the assumption that $\mathbf{S} = \mathbf{0}$.

2. *Social welfare maximizing operator:* A central operator optimizes the mobile storage service provision of all the EVs to maximize social welfare, which is defined as the surplus received by both the EVs and the electricity market participants, including the generators and load.

The precise mathematical description of these benchmarks depends on the type of EV drivers under consideration (commuters or on-demand drivers), and will be provided in subsequent sections.

We then consider the operation of EVs which operate in a decentralized manner to optimize their individual payoffs, thus participating in an EV battery sharing game. We define three game settings:

1. *Commuter EVs only:* The set of players is $\cup_{i,j \in \mathcal{N}} \mathcal{K}_{i,j}$, where each player has a decision of whether to provide mobile storage service or not. The payoff of player $k \in \mathcal{K}_{i,j}$ is defined as (5.5).

2. *On-demand EVs only:* The set of players is $\mathcal{L}$, where each player chooses from n^2 routes to provide the mobile storage service or not to provide the service. The payoff of player $\ell \in \mathcal{L}$ is defined as (5.8).

3. *Both commuter and on-demand EVs:* In this case, both types of players coexist, with their decisions and payoff functions defined as before.

We utilize *Nash Equilibrium* (NE) as the solution concept, under which no player has an incentive to unilaterally change its decision. As we are considering an aggregate game, i.e., each player's action only impact others' payoffs via the aggregate storage capacities, we will refer to the aggregate storage capacities induced by a NE as NE storage capacities. For each setting, we will compare the NE to the benchmarks discussed previously.

5.3 Commuter EVs: Fixed Routes

We now consider the setting where there are only commuter EVs providing mobile storage services to the grid, and characterize the market driven equilibrium outcome for the EV battery sharing game. Each route in the power network has a population of EV drivers $k \in \mathcal{K}_{i,j}$ characterized by their inconvenience cost θ_k, which are otherwise interchangeable. In order to define the optimal mobile storage service for each of the solution concepts, we partition the population of EVs on route $i \to j$ into $\mathcal{K}_{i,j}^+$ and $\mathcal{K}_{i,j}^-$ for each situation, where EVs in $\mathcal{K}_{i,j}^+$ provide mobile storage service, and EVs in $\mathcal{K}_{i,j}^-$ do not. We posit that the EVs

in $\mathcal{K}_{i,j}^+$ necessarily have a lower inconvenience cost than the EVs in $\mathcal{K}_{i,j}^-$ for each solution concept discussed in section 5.2 (which will be mathematically defined subsequently), i.e.,

Proposition 11. *For each solution concept discussed in this paper, there exists a threshold $\overline{\theta}_{i,j}$ such that*

$$\mathcal{K}_{i,j}^+ = \{k \in \mathcal{K}_{i,j} : \theta_k \leq \overline{\theta}_{i,j}\}, \quad i,j \in \mathcal{N}, \tag{5.10a}$$

$$\mathcal{K}_{i,j}^- = \{k \in \mathcal{K}_{i,j} : \theta_k > \overline{\theta}_{i,j}\}, \quad i,j \in \mathcal{N}. \tag{5.10b}$$

Proof. We split the discussion into two cases:

1. *Independent decisions by EVs:* Each EV makes a decision to provide mobile storage service based only on its payoff. The payoffs, and consequently the service decisions for two different EVs are only differentiated by their inconvenience cost θ_k. An EV with a higher θ_k will necessarily have a lower payoff (5.5), and if this EV decides to provide service, then any EV with a higher payoff (i.e., lower θ_k) will also provide service.

2. *Centrally controlled EVs:* From the perspective of the power system operator, EVs are undifferentiated except by their inconvenience costs. The system operator will preferentially choose EVs with lower inconvenience costs instead of those with higher inconvenience costs in order to minimize total social cost.

In both cases, there will be a marginal EV on route $i \to j$ with inconvenience cost $\overline{\theta}_{i,j}$ such that all EVs on that route with lower θ will provide service, and those with higher θ will not. $\square$

Benchmarks

We now characterize the operation in the benchmarks discussed in Section 5.2 when there are only commuters.

Myopic EV drivers

Each myopic EV owner traveling along $i \to j$ maximizes $\pi_k(s_k, \mathbf{0})$. The optimal decision would be to set

$$s_k^{\text{myop}} = \begin{cases} 1, & \text{if } \lambda_j^{(2)}(\mathbf{0}) - \lambda_i^{(1)}(\mathbf{0}) - \theta_k - \kappa \geq 0, \\ 0, & \text{otherwise}, \end{cases} \tag{5.11}$$

which gives us threshold inconvenience cost for each route

$$\overline{\theta}_{i,j}^{\text{myop}} = \lambda_j^{(2)}(\mathbf{0}) - \lambda_i^{(1)}(\mathbf{0}) - \kappa, \tag{5.12}$$

and the mobile storage proportion $S_{i,j}^{\text{myop}} = F_{i,j}(\overline{\theta}_{i,j}^{\text{myop}})$.

Social welfare maximizing operator

A social welfare maximizing operator solves the following problem:

$$\min_{\mathbf{S},\bar{\boldsymbol{\theta}}} \quad J(\mathbf{S}) + \sum_{i,j} \int_{\theta_k \leq \bar{\theta}_{i,j}} (\theta_k + \kappa) \, \mathrm{d}\, F(\theta_k), \tag{5.13a}$$

$$\text{s.t.} \quad S_{i,j} = F_{i,j}(\bar{\theta}_{i,j}), \quad i,j \in \mathcal{N}, \tag{5.13b}$$

where $J(\mathbf{S})$ is the optimal solution of the economic dispatch problem in (4.13). The social cost is taken to be the sum of generation cost, inconvenience and battery degradation costs for the EVs, minus the value of supplying electricity to loads. Then we have

Lemma 12. *The inconvenience cost threshold $\bar{\theta}_{i,j}^{sw}$ and the corresponding aggregate storage capacity $S_{i,j}^{sw}$, $i,j \in \mathcal{N}$, for the socially optimal operation is given by the solution of*

$$\bar{\theta}_{i,j}^{sw} = \lambda_j^{(2)}(\mathbf{S}^{sw}) - \lambda_i^{(1)}(\mathbf{S}^{sw}) - \kappa, \qquad\qquad i,j \in \mathcal{N}. \tag{5.14a}$$

$$S_{i,j}^{sw} = F_{i,j}(\bar{\theta}_{i,j}^{sw}), \qquad\qquad i,j \in \mathcal{N}. \tag{5.14b}$$

Proof. We can eliminate one variable in (5.13) by enforcing the equality constraint (5.13b). We set the gradient of the objective in the unconstrained problem to zero, i.e.

$$S_{i,j}^{\mathrm{sw}} : \nabla_{S_{i,j}} J(\mathbf{S})|_{\mathbf{S}^{\mathrm{sw}}} + (\bar{\theta}_{i,j}^{\mathrm{sw}} + \kappa) = 0. \tag{5.15}$$

From [8], we know that

$$\nabla_{S_{i,j}} J(\mathbf{S}) = -(\lambda_j^{(2)}(\mathbf{S}) - \lambda_i^{(1)}(\mathbf{S}))_+, \tag{5.16}$$

and we can ignore the positive part operator since a non-zero $S_{i,j}^{\mathrm{sw}}$ will necessitate a non-negative $\bar{\theta}_{i,j}^{\mathrm{sw}}$, which ensures that $\lambda_j^{(2)}(\mathbf{S}) - \lambda_i^{(1)}(\mathbf{S}) \geq 0$, and κ is necessarily non-negative. $\square$

Upon increasing mobile storage along route $i \to j$, the marginal increase in social welfare is given by the decrease in power system cost less the inconvenience and battery degradation costs incurred by the commuter EV, i.e.,

$$(\lambda_j^{(2)}(\mathbf{S}) - \lambda_i^{(1)}(\mathbf{S}))_+ - \theta_{i,j} - \kappa. \tag{5.17}$$

Nash equilibrium

Consider a situation where all the EVs are owned and operated by distributed entities, e.g., the case where they are all personal vehicles used for transport, and each EV driver participates in the EV battery sharing game independently. We can classify EVs into two groups: those which are providing mobile storage service at equilibrium and those which are not. At the equilibrium, no EV will be better off switching from one group to another.

At the NE, given the aggregate storage capacities, each EV maximizes its payoff, i.e.,

$$\max_{s_k} \quad \pi_k(s_k, \mathbf{S}). \tag{5.18}$$

If each EV has a small storage capacity, then the operational decision of one EV does not impact the LMPs, and

$$s_k^{\mathrm{NE}} = \sigma_{i,j}^{\mathrm{NE}}(\theta_k) = \begin{cases} 1, & \text{if } \pi_k(1, \mathbf{S}^{\mathrm{NE}}) \geq 0, \\ 0, & \text{otherwise,} \end{cases} \qquad (5.19)$$

for $k \in \mathcal{K}_{i,j}$. In other words, any EV which can obtain a non-negative payoff decides to provide mobile storage service.

Lemma 13. *The Nash equilibrium inconvenience cost threshold $\overline{\theta}_{i,j}^{NE}$ and the corresponding aggregate storage capacity $S_{i,j}^{NE}$, $i, j \in \mathcal{N}$ are given by the solution of*

$$\overline{\theta}_{i,j}^{NE} = \lambda_j^{(2)}(\mathbf{S}^{NE}) - \lambda_i^{(1)}(\mathbf{S}^{NE}) - \kappa, \qquad\qquad i, j \in \mathcal{N}. \qquad (5.20a)$$

$$S_{i,j}^{NE} = F_{i,j}(\overline{\theta}_{i,j}^{NE}), \qquad\qquad i, j \in \mathcal{N}. \qquad (5.20b)$$

Proof. Consider an EV with $\theta > \overline{\theta}_{i,j}^{\mathrm{NE}}$. We posit that at equilibrium, this EV does not provide mobile storage service. The payoff for this EV is given by

$$\lambda_j^{(2)}(\mathbf{S}^{\mathrm{NE}}) - \lambda_i^{(1)}(\mathbf{S}^{\mathrm{NE}}) - \kappa - \theta$$
$$< \lambda_j^{(2)}(\mathbf{S}^{\mathrm{NE}}) - \lambda_i^{(1)}(\mathbf{S}^{\mathrm{NE}}) - \kappa - \overline{\theta}_{i,j}^{\mathrm{NE}} = 0,$$

i.e., the payoff is negative, and the EV has no incentive to deviate from the equilibrium decision and start to provide mobile storage service.

Next, consider the complementary case, i.e., an EV with $\theta \leq \overline{\theta}_{i,j}^{\mathrm{NE}}$. We posit that at equilibrium, this EV will provide mobile storage service. The payoff for this EV is given by

$$\lambda_j^{(2)}(\mathbf{S}^{\mathrm{NE}}) - \lambda_i^{(1)}(\mathbf{S}^{\mathrm{NE}}) - \kappa - \theta$$
$$\geq \lambda_j^{(2)}(\mathbf{S}^{\mathrm{NE}}) - \lambda_i^{(1)}(\mathbf{S}^{\mathrm{NE}}) - \kappa - \overline{\theta}_{i,j}^{\mathrm{NE}} = 0,$$

i.e., is non-negative, and the EV has no incentive to deviate from the equilibrium decision and stop providing service. $\square$

We can relate the equilibrium mobile storage service with the socially optimal solution as:

Theorem 14. *Any aggregate storage capacity corresponding to the Nash equilibrium for commuter EVs supports the social welfare.*

Proof. There is a one-to-one correspondence of the socially optimal aggregate storage capacity given in (5.14) and the Nash equilibrium aggregate storage given in (5.20). $\square$
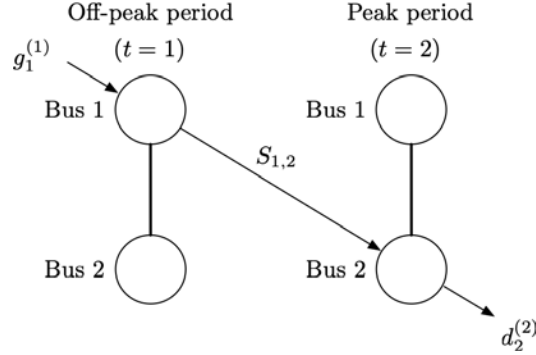
Figure 5.1: Two bus network

Example

Our results on the social welfare maximizing solution and NE depend on solving a system of
nonlinear equations. To gain explicit analytical insight, we consider a simple example with
two period and two buses shown in Fig. 5.1. For the network, bus 2 has a load at $t = 2$, and
bus 1 has a generator. There is some mobile storage capacity ($S_{1,2}$) which moves from bus 1
at $t = 1$ to bus 2 at $t = 2$. The generation cost is given by $C_t(g) = ag^2 + bg, t \in \{1, 2\}$ and
the value of supplying load is given by $B_t(d) = cd, t \in \{1, 2\}$. The LMPs for this network
are given by

$$\lambda_1^{(1)} = 2a \min\left\{S_{1,2}, \frac{c-b}{2a}\right\} + b, \quad \lambda_2^{(2)} = c. \tag{5.21}$$

The optimal mobile storage levels for each of the benchmarks for this network is given by

1. *Myopic EV drivers:* The LMPs when $\mathbf{S} = \mathbf{0}$ are $\lambda_1^{(1)} = b$, $\lambda_2^{(2)} = c$, and we have

$$S_{1,2}^{\text{myop}} = F_{1,2}(\overline{\theta}_{1,2}^{\text{myop}}) = F_{1,2}(c - b - \kappa). \tag{5.22}$$

2. *Social welfare maximizing operator:* The optimal decision is given by the solution of
the fixed point equation

$$S_{1,2}^{\text{sw}} = F_{1,2}(c - 2aS_{1,2}^{\text{sw}} - b - \kappa), \tag{5.23}$$

On comparing these values, we find

$$S_{1,2}^{\text{myop}} \geq S_{1,2}^{\text{sw}} = S_{1,2}^{\text{NE}}. \tag{5.24}$$

The intuition behind this is that myopic EV drivers tend to over-commit to providing mobile
storage service, since they do not factor the reduction of the LMP difference into their
decision.

5.4   On-Demand EVs: Flexible Routes

We now consider the setting where there are only on-demand EVs providing mobile storage services to the grid, and characterize the market driven equilibrium outcome for the EV battery sharing game. The network has a population of on-demand EVs $\ell \in \mathcal{L}$, which are characterized by their inconvenience cost θ_ℓ, and are otherwise indistinguishable. In order to define the optimal storage service, we partition the network-wide population of EVs into $\mathcal{L}^+$ and $\mathcal{L}^-$ for each of the solution concepts, where EVs in $\mathcal{L}^+$ provide mobile storage service on any one route in the power network and EVs in $\mathcal{L}^-$ do not provide mobile storage on any route. We can extend Proposition 11 and define a network-wide inconvenience cost threshold $\overline{\theta}$ for each solution concept, such that

$$\mathcal{L}^+ = \{l \in \mathcal{L} : \theta_\ell \leq \overline{\theta}\}, \tag{5.25a}$$

$$\mathcal{L}^- = \{l \in \mathcal{L} : \theta_\ell > \overline{\theta}\}. \tag{5.25b}$$

Benchmarks

We now characterize the operation of on-demand EVs in some of the benchmarks discussed in Section 5.2.

Myopic EV drivers

The myopic EV driver indexed by $\ell \in \mathcal{L}$ chooses $\mathbf{s}_\ell$ to maximize $\pi_\ell(\mathbf{s}_\ell, \mathbf{0})$. Since the only difference in payoffs for EVs is the inconvenience cost θ_ℓ, the route with the maximum potential payoff will attract all the myopic EV drivers. Let this route be $i^* \to j^*$, where

$$(i^*, j^*) = \underset{i,j}{\operatorname{argmax}} \ \lambda_j^{(2)}(\mathbf{0}) - \lambda_i^{(1)}(\mathbf{0}) - \kappa_{i,j}. \tag{5.26}$$

Then the decision of driver $\ell \in \mathcal{L}$ to provide service is

$$s_{\ell;i^*,j^*}^{\mathrm{myop}} = \begin{cases} 1, & \text{if } \lambda_{j^*}^{(2)}(\mathbf{0}) - \lambda_{i^*}^{(1)}(\mathbf{0}) - \kappa_{i^*,j^*} \geq \theta_\ell, \\ 0, & \text{otherwise}, \end{cases} \tag{5.27}$$

and with $s_{\ell;i,j}^{\mathrm{myop}} = 0$ for $(i,j) \neq (i^*, j^*)$. This gives us the inconvenience cost threshold

$$\overline{\theta}^{\mathrm{myop}} = \lambda_{j^*}^{(2)}(\mathbf{0}) - \lambda_{i^*}^{(1)}(\mathbf{0}) - \kappa_{i^*,j^*}, \tag{5.28}$$

where i^*, j^* are defined as in (5.26). The total storage capacity for route (i^*, j^*) is given by $S_{i^*,j^*}^{\mathrm{myop}} = F(\overline{\theta}^{\mathrm{myop}})$, and $S_{i,j}^{\mathrm{myop}} = 0$ for all other routes.

Social welfare maximizing operator

A central operator that maximizes social welfare (or equivalently minimizing the social cost) solves the following problem:

$$\min_{\mathbf{S}, \bar{\theta}} \quad J(\mathbf{S}) + \sum_{i,j} \kappa_{i,j} S_{i,j} + \int_{\theta_\ell \leq \bar{\theta}} \theta_\ell \, \mathrm{d}\, F(\theta_\ell) \tag{5.29a}$$

$$\text{s.t.} \quad \mathbf{S} \geq \mathbf{0}, \ \mathbf{1}^\top \mathbf{S} = F(\bar{\theta}), \tag{5.29b}$$

where $J(\mathbf{S})$ is the optimal cost of the economic dispatch problem in (4.13). The social cost is the sum of generation cost, inconvenience, travel and battery degradation costs for the EVs, minus the value of supplying electricity to loads.

We can define the storage capacity on each route by $S_{i,j}^{\mathrm{sw}}$, and we know that $\sum_{i,j} S_{i,j}^{\mathrm{sw}} = F(\bar{\theta}^{\mathrm{sw}})$, where $\bar{\theta}^{\mathrm{sw}}$ is the network-wide threshold of inconvenience costs determined by solving (5.29). From [8] we know that the value of increasing mobile storage capacity is given by

$$-\nabla_{S_{i,j}} J(\mathbf{S}) = (\lambda_j^{(2)}(\mathbf{S}) - \lambda_i^{(1)}(\mathbf{S}))_+, \tag{5.30}$$

which is the LMP increase along the route. However, increasing storage capacity along a route also increases the travel and inconvenience costs that need to be paid. The operator will add mobile storage capacity which maximizes the increase in social welfare

$$\left((\lambda_j^{(2)}(\mathbf{S}) - \lambda_i^{(1)}(\mathbf{S}))_+ - \theta_\ell - \kappa_{i,j} \right)_+. \tag{5.31}$$

We can ignore the inner positive part operator in this equation when we formulate our storage operation decision, since the LMP difference will necessarily be non-negative for the entire expression to be non-negative. The socially optimal storage operation of on-demand EVs can be formulated as a route choice

$$(i^*, j^*) = \underset{i,j}{\operatorname{argmax}} \ \lambda_j^{(2)}(\mathbf{S}^{\mathrm{sw}}) - \lambda_i^{(1)}(\mathbf{S}^{\mathrm{sw}}) - \kappa_{i,j}, \tag{5.32}$$

with a mobile storage service provision choice given by

$$s_{\ell;i,j}^{\mathrm{sw}} = 0, \quad \text{if } (i,j) \neq (i^*, j^*), \tag{5.33a}$$

$$s_{\ell;i^*,j^*}^{\mathrm{sw}} = \begin{cases} 1, \text{ if } \lambda_{j^*}^{(2)}(\mathbf{S}^{\mathrm{sw}}) - \lambda_{i^*}^{(1)}(\mathbf{S}^{\mathrm{sw}}) - \theta_\ell - \kappa_{i^*,j^*} \geq 0, \\ 0, \text{ otherwise.} \end{cases} \tag{5.33b}$$

This ensures that storage is only added if it increases the social welfare.

Lemma 15. *The network-wide inconvenience cost threshold for socially optimal operation of on-demand EVs is the solution of*

$$\bar{\theta}^{sw} = \lambda_{j^*}^{(2)}(\mathbf{S}^{sw}) - \lambda_{i^*}^{(1)}(\mathbf{S}^{sw}) - \kappa_{i^*,j^*}, \tag{5.34a}$$

$$\mathbf{1}^\top \mathbf{S}^{sw} = F(\bar{\theta}^{sw}), \tag{5.34b}$$

where i^*, j^* are defined as in (5.32).

Proof. 1. First, consider $\mathcal{L}^-$ is non-empty, i.e., there are some EVs which do not provide mobile storage along any route at the socially optimal solution. This means that the marginal increase in social welfare on adding an EV to any route in the network is non-positive, since otherwise the unutilized mobile storage would be dispatched along some route in the network. There are two types of routes in the network:

a) Route $i \to j$ has some non-zero mobile storage capacity, i.e., $S_{i,j}^{\mathrm{sw}} > 0$. The marginal increase in social welfare on adding an additional EV to this route is zero, and

$$\lambda_j^{(2)}(\mathbf{S}^{\mathrm{sw}}) - \lambda_i^{(1)}(\mathbf{S}^{\mathrm{sw}}) - \overline{\theta}^{\mathrm{sw}} - \kappa_{i,j} = 0. \tag{5.35}$$

We can ignore the positive part operator in (5.31) since $\overline{\theta}^{\mathrm{sw}}, \kappa_{i,j}$ are necessarily non-negative.

b) Route $i' \to j'$ has zero mobile storage capacity, i.e., $S_{i',j'}^{\mathrm{sw}} = 0$. Adding an EV to this route causes a decline in social welfare, i.e.

$$\lambda_{j'}^{(2)}(\mathbf{S}^{\mathrm{sw}}) - \lambda_{i'}^{(1)}(\mathbf{S}^{\mathrm{sw}}) - \overline{\theta}^{\mathrm{sw}} - \kappa_{i',j'} \le 0. \tag{5.36}$$

2. Second, consider $\mathcal{L}^-$ is empty, then $\sum_{i,j} S_{i,j}^{\mathrm{sw}} = \mathbf{1}^\top \mathbf{S}^{\mathrm{sw}} = 1$ and all EVs are deployed along one of the routes in the network. The network wide inconvenience cost threshold is $\overline{\theta}^{\mathrm{sw}} \ge \max_l \{\theta_l\}$, and at least one route has a non-negative payoff, i.e.,

$$\lambda_j^{(2)}(\mathbf{S}^{\mathrm{sw}}) - \lambda_i^{(1)}(\mathbf{S}^{\mathrm{sw}}) - \overline{\theta}^{\mathrm{sw}} - \kappa_{i,j} \ge 0 \text{ for some } i, j. \tag{5.37}$$

This indicates that if there were more EVs available with an inconvenience cost $\overline{\theta}^{\mathrm{sw}}$, it would be beneficial for them to provide mobile storage service.

□

Nash equilibrium

Consider a situation where all EVs are owned and operated by distributed agents, e.g., when they are owned by individuals who sign up on TNC platforms to earn money for providing mobile storage service. Each EV driver participates in an EV battery sharing game, and makes an independent decision on whether to provide mobile storage service and which route to provide it on based on the payoff $\pi_\ell(\mathbf{s}_\ell, \mathbf{S})$. At the equilibrium, EVs will provide service in a manner where no EV has an incentive to deviate from its chosen route and operation.

At the NE, given the aggregate storage capacities, each EV maximizes its own payoff, i.e., chooses a route and operational decision according to

$$\max_{\mathbf{s}_\ell} \quad \pi_\ell(\mathbf{s}_\ell, \mathbf{S}) \tag{5.38a}$$

$$\text{s.t.} \quad \mathbf{1}^\top \mathbf{s}_\ell \le 1, \tag{5.38b}$$

where $\mathbf{s}_\ell$ is the decision vector of $s_{\ell;i,j}$ for all routes on the network for driver ℓ. If each individual EV has a small storage capacity, then its operation decision will not impact LMPs and we can denote the optimal route choice of the marginal EV by

$$(i^*, j^*) = \underset{i,j}{\operatorname{argmax}} \, \lambda_j^{(2)}(\mathbf{S}^{\text{NE}}) - \lambda_i^{(1)}(\mathbf{S}^{\text{NE}}) - \kappa_{i,j}, \tag{5.39}$$

and the mobile storage service provision by

$$s_{\ell;i,j}^{\text{NE}} = 0, \quad \text{if} \, (i,j) \neq (i^*, j^*), \tag{5.40a}$$

$$s_{\ell;i^*,j^*}^{\text{NE}} = \begin{cases} 1, \text{if} \, \lambda_{j^*}^{(2)}(\mathbf{S}^{\text{NE}}) - \lambda_{i^*}^{(1)}(\mathbf{S}^{\text{NE}}) - \theta_\ell - \kappa_{i^*,j^*} \geq 0, \\ 0, \text{otherwise.} \end{cases} \tag{5.40b}$$

For the equilibrium mobile storage $\mathbf{S}^{\text{NE}}$, there are two dimensions: each EV which provides mobile storage service on route $i \rightarrow j$ at equilibrium will be no better off if (a) it decides to stop providing the service, or (b) if it switches to a different route. Additionally, each EV which does not provide mobile storage service will be no better off if it does so on any route in the network.

Lemma 16. *The network-wide inconvenience cost threshold at equilibrium $\overline{\theta}^{NE}$ and the corresponding aggregate storage capacity are given by the solution of*

$$\overline{\theta}^{NE} = \lambda_{j^*}^{(2)}(\mathbf{S}^{NE}) - \lambda_{i^*}^{(1)}(\mathbf{S}^{NE}) - \kappa_{i^*,j^*}, \tag{5.41a}$$

$$\mathbf{1}^\top \mathbf{S}^{NE} = F(\overline{\theta}^{NE}), \tag{5.41b}$$

where i^*, j^* are defined as in (5.39).

The Nash equilibrium operation of on-demand EVs providing mobile storage service is characterized through the following exhaustive list of cases, which can also serve as a proof of Lemma 16 by utilizing arguments similar to the ones in the proof for Lemma 13:

1. First, consider the case where $\mathcal{L}^-$ is not empty, i.e. there are some EVs which do not provide mobile storage service. Then, the marginal payoff for an additional EV on any route should be non-positive. There are two types of routes in the network:

   a) Route $i \rightarrow j$ has some non-zero mobile storage capacity, i.e. $S_{i,j} > 0$. At equilibrium, this route provides zero payoff and there is no incentive for an EV $\ell \in \mathcal{L}^-$ to provide service on this route, and

   $$\overline{\theta}^{\text{NE}} = \lambda_j^{(2)}(\mathbf{S}^{\text{NE}}) - \lambda_i^{(1)}(\mathbf{S}^{\text{NE}}) - \kappa_{i,j}. \tag{5.42}$$

   b) Route $i' \rightarrow j'$ has zero mobile storage capacity, i.e. $S_{i',j'} = 0$. This route has a non-positive payoff, which is why no EV chooses to provide service on that route, and

   $$\lambda_{j'}^{(2)}(\mathbf{S}^{\text{NE}}) - \lambda_{i'}^{(1)}(\mathbf{S}^{\text{NE}}) - \overline{\theta}^{\text{NE}} - \kappa_{i',j'} < 0. \tag{5.43}$$

2. Second, consider the case where $\mathcal{L}^-$ is empty, i.e. all the EVs available provide mobile storage service on one route or the other. Then we have

$$\bar{\theta}^{\text{NE}} = \lambda_{j_1}^{(2)}(\mathbf{S}^{\text{NE}}) - \lambda_{i_1}^{(1)}(\mathbf{S}^{\text{NE}}) - \kappa_{i_1,j_1} \tag{5.44a}$$

$$= \lambda_{j_2}^{(2)}(\mathbf{S}^{\text{NE}}) - \lambda_{i_2}^{(1)}(\mathbf{S}^{\text{NE}}) - \kappa_{i_2,j_2} \tag{5.44b}$$

$$\geq \lambda_{j_3}^{(2)}(\mathbf{S}^{\text{NE}}) - \lambda_{i_3}^{(1)}(\mathbf{S}^{\text{NE}}) - \kappa_{i_3,j_3} \tag{5.44c}$$

for all $i_1, j_1, i_2, j_2, i_3, j_3 \in \mathcal{N}$ where $S_{i_1,j_1}^{\text{NE}} > 0, S_{i_2,j_2}^{\text{NE}} > 0$ and $S_{i_3,j_3}^{\text{NE}} = 0$, i.e., the marginal payoff for routes with non-zero mobile storage capacity is the same throughout the network, and is higher than the marginal payoff for routes with zero mobile storage capacity at equilibrium. This indicates that if there were more EVs available with an inconvenience cost $\bar{\theta}^{\text{NE}}$, it would be profitable for them to provide mobile storage service.

We can relate the equilibrium mobile storage service to the socially optimal solution as:

Theorem 17. *Any inconvenience cost threshold $\bar{\theta}$ corresponding to the Nash equilibrium for on-demand EVs supports the social welfare.*

Proof. There is a one-to-one correspondence of the equilibrium inconvenience cost threshold in (5.41) and the socially optimal inconvenience cost threshold in (5.34). □

5.5 Hybrid: Commuter and On-Demand EVs

We now consider the setting where there is a mix of commuter and on-demand EVs providing mobile storage services to the grid, and characterize the market driven equilibrium outcome as an EV battery sharing game. There is a population of commuter EVs on each route characterized by their inconvenience costs $\theta_k, k \in \mathcal{K}_{i,j}$, and a network-wide population of on-demand EVs characterized by their inconvenience costs $\theta_\ell, \ell \in \mathcal{L}$. We denote the mobile storage capacity provided by commuter EVs with fixed routes by $\mathbf{S}^{\text{fix}}$, and the capacity provided by on-demand EVs with flexible routes by $\mathbf{S}^{\text{flex}}$. The total mobile storage capacity on all routes is represented by $\mathbf{S}$, and includes storage capacity from commuter and on-demand EVs. The two types of EVs provide the same service and are interchangeable in terms of value generated, but have different inconvenience, travel and battery degradation costs. In order to define the optimal storage service for each of the solution concepts, we partition the population of commuter EVs on each route into two sets: those which provide service ($\mathcal{K}_{i,j}^+$) and those which don't ($\mathcal{K}_{i,j}^-$). These sets are determined by a route specific inconvenience cost threshold $\bar{\theta}_{i,j}$. We also partition the network wide population of on-demand EVs into those which provide service on any route ($\mathcal{L}^+$) and those which don't ($\mathcal{L}^-$). These sets are determined by a network-wide inconvenience cost threshold $\bar{\theta}$.

Benchmark: social welfare maximizing operator

To maximize the social welfare, a central operator solves the following problem:

$$\min_{\substack{\mathbf{S}^{\text{fix}}, \mathbf{S}^{\text{flex}}, \\ \overline{\boldsymbol{\theta}}^{\text{fix}}, \overline{\boldsymbol{\theta}}^{\text{flex}}}} J(\mathbf{S}) + \sum_{i,j} \int_{\theta_k \leq \overline{\theta}_{i,j}^{\text{fix}}} (\theta_k + \kappa) \, \mathrm{d} F_{i,j}(\theta_k) + \int_{\theta_\ell \leq \overline{\theta}^{\text{flex}}} \theta_\ell \, \mathrm{d} F(\theta_\ell) + \sum_{i,j} \kappa_{i,j} S_{i,j}^{\text{flex}} \qquad (5.45\text{a})$$

$$\text{s.t.} \quad \mathbf{S}^{\text{flex}} \geq 0, \quad \mathbf{1}^\top \mathbf{S}^{\text{flex}} = F(\overline{\theta}^{\text{flex}}), \qquad (5.45\text{b})$$

$$S_{i,j}^{\text{fix}} = F_{i,j}(\overline{\theta}_{i,j}^{\text{fix}}), \quad i,j \in \mathcal{N}, \qquad (5.45\text{c})$$

where $\mathbf{S} = \mathbf{S}^{\text{fix}} + \mathbf{S}^{\text{flex}}$. From the perspective of the power system operator, it does not matter whether mobile storage capacity comes from commuter EVs ($\mathbf{S}^{\text{fix}}$) or on-demand EVs ($\mathbf{S}^{\text{flex}}$), and we can use the aggregate mobile storage capacity for our modeling. From [8], we know that the marginal value of adding mobile storage on a route is

$$\nabla_{S_{i,j}^{\text{fix}}} J(\mathbf{S}) = \nabla_{S_{i,j}^{\text{flex}}} J(\mathbf{S}) = -(\lambda_j^{(2)}(\mathbf{S}) - \lambda_i^{(1)}(\mathbf{S}))_+, \qquad (5.46)$$

which is the same for both commuter and on-demand EVs. The operator will add mobile storage capacity to maximize social welfare, i.e. will increase mobile storage capacity on a route as long as the marginal value is greater than or equal to the cost for either type of EV, i.e.

$$\lambda_j^{(2)}(\mathbf{S}) - \lambda_i^{(1)}(\mathbf{S}) \geq \overline{\theta}_{i,j}^{\text{fix}} + \kappa \qquad (5.47\text{a})$$

$$\lambda_j^{(2)}(\mathbf{S}) - \lambda_i^{(1)}(\mathbf{S}) \geq \overline{\theta}^{\text{flex}} + \kappa_{i,j}. \qquad (5.47\text{b})$$

The operator will prioritize dispatching on-demand EVs to the route with the greatest marginal increase in social welfare. We can ignore the positive part operator in this expression, since the sum of costs on the right hand side is non-negative by definition.

Lemma 18. *The inconvenience cost thresholds for the socially optimal storage operation of commuter and on-demand EVs are given by the joint solution of (5.14) and (5.34), where i^*, j^* are defined as in (5.32) and prices are determined by the aggregate mobile storage capacity:*

$$\mathbf{S}^{sw} = \mathbf{S}^{fix, \, sw} + \mathbf{S}^{flex, \, sw} \qquad (5.48\text{a})$$

$$\mathbf{1}^\top \mathbf{S}^{flex, \, sw} = F(\overline{\theta}^{flex, \, sw}), \qquad (5.48\text{b})$$

$$S_{i,j}^{fix, \, sw} = F_{i,j}(\overline{\theta}_{i,j}^{fix, \, sw}), \qquad\qquad i,j \in \mathcal{N}, \qquad (5.48\text{c})$$

$$\overline{\theta}^{flex, \, sw} = \lambda_{j^*}^{(2)}(\mathbf{S}^{sw}) - \lambda_{i^*}^{(1)}(\mathbf{S}^{sw}) - \kappa_{i^*, j^*}, \qquad (5.48\text{d})$$

$$\overline{\theta}_{i,j}^{fix, \, sw} = \lambda_j^{(2)}(\mathbf{S}^{sw}) - \lambda_i^{(1)}(\mathbf{S}^{sw}) - \kappa, \qquad\qquad i,j \in \mathcal{N}. \qquad (5.48\text{e})$$

Proof. The marginal increase in social welfare upon adding commuter EVs is given by (5.17), and the operator will add mobile storage using commuter EVs along route $i \rightarrow j$ as long as

the marginal value is positive. Similarly, the socially optimal decision for on-demand EVs is to add mobile storage as long as the marginal value is positive as discussed in the proof for Lemma 15. Commuter EVs and on-demand EVs interact with each other through their effect on the electricity prices λ. The marginal increases in social welfare on adding mobile storage through commuter EVs (5.17) or on-demand EVs (5.31) are only related through prices which depend on aggregate mobile storage capacity, and jointly solving the set of equations in Lemma 18 will resolve the interdependencies and give us the socially optimal solution. $\qquad\square$

Joint Nash equilibrium

Consider the situation where all of the EVs are operated independently irrespective of their type. Each EV driver participates in an EV battery sharing game, and makes an independent decision to provide mobile storage service and chose a route (for on-demand EVs) in order to maximize $\pi_k(s_k, \mathbf{S})$ or $\pi_\ell(\mathbf{s}_\ell, \mathbf{S})$ as appropriate. At the equilibrium, there will be a combination of commuter and on-demand mobile storage on each route. No commuter EV should be better off if it switches from $\mathcal{K}_{i,j}^+$ to $\mathcal{K}_{i,j}^-$ or vice versa (characterized by $\overline{\theta}_{i,j}^{\text{fix, NE}}$). Similarly, no on-demand EV should be better off switching from $\mathcal{L}^+$ to $\mathcal{L}^-$ or vice versa (characterized by $\overline{\theta}^{\text{flex, NE}}$), or by switching routes. Note that we model each type of EV as a distinct type of resource, and a commuter EV can not switch to being an on-demand EV, or vice versa. The 'joint' aspect of the equilibrium is that both types of EVs make decisions that place them at an NE. The storage capacities at equilibrium are given by

$$\mathbf{1}^\top \mathbf{S}^{\text{flex, NE}} = F^{\text{flex}}(\overline{\theta}^{\text{flex, NE}}), \tag{5.49}$$

$$S_{i,j}^{\text{fix}} = F_{i,j}^{\text{fix}}(\overline{\theta}_{i,j}^{\text{fix, NE}}), \qquad\qquad i,j \in \mathcal{N}, \tag{5.50}$$

where $F^{\text{flex}}(\cdot), F_{i,j}^{\text{fix}}(\cdot)$ are the cumulative distributions of inconvenience costs of on-demand and commuter EVs on that route respectively. The equilibrium decision by a commuter EV is given by

$$s_{k;i,j}^{\text{fix, NE}} = \begin{cases} 1, & \text{if } \lambda_j^{(2)}(\mathbf{S}^{\text{NE}}) - \lambda_i^{(1)}(\mathbf{S}^{\text{NE}}) - \theta_k - \kappa \geq 0 \\ 0, & \text{otherwise.} \end{cases} \tag{5.51}$$

The equilibrium decision by an on-demand EV is given by the route choice

$$(i^*, j^*) = \underset{i,j}{\operatorname{argmax}} \, \lambda_j^{(2)}(\mathbf{S}^{\text{NE}}) - \lambda_i^{(1)}(\mathbf{S}^{\text{NE}}) - \kappa_{i,j}, \tag{5.52}$$

and the mobile storage service provision by

$$s_{\ell;i,j}^{\text{flex, NE}} = 0, \quad \text{if } (i,j) \neq (i^*, j^*), \tag{5.53a}$$

$$s_{\ell;i^*,j^*}^{\text{flex, NE}} = \begin{cases} 1, \text{if } \lambda_{j^*}^{(2)}(\mathbf{S}^{\text{NE}}) - \lambda_{i^*}^{(1)}(\mathbf{S}^{\text{NE}}) - \theta_\ell - \kappa_{i^*,j^*} \geq 0, \\ 0, \text{otherwise.} \end{cases} \tag{5.53b}$$

We can characterize the Nash equilibrium by considering the exhaustive list of cases:

1. For a route $i \to j$, consider $\mathcal{K}_{i,j}^-$ and $\mathcal{L}^-$ are not empty, i.e., there are some commuter and on-demand EVs not providing mobile storage service. Then the marginal payoff for either type of EV is non-positive.

   a) $S_{i,j}^{\text{fix}} \neq 0$ and $S_{i,j}^{\text{flex}} \neq 0$; then the marginal payoff for both type of EVs on that route should be zero, i.e.

   $$\overline{\theta}^{\text{flex, NE}} = \lambda_j^{(2)}(\mathbf{S}^{\text{NE}}) - \lambda_i^{(1)}(\mathbf{S}^{\text{NE}}) - \kappa_{i,j}, \tag{5.54a}$$

   $$\overline{\theta}_{i,j}^{\text{fix, NE}} = \lambda_j^{(2)}(\mathbf{S}^{\text{NE}}) - \lambda_i^{(1)}(\mathbf{S}^{\text{NE}}) - \kappa. \tag{5.54b}$$

   b) $S_{i,j}^{\text{fix}} = 0$, which means

   $$\lambda_j^{(2)}(\mathbf{S}^{\text{NE}}) - \lambda_i^{(1)}(\mathbf{S}^{\text{NE}}) - \kappa < \min_k \theta_{k;i,j}.$$

   c) $S^{\text{flex}} = 0$, which means

   $$\lambda_j^{(2)}(\mathbf{S}^{\text{NE}}) - \lambda_i^{(1)}(\mathbf{S}^{\text{NE}}) - \kappa_{i,j} < \overline{\theta}^{\text{flex, NE}}.$$

2. For a route $i \to j$, consider $\mathcal{K}_{i,j}^-$ is empty, i.e., all commuter EVs provide mobile storage service. Then $S_{i,j}^{\text{fix, NE}} = 1$, and

   $$\lambda_j^{(2)}(\mathbf{S}^{\text{NE}}) - \lambda_i^{(1)}(\mathbf{S}^{\text{NE}}) - \overline{\theta}_{i,j}^{\text{fix, NE}} - \kappa \geq 0. \tag{5.55}$$

3. Consider $\mathcal{L}^-$ is empty, i.e., all on-demand EVs are providing mobile storage service. Then $\sum_{i,j} S_{i,j}^{\text{flex, NE}} = 1$, and

   $$\lambda_j^{(2)}(\mathbf{S}^{\text{NE}}) - \lambda_i^{(1)}(\mathbf{S}^{\text{NE}}) - \overline{\theta}^{\text{flex, NE}} - \kappa_{i,j} \geq 0 \tag{5.56}$$

   for at least one route $i \to j$ in the network.

Except for the first situation, we cannot explicitly relate the equilibrium service by commuter and on-demand EVs.

Lemma 19. *The inconvenience cost thresholds for the equilibrium operation of commuter and on-demand EVs are given by the joint solution of (5.20) and (5.41), where i^*, j^* are defined as in (5.39) and prices are determined by the aggregate mobile storage capacity $\mathbf{S}^{NE} = \mathbf{S}^{fix, NE} + \mathbf{S}^{flex, NE}$.*

Proof. Commuter EVs and on-demand EVs interact with each other through their effect on the electricity prices λ. The payoff for either type of EV depends only on the aggregate mobile storage capacity, and jointly solving the set of equations in (5.20) and (5.41) will resolve the interdependencies and give us the equilibrium operation. $\square$

Theorem 20. *Any inconvenience cost thresholds for commuter and on-demand EVs corresponding to a joint Nash equilibrium also support the social welfare.*

Proof. There is a one-to-one correspondence between the equations which determine inconvenience cost thresholds for the socially optimal solution and the Nash equilibrium. $\square$

5.6   Discussion

We have formulated and analyzed a network EV battery sharing game, where distributed EVs provide mobile energy storage service to the grid. We modeled two different EV behaviors: commuter EVs which travel on fixed routes, and on-demand EVs which can travel on any route in the power network. Our results suggest that the NE will support social welfare in settings where each EV driver is an infinitesimally small entity (and has no market power), and when only two time periods are considered. These results are robust across any combination of the different EV types. In future work, we plan to study the impact of market power for a collection of EVs, when they are coordinated by an EV aggregator or a transportation network company. We are also interested in extending our work to settings with multiple time periods. Since it is known that storage devices across the network may complement instead of substitute each other [52], our positive results for competitive EV-based mobile storage may only hold under certain network congestion patterns when more than two time slots are considered.

Part III

Aggregations of Energy Prosumers

Chapter 6

Optimal Composition of Prosumer Aggregations

In previous chapters, we discussed how flexible consumers and EV battery operators can interact with wholesale power markets and utility programs. Distributed resources can also bypass the utility and participate in local energy aggregations. In this chapter, we introduce the concept of prosumers and discuss the setup of a prosumer aggregation. The results presented here were published in [4], [6].

6.1 Introduction

A *prosumer* is an entity that is capable of *pro*ducing energy alongside being a con*sumer* through the presence of local generation and energy storage devices. An example of this are smart buildings, who often invest in energy resources in the form of local generation (photovoltaic arrays, diesel generators) and energy storage (batteries) which can be used to offset loads, reduce demand charges and optimize grid consumption. They can profit from these resources, e.g. by charging their batteries during low price hours and selling generation to the utility during peak price hours, thus demonstrating their prosumer behavior. However, local generation and storage is not always a profitable proposition: buildings have to invest in over-capacity generation and storage to accommodate the variability in their loads due to fluctuating occupancy and weather conditions. Additionally, as net-metering programs are phased out, utilities typically buy energy from distributed resources at a lower price [32]. These underutilized energy resources can become profitable when prosumers trade their surplus energy with other buildings rather than selling to the utility. *Prosumer aggregations* are coalitions set up to facilitate such energy sharing and trading.

In this chapter, we consider a central aggregator which facilitates energy trades within the aggregation and presents the net deficit/surplus to the utility as a single customer. The aggregation's total cost is the cost of trading the deficit/surplus with the utility. Each individual prosumer has to pay for its internal energy trades as well as its share of the utility
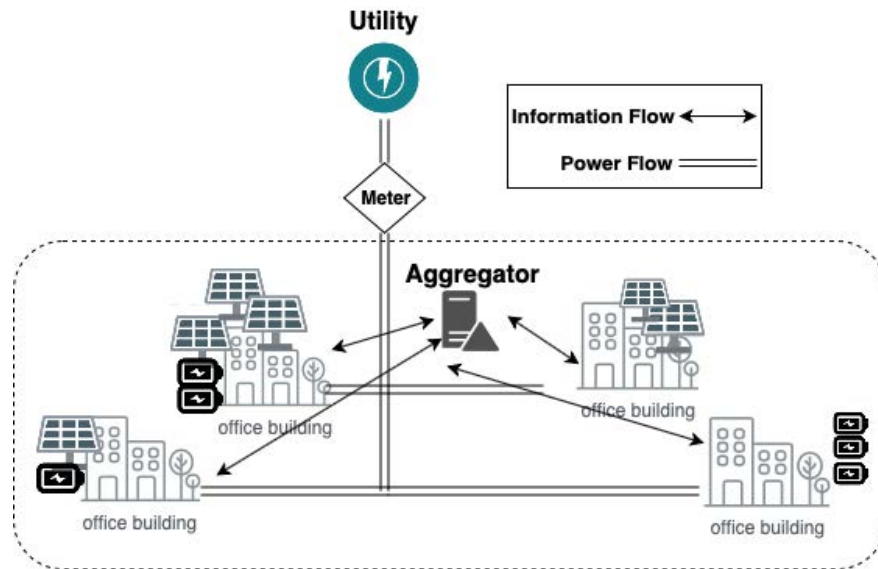
Figure 6.1: Social net metering in a prosumer aggregation

procurement. This model of aggregation does not require setting up new infrastructure, and is illustrated in Fig. 6.1. Similar contracts for virtual net-metering exist in the United States [60], and power flow occurs only between the utility and prosumers. The aggregator and prosumers share information to settle trades and manage payments, and the aggregator does not need to balance power flow or own physical infrastructure. Such aggregations can be designed with a variety of motives: cooperative cost savings for participants, increasing local renewable consumption, improving utilization of resources, or to maximize the profit of private investors.

There are two important questions we must address for aggregation design: (a) which prosumers would form the most beneficial aggregation, and (b) what value would additional prosumers add to an existing aggregation? Estimating the value of additional participants is a complex proposition due to the inter-dependencies between members of an aggregation. Prosumers share energy with each other, and an additional participant will affect all aggregation members. In this chapter, we focus on providing results on the optimal composition of aggregations and validating them with transactive control mechanisms borrowed from literature.

Related work

The dynamics of a prosumer aggregation can be estimated empirically, and agent based models have been recognized as an important tool for such simulations. In [19], prosumer agents are modeled by function and interact with each other in a peer to peer fashion to trade energy. In [22], agents are modeled for generation, consumption, market clearing and

coordination functions in an aggregation. These modeling techniques can be used to simulate setups with different participant and resource combinations, and the difference in costs can be used to evaluate individual prosumers. However, these methods require the knowledge of load and energy resources owned by each prosumer for accurate modeling.

Theoretical frameworks for designing optimal aggregations are also an active area of work. In [58], prosumers are optimally aggregated in a cooperative microgrid using coalitional game theory. The optimal sizing of energy resources in a microgrid is calculated using mixed-integer linear programming in [77]. In [55], the microgrid resource planning problem is cast as the upper level of a bilevel program which aims to optimize investment costs along with system reliability. Research in this area mainly focuses on optimizing resource investments, and the problem of evaluating a new prosumer using numerical metrics is not as widely studied.

The problem of controlling prosumer aggregations has also been investigated, like in [59] where a pricing method (VCG mechanism) is developed for demand side management with the aim of maximizing social welfare. A variety of papers develop price based controls: [38] develops a price to minimize load variation, and [42] develops a price based on supply-demand ratio to incentivize energy sharing.

Contributions

We develop a metric to estimate the degree of complementarity for a centrally controlled aggregation, i.e. we develop an expression which can be used to estimate the value of adding a prosumer or energy resource which would otherwise have operated independently outside the aggregation. This metric can be used to evaluate investments in new resources, or to prioritize the addition of certain prosumers. We also test the metric using simulations in an agent based aggregation model with market mechanisms from literature and real data.

The chapter is organized as follows: Section 6.2 introduces the prosumer and aggregator models, Section 6.3 lays out the main results, Section 6.4 validates the results through numerical simulations, and Section 6.5 concludes the chapter.

6.2 Model

We now set up the optimization problems that define the prosumer and aggregator. A prosumer is modeled as a cost-minimizing rational agent, while an aggregator can have a variety of objectives as discussed earlier.

Prosumer model

In any time period t, the prosumer has energy demand $d^{(t)}$, local generation $g^{(t)}$, and storage operation $u^{(t)}$. The building's net load at time t is given by

$$z^{(t)} = d^{(t)} - g^{(t)} + u^{(t)} \tag{6.1}$$

where charging storage is a net load, i.e. a positive $u^{(t)}$.

Define $\boldsymbol{\pi}_b$ to be the time-of-use rate at which prosumers buy energy, and $\boldsymbol{\pi}_s$ as the rate at which they sell surplus energy. Utilities typically have different buy and sell prices [32], as they move towards phasing out net-metering programs and incorporating distributed energy resources in wholesale markets. A prosumer can modify its energy consumption over the course of the day to minimize its energy bill, e.g. by storing energy in the battery during low price/surplus generation time periods, and discharging during peak price hours. However, battery life is affected by the number of charge/discharge cycles it goes through, and any usage of the battery costs money which can be modeled as a per cycle amortized battery cost. The optimization problem solved by the prosumer is

$$\min_{\mathbf{u}} \quad J_P(\boldsymbol{\pi}_b, \boldsymbol{\pi}_s) = \sum_{t=1}^{T} \left[\pi_b^{(t)} z_+^{(t)} + \pi_s^{(t)} z_-^{(t)} + \pi_{\text{bat}} |u^{(t)}| \right] \tag{6.2a}$$

$$= \boldsymbol{\pi}_b^\top \mathbf{z}_+ + \boldsymbol{\pi}_s^\top \mathbf{z}_- + \pi_{\text{bat}} \mathbf{1}^\top |\mathbf{u}| \tag{6.2b}$$

$$\text{s.t.} \qquad 0 \leq L\mathbf{u} \leq c \tag{6.2c}$$

where $\mathbf{u}$ represents the vector of battery charged/discharged energy over time with positive values denoting battery charging, $\boldsymbol{\pi}_b, \boldsymbol{\pi}_s$ represent the time vectors of utility buy and sell prices, $\mathbf{z}_+, \mathbf{z}_-$ represent the time vectors for positive and negative net demand curves respectively, and negative demand corresponds to generation. The optimization objective (6.2a) incorporates the cost of procuring net demand $z_+^{(t)}$ at the buy price, the revenue from selling net generation $z_-^{(t)}$ at the sell price, and the cost of battery degradation evaluated with π_{bat}. The battery constraints (6.2c) are on the state of charge and charging speed, and incorporate the one way battery efficiency η. A detailed explanation of the model can be found in [4].

If the utility had a net metering program ($\boldsymbol{\pi}_b = \boldsymbol{\pi}_s$), the optimization problem in (6.2) reduces to a linear program. Without net metering, the objective (6.2a) is a piece-wise linear function (and convex, under the assumption that $\boldsymbol{\pi}_b \geq \boldsymbol{\pi}_s$), and the optimization problem (6.2) is a convex program. Any uncertainty in load and generation can be incorporated in the objective through a stochastic optimization problem, however we do not do so for simplicity of exposition.

Aggregator model

We now develop a model for the prosumer aggregator which coordinates energy usage across prosumer participants.

Centrally controlled aggregation

From the perspective of coordination complexity, the simplest model is a centrally controlled aggregation where the aggregator has direct control over the storage and flexibility resources of all the prosumer participants. Such a setup could potentially exist when the aggregator

is designed to maximize the social welfare of the aggregation as a whole, i.e. minimize the utility bill and battery operation costs. We can model this problem as

$$\min_{\mathbf{u}_i, i \in S} \quad J_S = \boldsymbol{\pi}_b^\top \Big(\sum_{i \in S} \mathbf{z}_i\Big)_+ + \boldsymbol{\pi}_s^\top \Big(\sum_{i \in S} \mathbf{z}_i\Big)_- + \pi_{bat} \mathbf{1}^\top \Big|\sum_{i \in S} \mathbf{u}_i\Big| \tag{6.3a}$$

$$\text{s.t.} \qquad\qquad \mathbf{0} \leq L\mathbf{u}_i \leq c_i \mathbf{1} \,\forall i \in S \tag{6.3b}$$

where the objective (6.3a) represents the utility bill and battery operation costs of the aggregation as a whole, and the constraint (6.3b) represents the battery operation constraints. There are a few reasons why centralized control schemes may not be implementable: prosumers may be unwilling to cede control of privately owned resources to an external authority, and may be interested in minimizing their own costs rather than contributing to social welfare.

Aggregator as a market maker

We consider a setup where the aggregator trades energy with prosumers by operating a centralized clearing-house. The aggregator sets a price that reflects market dynamics, then sells energy to net consumers and buys energy from net generators at that price. It balances the net deficit/surplus by trading with the utility at the utility buy/sell price. Pricing schemes for aggregators have been explored in literature [36], [38], and the market-maker problem can be formalized as

$$\min_{\mathbf{p}_b, \mathbf{p}_s} \quad \Big|\sum_i \big(\mathbf{p}_b^\top \mathbf{z}_{i+} + \mathbf{p}_s^\top \mathbf{z}_{i-}\big) - \boldsymbol{\pi}_b^\top \Big(\sum_i \mathbf{z}_i\Big)_+ - \boldsymbol{\pi}_s^\top \Big(\sum_i \mathbf{z}_i\Big)_-\Big| \tag{6.4a}$$

$$\text{s.t.} \qquad\qquad \mathbf{z}_i = \mathbf{d}_i - \mathbf{g}_i + \mathbf{u}_i^* \quad \forall i \in S \tag{6.4b}$$

$$\mathbf{u}_i^* = \operatorname{argmin}_{\mathbf{u}} J_P(\mathbf{p}_b, \mathbf{p}_s) \quad \forall i \in S \tag{6.4c}$$

where $\mathbf{p}_b, \mathbf{p}_s$ are the buy and sell prices set by the aggregator which the prosumers respond to by optimizing operation as in (6.2). The aggregator aims to minimize the difference in revenue from prosumer trades and the cost of utility procurement, i.e. set a price that reflects the market equilibrium accurately.

Agent Based Modeling for Aggregations: Pricing energy in prosumer aggregations is made complex by the fact that prices that depend on prosumers' operation will in turn modify prosumers' optimal storage operation. This results in two-way dependencies between price and storage operation, which are modeled as a bilevel optimization problem in (6.4). The actions of one prosumer affect not only its own cost, but also the costs of other participants. While there are methods to solve bilevel problems efficiently [51], the actual interdependencies can not be explicitly formulated. Agent based models can be used to resolve the effects of each prosumer's actions through Monte Carlo simulations. Table 6.1 defines the elements in an agent based model of a prosumer aggregation.

Table 6.1: General elements of an agent based modeling scheme and its analogues in the prosumer aggregation model

General Element	Analogue in Prosumer Aggregation
Agent	Building, Aggregator
Decision Making Heuristic	Cost minimization
Adaptive Response	Response to changing electricity prices
Interaction Topology	Interactions with aggregator as in Figure 6.1
Environment	Utility policies, actions of other buildings in the aggregation

6.3 Results

In this section, we develop our main results on the optimal composition of prosumer aggregations. We start by making some observations on the value proposition of aggregations.

1) The value of an aggregation derives from a difference in utility buy and sell prices, i.e. $\boldsymbol{\pi}_b - \boldsymbol{\pi}_s$, and the marginal value increases with the price difference. Prosumers trading energy with each other essentially perform price arbitrage over the utility price differential, and its value exists only when the differential is non-zero.

2) The minimum social (total) cost is achieved in a centrally controlled aggregation. That cost is a lower bound for the total cost that can be achieved through any other control policy. The central authority that aims to maximize social welfare solves the optimization problem in (6.3) which has as its objective the total cost (6.3a), and only has the physical constraints on battery operation (6.3b) which would exist in any other control mechanism as well. It is the least constrained problem possible with this objective, and hence achieves the lowest possible total cost. This does not mean that each prosumer is at its individual optimum, as battery operation is optimized for social welfare which might not coincide with each prosumer's objectives.

Note: In this work, we do not consider the problem of mechanism design and instead focus on theoretical guarantees for costs for centrally controlled aggregations. Any market mechanism will achieve higher costs than these bounds, but the results will guide us in aggregation design.

We conduct the rest of our analysis for an aggregation which aims to minimize total cost. We realize that this does not capture the self interested nature of the participating prosumers, and while validating our results we will use mechanisms that use price signals to coerce socially beneficial actions from participants that are modeled as rational economic agents. Having laid down the basis of our analysis, we now set out to answer the question: what is an optimal aggregation, i.e. given a set of buildings, which ones should cooperate and decide to form an aggregation?

3) Aggregations are superadditive, i.e. larger aggregations result in higher social welfare. The largest possible aggregation achieves the lowest total cost, and adding a participant

to an aggregation will always benefit the aggregation as a whole as well as the additional participant. However, other factors may constrain the expansion of a prosumer aggregation: communication infrastructure required, willingness of participants to share information and cede control of their storage resources, and regulatory restrictions on how large social net metering aggregations can be. In that case, an existing aggregation may have to prioritize admitting some participants, and will need to identify which prosumers are good additions to the aggregation. We now state our main result which devises a metric to evaluate prosumers.

Result 21. *In order to maximize social welfare, an aggregation should preferentially add a participant k that maximizes the **degree of complementarity** to the existing participants S, i.e. has an optimally complementary consumption curve. A lower bound on the degree of complementarity can be calculated as*

$$\frac{\boldsymbol{\pi}_b^\top - \boldsymbol{\pi}_s^\top}{2} \left(\left| \sum_{i \in S} \mathbf{z}_i^* \right| + |\mathbf{z}_k^*| - \left| \sum_{i \in S} \mathbf{z}_i^* + \mathbf{z}_k^* \right| \right) \tag{6.5}$$

where $\mathbf{z}_i^*, \mathbf{z}_k^*$ are the optimal consumption curves for prosumers in the existing aggregation S and the new entrant k respectively.

Proof. The optimal social cost for a prosumer aggregation S and joint aggregation $S \cup \{k\}$ is obtained by solving (6.3), and the optimal cost for the isolated prosumer is obtained from problem (6.2). The marginal increase in social welfare from admitting a participant k is given by the decrease in social cost

$$J_S^* + J_k^*(\boldsymbol{\pi}_\mathrm{b}, \boldsymbol{\pi}_\mathrm{s}) - J_{S \cup \{k\}}^* \tag{6.6}$$

The constraints on the enlarged aggregation are the same as the constraints on the original aggregation S and the prosumer k. Using the triangle inequality and the fact that the enlarged aggregation's objective is the sum of the objectives for aggregation S and prosumer k, the objective in (6.3a) can be lower bounded by the expression in (6.5). $\square$

The gap between the actual marginal value of aggregation (6.6) and the lower value estimated by the degree of complementarity (6.5) arises from the joint optimization of the new entrant and existing aggregation. Initially, the participants are operating storage in order to maximize their own individual value, and their cooperative behavior on forming a joint aggregation improves the social welfare.

From the above, it follows that *an aggregation should preferentially invest in generation resources that maximize the degree of complementarity to the existing participants, which is lower bounded by*

$$\frac{\boldsymbol{\pi}_b^\top - \boldsymbol{\pi}_s^\top}{2} \left(\left| \sum_{i \in S} \mathbf{z}_i^* \right| + |\mathbf{g}| - \left| \sum_{i \in S} \mathbf{z}_i^* + \mathbf{g} \right| \right) \tag{6.7}$$

where $\mathbf{z}_i^*$ is defined in Result 21, and $\mathbf{g}$ is the generation curve. It also follows that *an aggregation should preferentially incentivize prosumers to shift loads which result in a consumption*

curve change that maximizes the degree of complementarity to the existing participants, which is lower bounded by

$$\frac{\boldsymbol{\pi}_b^\top - \boldsymbol{\pi}_s^\top}{2} \left(\left| \sum_{i \in S} \mathbf{z}_i^* \right| + |\Delta \mathbf{d_k}| - \left| \sum_{i \in S} \mathbf{z}_i^* + \Delta \mathbf{d_k} \right| \right) \tag{6.8}$$

where $\mathbf{z}_i^*$ is defined in Result 21, and $\Delta \mathbf{d_k}$ is the load shift.

An aggregation may have to make an initial evaluation of prosumers based on data that can be shared without privacy concerns. Empirical agent based methods require the knowledge of energy resources owned by each prosumer, which could be considered private information. Our result only uses metered consumption data, i.e. the energy exchanges with the utility ($\mathbf{z}_k$). The expression in (6.5) can be evaluated with the current net consumption curves of the aggregation and the new prosumer, and can predict which prosumers would be the most profitable partners to admit into the aggregation. This lower bound only holds for centrally controlled aggregations, and other control mechanisms may deviate from this.

The marginal reduction in cost (6.6) will be distributed within the aggregation, and a larger reduction does not necessarily mean that each individual prosumer will be better off- it just means that there is more on the table to be distributed. The metric in (6.5) depends on both the magnitude and timing of the net demand curves, and a test for complementarity can be devised that accounts for profit sharing.

6.4   Simulations

While the results in Section 6.3 are only applicable to a centrally controlled aggregation, research has been undertaken to devise transactive control schemes and market mechanisms that can influence prosumer behavior to achieve close-to-optimal social welfare. We use a transactive control scheme to verify our results, namely the *supply-demand ratio (SDR) driven price* proposed in [42] where the ratio of supply and demand determines the buy and sell prices within the aggregation. These prices depend on the aggregation's operating status, and in turn influence prosumer operation which creates the need to set them in an iterative manner to manage the mutual inter-dependencies. We design an agent based model in Python that includes the elements in Table 6.1 and can implement iterative pricing schemes.

Model Details: The prosumer behavior is modeled to optimize (6.2), and two aggregator models are considered: a market maker that solves (6.4), and a central controller that solves (6.3). The bilevel problem in (6.4) is solved in an iterative manner, where the aggregator determines a price based on the supply-demand ratio that minimizes the upper level objective and conveys it to the prosumer participants who then optimize their storage operation and convey a net consumption curve back to the aggregator. In the central controller aggregator model, the aggregator directly optimizes and controls battery operation.

Data Sources: ToU pricing is obtained from [48] and battery costs are estimated from [20]. Battery one-way efficiency is taken to be 95%. Prosumers are modeled using load data
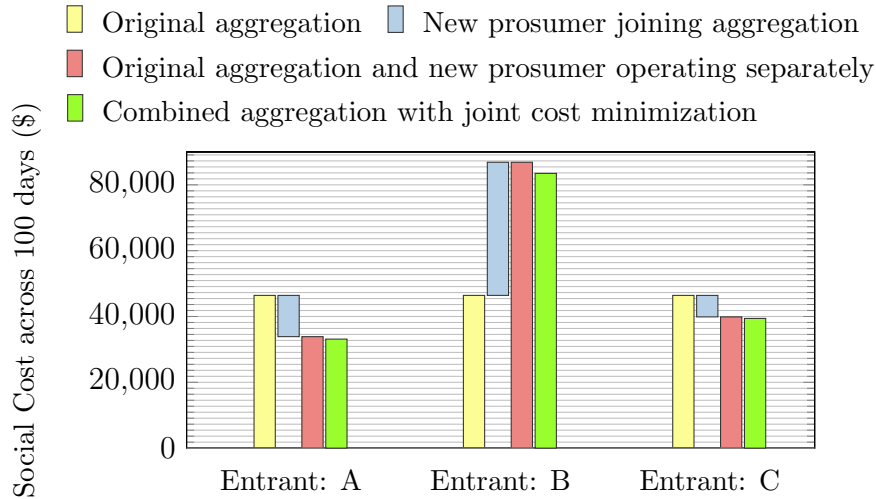
Figure 6.2: Comparison of costs for an aggregation *before* and *after* adding a new prosumer. We compare the sum of costs of the disjoint prosumer and original aggregation before the new prosumer is added (red bar) with the social cost after the new prosumer is added, i.e. when the joint cost is co-optimized (green bar). Adding a prosumer is always beneficial, but the value of each prosumer is different. Prosumer B is the most valuable entrant as its addition leads to the greatest decrease in cost (difference between red and green bars).

taken from [46] with demand of the order of $10 - 200$ kW, and the simulations use varying levels of battery installations and PV array sizes for each of the prosumers. PV energy output is estimated using [41]. To build a robust cost estimate, Monte Carlo simulations are done spanning a set of 100 days across the year to incorporate seasonal variations.

We consider an aggregation of 5 office buildings (*Original aggregation* in Fig 6.2) and evaluate three new potential participants: A, B and C. A and C are net producers, with A having a lower (negative) cost than C. B is a net consumer with a positive cost. Fig 6.2 compares the sum of costs of the new entrant and original aggregation with the cost for the joint aggregation, i.e. after the new prosumer is added to the aggregation and their costs are jointly optimized. As a validation of our remarks in Section 6.3, the cost of the combined aggregation is always lower than the sum of costs of the constituents. Further, prosumer B is the most valuable addition to the aggregation as it results in the greatest decrease in cost (difference between the red and green bars in Fig 6.2), *even though it is a net consumer and has a positive individual cost*. This indicates that estimating complementarity is not a trivial problem, and validates the importance of our result.

In Fig 6.3 we compare the marginal value (6.6) with the degree of complementarity (6.5) for two different control schemes in order to validate our main result. Result 21 aims to develop a *lower bound for the marginal value for centrally controlled aggregations*, and our simulations validate that. The central control paradigm is consistently able to achieve the
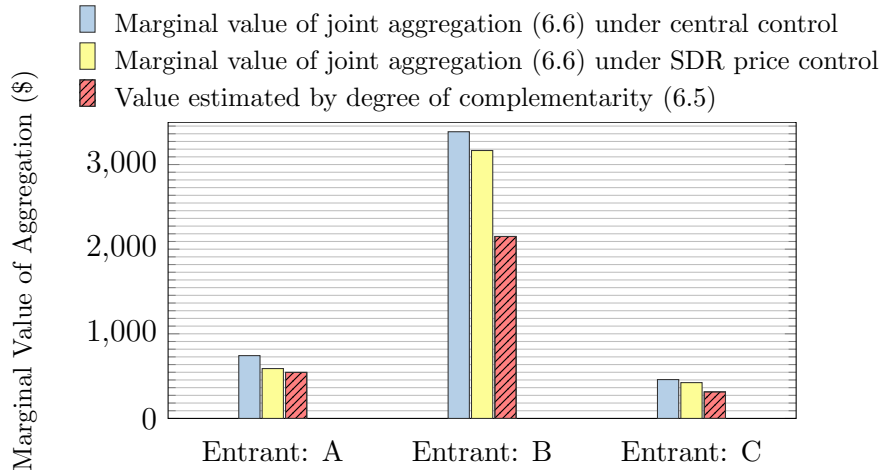
Figure 6.3: Comparison of the marginal benefit of forming a joint aggregation with a new prosumer (6.6) with the degree of complementarity of that prosumer (6.5). We compare the actual cost reduction with the estimate developed in (6.5) under two control paradigms: central and SDR price control.

highest value of aggregation, validating our remarks in Section 6.3.

The simulation results presented here are intended to serve as a validation of our theoretical results, and larger case studies might be needed to experimentally quantify the benefit of these results for a wider building population.

6.5 Discussion

In this chapter, we developed ideas around the optimal composition of aggregations and quantified the value added by new members or additional resources. Specifically, we developed a metric for the degree of complementarity of a prosumer with an existing aggregation, and extended this result to generation and load shift resources. We also validated our results with simulations in an agent based modeling framework with transactive control schemes and real building data.

We now discuss the practical implications of our result. If a profit seeking entity such as a commercial DER aggregator were to manage a prosumer aggregation, it would introduce *friction* in the system. Some of the marginal value of the aggregation would go towards profits, and any new participant would have to achieve a degree of complementarity above a minimum threshold level to guarantee a certain profit margin. From the utility's perspective, a prosumer aggregation which profits off the utility buy-sell price difference is taking a share of what would normally accrue to the utility. However, there are many reasons a utility would still permit social/virtual net-metering as described in this chapter. First, prosumers

do have some market power, as they could defect from the utility and form a microgrid with additional investment. Second, regulatory mandates could force utilities to allow such schemes, as the presence of aggregations incentivizes investments in distributed generation as well as local consumption, leading to a reduction in carbon emissions.

Chapter 7

Pricing in Prosumer Aggregations using Reinforcement Learning

In the previous chapter, we discussed what an optimal prosumer aggregation would look like by developing a metric for the degree of complementarity. In this chapter, we discuss how a similar aggregation could be managed by using reinforcement learning to set prices for energy sharing within the aggregation. The results presented in this chapter were published in [10].

7.1   Introduction

Traditional consumers like buildings are increasingly investing in distributed energy resources such as solar panels and battery backups, and electrifying loads like vehicles. These resources can be used to supply the building's own demand, shave the peak load to reduce demand charges, or to increase resiliency in the face of grid failure or power shutoff and enable consumers to become **prosumers**, i.e. be electricity *producers* as well. However, such resources may remain underutilized, or be sized over-capacity to account for weather and load variability. Prosumers can profit from trading their surplus energy with other prosumers and improving resource utilization. Utilities have typically accommodated distributed energy resources (DERs) through net-metering programs that compensate producers at the retail tariff. However, retail tariffs are much higher than wholesale energy market prices, and utilities have begun to phase out net metering programs in favor of direct market participation of DERs through aggregations. Prosumers can increase their profitability if they trade energy with other prosumers using social net-metering schemes implemented by utilities [32]. In these schemes, communities can share energy resources while presenting the net consumption to the utility as a single entity.

In this chapter, we consider prosumer aggregations that facilitate trading between participants in the aggregation, and then balance the net load by purchasing from or selling to the utility. They can be formed with a variety of motives: private entities could manage
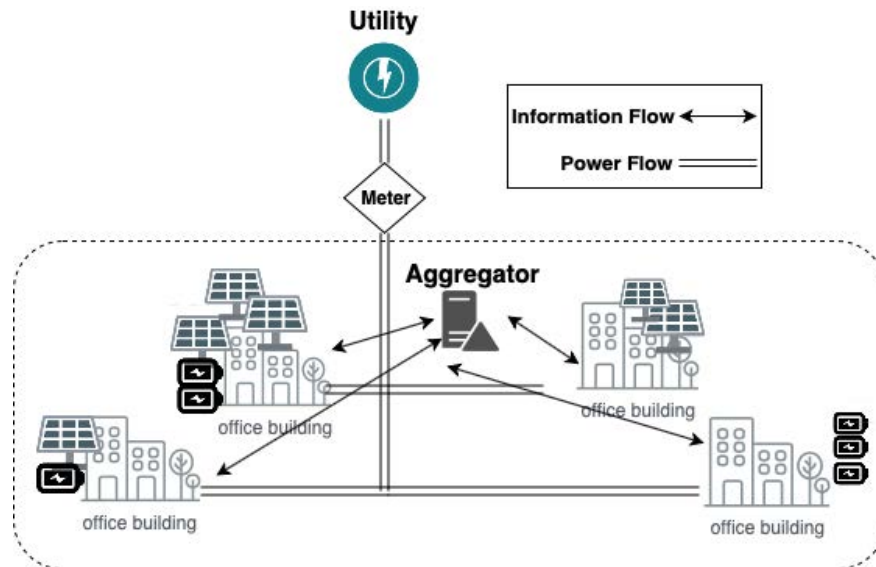
Figure 7.1: Social net metering in a prosumer aggregation

aggregations for a fee or for a profit, and participants could form cooperative aggregations to maximize social welfare. Each aggregation has control the energy consumption and production of its participants, either through direct control or through some signal which can convey operational information to the participants. Realistically, prosumers will have independent cost minimization objectives, and will seek to optimize the operation of their resources for their own profit. Coordinating independent entities which are separately owned and managed is a difficult task, and **transactive control** is a strategy which uses the price of electricity to influence the operation of prosumers. For a prosumer, responding to a day-ahead price is easier than estimating load/ generation schedules required to participate in a market, or responding to real time prices. The aggregator can communicate time-of-use rates a day ahead to aggregation participants, who can then schedule their operation in response to energy prices similar to utility time-of-use rate plans. The aggregator has the task of designing prices that achieve the aggregation's objectives while dealing with an uncertain environment: *first*, the response of prosumers to energy prices is not known to the aggregator, and *second*, loads and generation are not perfectly predictable and have inherent occupancy and weather driven uncertainty.

Pricing resources in an uncertain environment is a task well suited for a data driven controller such as an RL algorithm, which motivates our work presented in this chapter.

Contributions: We propose the use of Reinforcement Learning (RL) for pricing in local energy markets, and use it to develop a pricing mechanism that does not need explicit participant models or any operational information about prosumers. The proposed RL controller can replace iterative pricing methods commonly found in literature by learning

to estimate market settlement and profit maximizing prices for the aggregator in a one-shot manner using historical and forecast data, and motivates further research in RL based methods for pricing.

7.2 Background

In this section, we build background for the two main themes of this chapter: prosumer aggregations and RL.

Prosumer aggregations

Recent regulations have opened up multiple avenues for distributed energy resources (DERs) to participate in energy markets. However, wholesale markets have minimum participation sizes and may require DERs to construct demand and supply bids. Virtual microgrids and DER aggregations offer a pathway for prosumers to trade energy locally instead of participating in energy markets.

Researchers have worked on developing methods to control such aggregations. While microgrids have traditionally controlled distributed resources through a central authority dictating consumption/generation decisions, this can not be implemented in a situation where self-interested prosumers want to aggregate without ceding control of their operational decisions. [38] considers a microgrid central controller trying to shape the load curves of participants by employing participant differentiated real time pricing. [36] studies the problem of minimizing deviation from day ahead estimates through pricing, and [73] models a hierarchical optimization problem to solve the aggregation control problem. We model a similar hierarchical optimization in Section 7.3.

Aggregations commonly employ iterative pricing methods: [72] models prosumer trades as a Nash Bargaining problem, and solves it by decomposing it into two sequential problems which are solved iteratively using alternating direction method of multipliers (ADMM). This involves communicating price and energy consumption information back and forth between the aggregator and participants. Similarly, [42] develops a pricing model for a prosumer aggregation but settles on a price in an iterative manner. These methods have a couple of disadvantages: first, they require the participants to communicate back-and-forth with the aggregator which requires two-way communication infrastructure; second, prosumers are required to develop demand forecasts, which can unnecessarily raise the computational barrier for entry.

There is a need to devise methods to optimize the aggregator objective without relying on participant load/generation forecasts and without an iterative back and forth with prosumers, and this is the gap we try to address in this work.

Reinforcement learning

RL is a type of agent-based machine learning where a complex system is controlled through actions that optimize the system in some manner [66]. The actions seek to optimize the expected sum of rewards for actions (a_t) and states (s_t) in a policy parameterized by θ; i.e., $J(\theta) = \mathbb{E}\sum_{s_t,a_t \sim p_\pi}[r(s_t,a_t)]$. RL has been applied to a number of demand response situations in prosumer microgrids, but almost all the work centers on agents that directly schedule resources [71]. RL architectures can vary widely, for example [39] deploys a fuzzy Q-learning multi-agent that learns to coordinate appliances to increase reliability. In another illustrative example, [45] manages a battery directly using batch Q-learning. However, there are few works where the RL controller is a price setter in a market. In [44] RL has been used to estimate dynamic prices in a multi agent environment of demand response assets. To the best of our knowledge, RL has not been used to preemptively solve for equilibrium price in markets.

We propose the use of Soft Actor Critic, an RL architecture that tries to maximize the entropy of its actions to better explore the search space [30]. Actor-Critic architectures are composed of policy networks that suggest actions (*actors*) and value estimation networks that estimate the expected reward of the next state (*critics*), thereby guiding the actor network's learning [40]. How an agent prioritizes exploration vs. exploitation can be influenced by the inclusion of an entropy parameter e which is valued by an entropy maximizing framework, i.e. $J(\theta) = \mathbb{E}\sum_{s_t,a_t \sim p_\pi}[r(s_t,a_t) + w_e e]$, weighting e by some value w_e.

7.3   Methods

We model the prosumer and aggregator behavior as solutions to optimization problems, and then introduce the RL controller that we use to estimate prices in a day ahead manner.

Prosumer model

A prosumer typically has a combination of loads (flexible and inflexible), local generation and energy storage. We can denote the net energy consumption as $z^{(t)} = d^{(t)} - g^{(t)} + u^{(t)}$ where in any time period t, the prosumer has energy demand $d^{(t)}$, local generation $g^{(t)}$, and storage operation $u^{(t)}$. The prosumer purchases its net load at a time-of-use rate $\pi_b(t)$, and sells back any excess generation at $\pi_s(t)$. These prices are typically different [32], as utilities remove or disincentivize net-metering programs. The prosumer optimization problem (P-OPT) can be formulated as

$$\text{P-OPT}(\boldsymbol{\pi}_b, \boldsymbol{\pi}_s): \min_{\mathbf{u}} \quad \sum_{t=1}^{T}\left[\pi_b^{(t)} z_+^{(t)} + \pi_s^{(t)} z_-^{(t)} + \pi_{bat}|u^{(t)}|\right] \tag{7.1a}$$

$$= \boldsymbol{\pi}_b^\top \mathbf{z}_+ + \boldsymbol{\pi}_s^\top \mathbf{z}_- + \pi_{bat}\mathbf{1}_T^\top|\mathbf{u}| \tag{7.1b}$$

$$\text{s.t.} \qquad 0 \le L\mathbf{u} \le c \tag{7.1c}$$

where $\mathbf{u}$ represents the vector of battery charge/discharge over time with positive values denoting battery charging, $\boldsymbol{\pi_b},\boldsymbol{\pi_s}$ represent the time vectors of buy and sell prices, and $\mathbf{z_+},\mathbf{z_-}$ represent the time vectors for net positive demand and net negative demand (net generation) respectively. The optimization objective (7.1a) incorporates the cost of procuring any net demand z_+ at the buy price, the revenue from selling any net surplus energy generation z_- at the sell price, as well as the cost of battery degradation evaluated with π_{bat}. The constraint (7.1c) encapsulates physical constraints on the state of charge for energy storage, charging speed constraints, and the one way battery efficiency η. More details can be found in [4].

Aggregator model

Aggregators can be operated as central clearing houses where energy trades are balanced, and the net consumption is procured from the utility which acts as the outside option. All prosumers purchase their net energy needs from the aggregator at a price set by the aggregator. The aggregator is constrained in its choice of prices: if it is worse then the outside option (the utility), prosumers will have no incentive to trade with it. This constraint is encapsulated as $\boldsymbol{\pi_s} \leq \boldsymbol{\lambda_s}, \boldsymbol{\lambda_b} \leq \boldsymbol{\pi_b}$, where $\boldsymbol{\lambda_s}, \boldsymbol{\lambda_b}$ represent the aggregator-set sell and buy prices respectively. Aggregations can be formed with multiple objectives, and we explore two particular objectives: profit maximization and market balancing.

For-profit aggregator

Aggregators can aim to maximize the profit they earn for acting as a trade facilitator, and in a situation with perfect information they would solve the following bilevel optimization problem to set prices:

$$\max_{\boldsymbol{\lambda_b},\boldsymbol{\lambda_s}} \quad \left[\boldsymbol{\lambda}_b^\top \sum(\mathbf{z}_+^*) + \boldsymbol{\lambda}_s^\top \sum(\mathbf{z}_-^*)\right] - \left[\boldsymbol{\pi}_b^\top (\sum \mathbf{z}^*)_+ + \boldsymbol{\pi}_s^\top (\sum \mathbf{z}^*)_-\right] \tag{7.2a}$$

$$\text{s.t.} \qquad\qquad\qquad \boldsymbol{\pi_s} \leq \boldsymbol{\lambda_s}, \boldsymbol{\lambda_b} \leq \boldsymbol{\pi_b} \tag{7.2b}$$

$$\mathbf{z}^* = \mathbf{d} - \mathbf{g} + \mathbf{u}^*; \mathbf{u}^* = \underset{\mathbf{u}}{\arg\min}\,\text{P-OPT}(\boldsymbol{\lambda_b},\boldsymbol{\lambda_s}) \tag{7.2c}$$

where the objective in Eq. 7.2a represents the net profit for the aggregator, i.e. the revenue from sales to the prosumers minus the cost of procuring the net energy demand from the utility. $\sum(\mathbf{z}_+^*), \sum(\mathbf{z}_-^*)$ are the sum of each prosumer's demand and generation taken separately, while $(\sum \mathbf{z}^*)_+, (\sum \mathbf{z}^*)_-$ are the net demand and generation of the aggregation once all internal trades have been balanced.

Market solving aggregator

The aggregation can be set up to operate a local energy market where prosumers negotiate with each other and eventually trade at the market equilibrium price. Instead of requiring prosumers to develop demand and supply bids and engage in negotiations, the aggregator can set prices that reflect the market equilibrium in a day ahead manner. Such an aggregator
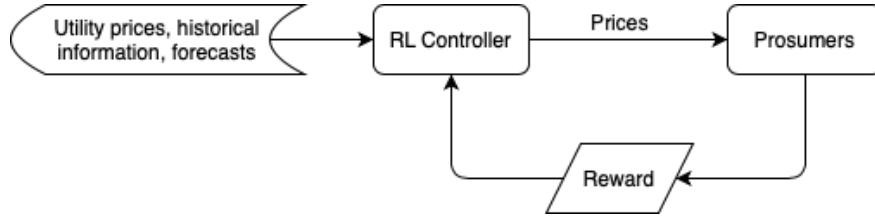
Figure 7.2: Reinforcement Learning control flow

will aim to reduce the difference between day ahead estimated price and market settlement
price, which is equivalent to ensuring a net zero profit/loss situation for the aggregator. This
problem can be formulated as

$$\min_{\boldsymbol{\lambda}_b, \boldsymbol{\lambda}_s} \quad \left| \left[\boldsymbol{\lambda}_b^\top \sum (\mathbf{z}_+^*) + \boldsymbol{\lambda}_s^\top \sum (\mathbf{z}_-^*) \right] - \left[\boldsymbol{\pi}_b^\top (\sum \mathbf{z}^*)_+ + \boldsymbol{\pi}_s^\top (\sum \mathbf{z}^*)_- \right] \right| \tag{7.3a}$$

$$\text{s.t.} \qquad\qquad \text{Eq. 7.2b, Eq. 7.2c} \tag{7.3b}$$

Note that the objective (Eq. 7.3a) is the absolute value of the objective for the for-profit
aggregator (Eq. 7.2a).

Transactive control using RL

The problems modeled in Section 7.3 are hierarchical optimization problems, and do not have
a closed-form solution without some form of information sharing between the aggregator and
prosumers. As discussed in other papers which use ADMM and iterative pricing methods
(Section 7.2), decentralized pricing methods require iterations to converge to a solution. We
develop an RL controller that relies on a day-ahead price set using historical price information
and generation forecasts. The transactive controller does not iterate over prices, and instead
learns to estimate future prices in a one-shot manner. Our search space of possible prices is
simple enough to be covered by an entropy maximizing agent, and we employ a Soft Actor-
Critic (SAC) architecture to do so. The reward for the for-profit aggregator is computed
as the objective expressed in Eq. 7.2a, and the reward for the market solving aggregator is
computed by the objective in Eq. 7.3a. We simulate the behavior of our controller under
uncertain generation forecasts and compare it to baseline iterative pricing algorithms in
Section 7.4.

7.4   Results

We will now describe our results for each of the two objectives: market solving and profit
maximization, prefaced by an explanation of our data, architecture and training process. We
model this problem after an environment to simulate demand response in office buildings

[63]. Each step in the environment is a day where the RL controller broadcasts prices to the prosumers, who modify their energy storage and consumption to minimize their costs, and the controller uses their consumption data to calculate its reward.

Implementation   We use the stable-baselines fork of OpenAI baselines [33], and our other implementation choices are detailed in our Github repository [62]. The final run presented here was distributed across 24 CPUs for 12 hours each. The Q-factor loss shown in Fig. 7.5 is one of many metrics that represents the neural network's training. The market solving controller's reward (Eq. 7.3a) is always negative. For the simulations presented in this work, the utility pricing is obtained from [48] and the prosumers considered are commercial office buildings modeled using load data taken from [46] with additional details presented in [4].

Marginal benefit of aggregation

We compare the system costs in the presence and absence of a profit-maximizing aggregator for two different levels of prosumer solar generation and battery capacity. As can be seen in Fig. 7.3, the RL controller reduces the system costs and provides value which can be distributed among the aggregator and prosumers.
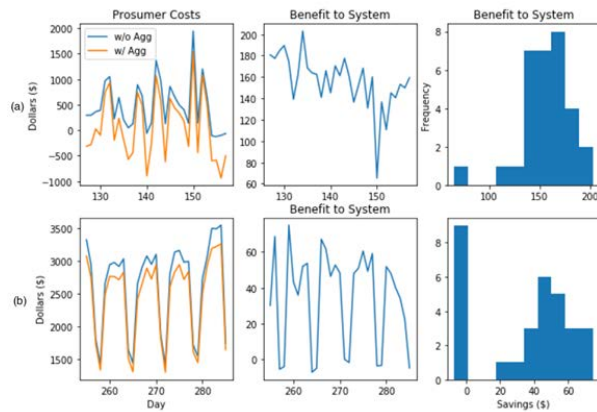
Figure 7.3: Comparing system costs, i.e. sum of aggregator and prosumer costs with and without a profit maximizing RL controller for two resource levels: a) Medium, and b) Small

Comparison with iterative pricing

We compare the market solving RL controller with an iterative pricing scheme that aims to achieve market equilibrium through back and forth negotiations with prosumers [4]. In this case, the objective is to drive the aggregator profit close to zero. The RL controller has a smoother profit on average, i.e it exhibits lower deviations than the iterative pricing

algorithm as can be seen in Fig. 7.4. We believe that expanding training and shaping the
observation space could potentially improve the performance of the RL controller.

Figure 7.4: Comparing aggregator profit for market solving prices with iterative pricing and
RL controller
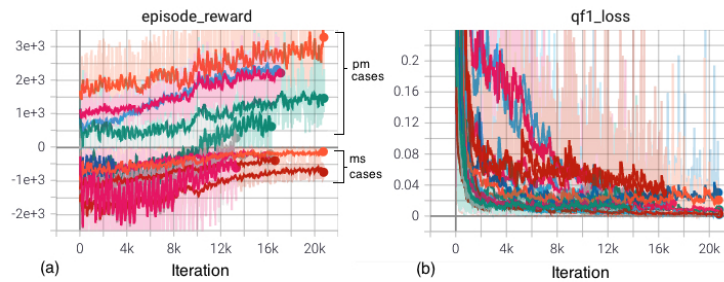
Figure 7.5: Training curves for reward and Q-factor loss. The concave shape indicates an
approach to convergence

7.5   Discussion

RL controllers are particularly well suited for dynamic data driven environments with un-
known, complex, and time-varying system models, e.g., with changing prosumer resources.
The novelty of our proposition is in using RL to preemptively price energy in local mar-
kets, but is accompanied by many challenges that will need to be addressed for practical
applicability.

Safety: An RL controller might generate prices that result in infeasible operation. We
tackle this by using utility-set prices to enforce limits on the aggregator prices $\boldsymbol{\lambda}_s, \boldsymbol{\lambda}_b \in [\boldsymbol{\pi}_s, \boldsymbol{\pi}_b]$.
An additional safety check would involve validating these prices through a single back-and-
forth communication with prosumers to ensure that their operation does not exceed system

limits. Probabilistic guarantees for RL controllers can be used [13]. Additionally, supervised RL can help guarantee safety at the outset [56].

Efficiency: While the large number of training iterations represent a greater computational burden than iterative pricing methods, the RL controller will reduce the computational burden on each individual prosumer by eliminating the need to construct forecasts or demand/supply bids. Further, each prosumer's computations occur in parallel and adding new prosumers to the aggregation does not increase the problem complexity.

Robustness: Adversarial training is a useful method to construct robust RL controllers [49], and can be extended to our setup.

Optimality: Research has been done in bounding the sub-optimality of RL policies using policy certificates [21], and research in this area can help provide guarantees for our RL controller as well.

Practical Implementation: The training iterations needed are a barrier to use of an RL controller in a prosumer aggregation in practice. However, there are numerous enhancements we propose to address this. First, *meta-learning:* a large part of the training can take place in a simulation environment which can use a rules-based heuristic as a starting point, and use exogenous parameters to create a distribution of unique systems to train on (i.e. domain randomization.) A technique like Model Agnostic Meta-Learning can train in the different simulations to approximate a starting distribution for policy network weight initializations [25]. However, the accuracy of the simulation model will determine how effective the RL controller is when it transitions to an actual aggregation. Second, *planning*: a Dyna-like auxiliary model, either generative (i.e. GANs) or predictive (i.e. regression or neural nets), could train with the agent and help augment data [67]. Third, *offline learning* can incorporate data from other microgrids using techniques in the causal methods literature to help adequately perform the data fusion necessary[26]. However, validating these ideas will require more work.

In practice, either formulation of the aggregator could be implemented: a profit-seeking entity could operate the controller, or a prosumer cooperative could aim to facilitate trades between members. In this work, we model the utility as the outside alternative. As prosumer aggregations grow larger, they may participate in wholesale energy markets instead of purchasing energy from utilities, and will have to adapt to variable energy market prices as well as having to generate estimates of their own consumption and production. RL algorithms have been previously used to optimize market participation, and these would be complementary to the model we present here. The use of reinforcement learning for pricing continues to be an active area of research, with follow up studies conducted in [35].

Chapter 8

Conclusion

8.1 Summary

This thesis summarizes a few key challenges associated with three main trends shaping the transition to a low-emissions grid: the rise of distributed energy resources, the need for demand side flexibility, and the intersection of the transportation and power network. Each of the chapters in this thesis examines a specific challenge, and presents a potential solution.

The first part of the thesis focuses on challenges associated with harnessing demand side flexibility, both for aggregators participating in electricity markets and for climate conscious consumers. These challenges are particularly relevant due to the rise of clean electricity generation, which is intermittent and uncontrollable. Power system operators will increasingly rely on demand side flexibility to accommodate the variability on the supply side, and flexible consumers can harness this resource both to earn money and to reduce their carbon footprint. In Chapter 2, we discussed problems related to optimizing demand response participation for flexible consumers in utility contract programs, and presented a complementarity metric which can be used to form optimal aggregations of flexible consumers. In Chapter 3, we discussed how flexible energy consumption can also have an impact on CO_2 emissions by prioritizing the time periods at which consumers shift and shed loads.

The second part of this thesis focuses on electrified transportation and the intersection of this new resource with the power network. The vast majority of new battery capacity will be embedded in electric vehicles, and it is essential that power system operators harness this *mobile* storage capacity optimally. In Chapter 4, we discussed how electric vehicle batteries can participate in the power network as mobile storage. We considered this new resource from the power system operator's perspective, derived expressions for the marginal value of the mobile storage resource, and developed algorithms for optimal relocation. In Chapter 5, we considered an electric vehicle battery sharing game, where owners can choose to use their batteries and participate as mobile storage in power networks. We modeled two different types of EV behaviors, analyzed the equilibrium operation and put it in the context of the social welfare.

The third part of the thesis deals with *prosumers*, i.e., consumers that have *production* capability through on-site generation and storage. Prosumers can increase the utilization of their onsite resources by forming local energy markets (aggregations), where the setup and operation of such aggregations is an open research question. In Chapter 6, we considered prosumer aggregations, how they can help incentivize greater investment in distributed energy resources, and how prosumer aggregations can be set up in an optimal manner. In Chapter 7, we turned to the problem of operating these prosumer aggregations, and devised a reinforcement learning mechanism to set prices in prosumer aggregations in order to maximize either aggregator profit or social welfare.

8.2   Open Challenges

This thesis touched on specific questions associated with each of the three trends affecting the transition to a low-emissions grid. However, there remain open questions associated with each of these trends.

Demand side flexibility

One big hurdle in utilizing demand side flexibility as a resource in the power grid is its low reliability. Utility and power system operators do not have the confidence that consumers will reliably and adequately curtail their energy consumption when called upon to do so. Further, they do not have accurate estimates of what the load curtailment will be, even in a probabilistic sense. Power system operators and utilities can only schedule resources that they have a certain level of insight into, for example through forecasts or uncertainty spreads. In order to make demand side flexibility a reliable resource for the power grid, it is essential that forecasting models for flexible load capability are developed.

These forecasts are also useful for flexible consumers that are bidding into demand response programs, as they can be used to improve the profits that consumers earn from their participation in these programs. Additionally, flexibility forecasts are necessary in order to optimize the emissions impact of flexible energy consumption, since the efficacy and optimal timing of the load shift or load shed actions depends on the amount and type of flexible load available at each time period.

Alongside improving forecasts, it is important to bring more flexible loads 'online', i.e., make them capable of providing demand side flexibility at short notice. There are multiple technological challenges associated with unlocking new sources of demand side flexibility, such as the need for advances in controls and communications infrastructure through which we can make existing devices 'smart', i.e., capable of modulating their energy consumption in response to an outside signal. Further, there are new flexible resources coming online each day as loads such as vehicles and heat pumps are electrified, and they can act as additional sources of demand side flexibility. These newly electrified loads will have different patterns of energy consumption than existing loads in the power network, and it may be necessary

to develop new market mechanisms in order to accommodate the specific kind of flexibility that they can offer.

Electric vehicles and the power network

With the increase in the share of electric vehicles in the transportation network, electric vehicle charging will be the fastest growing end-use load for the power system. Power system operators and utilities are already struggling to accommodate this new load, particularly in congested sections of the distribution grid. However, electric vehicles are not only an additional load, but also a resource due to the embedded batteries which can be harnessed by the power system operator. Utilities across the world are running pilots and testing programs to figure out what the optimal model of engagement with electric vehicles should be. Given that we are in the early stages of electric vehicle penetration, there is no clear winner among the possible modes of engagement - whether it will be driven through third party platforms that enable electric vehicles to participate in power markets, or through special programs run by utilities and distribution system operators.

There are three main ways in which electric vehicles can interface with the power network. The first is through their function as an electricity consumer, i.e., through their charging operation. Accommodating this new load is an infrastructure problem, as both generation and transmission/distribution capacity will need to be ramped up to get electricity to the EV batteries that need it. Managed charging is increasingly being explored as a solution to a myriad of problems - being able to shift the time of charging can enable electric vehicles to use cleaner and cheaper electricity, and help system operators avoid expensive upgrades. There are multiple models to encourage managed charging, like imposing dynamic/time-varying retail tariffs for EVs, providing one-off incentives, and directly controlling charge flow for centrally managed charging networks.

The second way for electric vehicles to participate in the power network is as stationary storage. Bus and truck fleets have predictable schedules and downtimes, and the batteries embedded in them can be used as grid connected storage when they're parked. Car manufacturers such as Ford have already rolled out car models whose batteries can be used as stationary storage to power homes in case of grid outages. It remains to be seen whether electric vehicle batteries will predominantly be used as backup or emergency batteries, or whether they will actively engage in electricity markets as stationary storage.

The third model of engagement for electric vehicles is by acting as mobile storage in the power network. In Chapters 4 and 5, we talked about how the power system operator and individual EV drivers will approach the mobile storage resource. However, simulations conducted on a section of the power grid in the PJM territory show that a passenger EV acting as mobile storage would not make much money [9]. Currently, the costs of using high energy-density Li-ion batteries embedded in electric vehicles as mobile storage outweigh the monetary value. However, with changing grid congestion conditions, mobile storage in the form of moving EVs could become a valuable resource in certain parts of the grid at certain times of the year, particularly as an alternative during critical emergencies. Additionally,

shifting energy consumption across time and locations can also be thought of as mobile storage. For example, if an EV driver chooses to charge their car at their workplace during the afternoon instead of at home during the night, that action can be thought of as a 'mobile battery': injecting power into the grid near the driver's home at night, and then drawing power from the grid near the driver's workplace during the day. Such load shift actions can be modeled using the mobile storage formulation in Chapter 4, and can be considerably cheaper to implement.

Prosumers

One of the ways in which distributed energy resources will participate in the larger power network is through local energy markets and aggregations. There are other market participation models, e.g., through direct market participation of a share of the resource. While there have been many pilots and test beds for prosumer aggregations, there are few functioning examples of such local energy markets in practice. Part of that is due to the regulatory environment around such aggregations. Recently, there have been strides towards incorporating virtual power plants, i.e., collections of distributed resources functioning as a power supplier into the larger power grid. The profitability of such aggregations remains to be seen, and will be impacted by the reliability and availability of the constituent resources.

The other aspect of prosumer aggregations is the control mechanism or pricing algorithm that influences prosumers' actions. We presented a reinforcement learning (RL) controller to set prices in such an aggregation; however, the use of RL for pricing faces challenges in implementation. Utilities are regulated on safety and reliability, and consumers are unlikely to accept prices that are not interpretable, particularly if they come from a black box machine learning model. Further research on setting prices that are fair and have optimality guarantees is necessary, and remains an active area of research.

8.3   The Big Picture

The move to clean energy sources is driving a transition in power systems across the world, and distributed energy resources which are variable and operated independently will need new market participation models to integrate with the power grid. These models include direct participation in wholesale markets, as we discussed for mobile storage, or local energy markets as we discussed for prosumers. Another form of participation can be through specific contract mechanisms for a specialized service, as discussed for demand response. There is work being done to figure out which new participation model will work best for each resource, both in academic literature and through pilots run by power system stakeholders. As the market matures, new technologies emerge and cost curves change, the participation model for each kind of resource might change as well.

Another aspect of these resources is that they can serve as alternatives to traditional infrastructure. In this role, they can enable a power system transition from a centrally

controlled system with high inertia generators to a distributed, variable and intermittent resource mix. For example, demand side flexibility and batteries can be used to maintain the power balance on the grid, mobile storage can serve as an alternative to transmission line capacity or other forms of storage, and setting up local energy markets can be an alternative to expanding transmission and distribution infrastructure.

For each of these resources, the most valuable service that they can provide to the power system and the optimal participation model to enable that service will depend on the grid conditions: the renewables penetration, the system configuration and market regulations that govern it. In the move to a clean power grid, the rise of distributed energy resources, the need for demand side flexibility, and the participation of electric vehicles in the power grid will enable a market transition with new participation models and market mechanisms.

Bibliography

[1]   URL: https://dataminer2.pjm.com/feed/da%5C_hrl%5C_lmps.

[2]   URL: https://afdc.energy.gov/fuels/electricity%5C_charging%5C_home.html.

[3]   United States Environmental Protection Agency. *EPA Greenhouse Gas Inventory Data Explorer*. URL: https://cfpub.epa.gov/ghgdata/inventoryexplorer/#allsectors/allsectors/allgas/econsect/current.

[4]   Utkarsha Agwan. "Optimal Prosumer Aggregations: Design and Modeling". In: (2020).

[5]   Utkarsha Agwan, Samuel Bobick, Srinath Rangan, Kameshwar Poolla, and Costas J Spanos. "Time Varying Marginal Emissions Intensity of Energy Consumption: Implications for Flexible Loads". In: *Findings* (2023).

[6]   Utkarsha Agwan, Kameshwar Poolla, and Costas J Spanos. "Optimal Composition of Prosumer Aggregations". In: *2021 IEEE PES Innovative Smart Grid Technologies Europe (ISGT Europe)*. IEEE. 2021, pp. 1–5.

[7]   Utkarsha Agwan, Junjie Qin, Kameshwar Poolla, and Pravin Varaiya. "Electric vehicle battery sharing game for mobile energy storage provision in power networks". In: *2022 IEEE 61st Conference on Decision and Control (CDC)*. IEEE. 2022, pp. 6364–6370.

[8]   Utkarsha Agwan, Junjie Qin, Kameshwar Poolla, and Pravin Varaiya. "Marginal Value of Mobile Energy Storage in Power Network". In: *2021 60th IEEE Conference on Decision and Control (CDC)*. IEEE. 2021, pp. 4936–4943.

[9]   Utkarsha Agwan, Junjie Qin, Kameshwar Poolla, and Pravin Varaiya. "Mobile Energy Storage in Power Network: Marginal Value and Optimal Operation". In: *arXiv preprint arXiv:2303.09704* (2023).

[10] Utkarsha Agwan, Lucas Spangher, William Arnold, Tarang Srivastava, Kameshwar Poolla, and Costas J Spanos. "Pricing in prosumer aggregations using reinforcement learning". In: *Proceedings of the Twelfth ACM International Conference on Future Energy Systems*. 2021, pp. 220–224.

[11] Utkarsha Agwan, Costas J Spanos, and Kameshwar Poolla. "Asset Participation and Aggregation in Incentive-Based Demand Response Programs". In: *2021 IEEE International Conference on Communications, Control, and Computing Technologies for Smart Grids (SmartGridComm)*. IEEE. 2021, pp. 89–94.

[12] Utkarsha Agwan, Costas J Spanos, and Kameshwar Poolla. "Optimizing participation of buildings and aggregations in incentive-based demand response programs". In: *Proceedings of the 9th ACM International Conference on Systems for Energy-Efficient Buildings, Cities, and Transportation*. 2022, pp. 278–279.

[13] Edoardo Bacci and David Parker. "Probabilistic guarantees for safe deep reinforcement learning". In: *International Conference on Formal Modeling and Analysis of Timed Systems*. Springer. 2020, pp. 231–248.

[14] Eilyan Bitar, Pramod Khargonekar, and Kameshwar Poolla. "On the marginal value of electricity storage". In: *Systems & Control Letters* 123 (2019), pp. 151–159.

[15] Subhonmesh Bose and Eilyan Bitar. "The marginal value of networked energy storage". In: *arXiv preprint arXiv:1612.01646* (2016).

[16] Raffaele Carli, Mariagrazia Dotoli, and Vittorio Palmisano. "A distributed control approach based on game theory for the optimal energy scheduling of a residential microgrid with shared generation and storage". In: *2019 IEEE 15th International Conference on Automation Science and Engineering (CASE)*. IEEE. 2019, pp. 960–965.

[17] Cara Carmichael, James Mandel, Henry Richardson, Edie Taylor, and Connor Usry. *The Carbon Emissions Impact of Demand Flexibility*. Tech. rep. RMI, 2021. URL: `rmi.org/our-work/buildings/`.

[18] McKinsey & Co. "Battery 2030: Resilient, sustainable, and circular". In: (2023).

[19] Christopher M Colson and M Hashem Nehrir. "Algorithms for distributed decision-making for multi-agent microgrid power management". In: *2011 IEEE Power and Energy Society General Meeting*. IEEE. 2011, pp. 1–8.

[20] Claire Curry. *Lithium-Ion Battery Costs and Market*. 2017. URL: `data.bloomberglp.com/bnef/sites/14/2017/07/BNEF-Lithium-ion-battery-costs-and-market.pdf`.

[21] Christoph Dann, Lihong Li, Wei Wei, and Emma Brunskill. "Policy certificates: Towards accountable reinforcement learning". In: *International Conference on Machine Learning*. PMLR. 2019, pp. 1507–1516.

[22] YS Foo Eddy, Hoay Beng Gooi, and Shuai Xun Chen. "Multi-agent system for distributed management of microgrids". In: *IEEE Transactions on power systems* 30.1 (2014), pp. 24–34.

[23] Consolidated Edison. *Commercial Demand Response Program Guidelines*. 2021.

[24] *FERC Order 745*. https://www.ferc.gov/sites/default/files/2020-06/Order-745.pdf. 2011.

[25] Chelsea Finn, Pieter Abbeel, and Sergey Levine. "Model-Agnostic Meta-Learning for Fast Adaptation of Deep Networks". In: *CoRR* abs/1703.03400 (2017). arXiv: `1703.03400`. URL: `http://arxiv.org/abs/1703.03400`.

[26] Andrew Forney and Elias Bareinboim. "Counterfactual Randomization: Rescuing Experimental Studies from Obscured Confounding". In: *Proceedings of the AAAI Conference on Artificial Intelligence* 33.01 (July 2019), pp. 2454–2461. DOI: `10.1609/aaai.v33i01.33012454`. URL: `https://ojs.aaai.org/index.php/AAAI/article/view/4090`.

[27] Natalie Mims Frick, Eric Wilson, Janet Reyna, Andrew Parker, Elaina Present, Janghyun Kim, Tianzhen Hong, Han Li, and Tom Eckman. "End-Use Load Profiles for the US Building Stock: Market Needs, Use Cases, and Data Gaps". In: (2019).

[28] L. Gacitua, P. Gallegos, R. Henriquez-Auba, A. Lorca, M. Negrete-Pincetic, D. Olivares, A. Valenzuela, and G. Wenzel. "A comprehensive review on expansion planning: Models and tools for energy policy analysis". In: *Renewable and Sustainable Energy Reviews* 98 (2018), pp. 346–360. ISSN: 1364-0321. DOI: `https://doi.org/10.1016/j.rser.2018.08.043`. URL: `https://www.sciencedirect.com/science/article/pii/S1364032118306269`.

[29] Brian Gerke, Giulia Gallo, Sarah Smith, Jingjing Liu, Peter Alstone, Shuba Raghavan, Peter Schwartz, Mary Ann Piette, Rongxin Yin, and Sofia Stensson. "The California demand response potential study, phase 3: final report on the shift resource through 2030". In: (2020).

[30] Tuomas Haarnoja, Aurick Zhou, Pieter Abbeel, and Sergey Levine. "Soft actor-critic: Off-policy maximum entropy deep reinforcement learning with a stochastic actor". In: *International Conference on Machine Learning*. PMLR. 2018, pp. 1861–1870.

[31] Guannan He, Jeremy Michalek, Soummya Kar, Qixin Chen, Da Zhang, and Jay F Whitacre. "Utility-Scale Portable Energy Storage Systems". In: *Joule* 5.2 (2021), pp. 379–392.

[32] Rodrigo Henriquez-Auba, Patricia Pauli, Dileep Kalathil, Duncan S Callaway, and Kameshwar Poolla. "The Sharing Economy for Residential Solar Generation". In: *2018 IEEE Conference on Decision and Control (CDC)*. IEEE. 2018, pp. 7322–7329.

[33] Ashley Hill, Antonin Raffin, Maximilian Ernestus, Adam Gleave, Anssi Kanervisto, Rene Traore, Prafulla Dhariwal, Christopher Hesse, Oleg Klimov, Alex Nichol, Matthias Plappert, Alec Radford, John Schulman, Szymon Sidor, and Yuhuai Wu. *Stable Baselines*. `https://github.com/hill-a/stable-baselines`. 2018.

[34] International Energy Agency. *Global EV Outlook 2021*. Tech. rep. IEA Paris, Note = `https://www.iea.org/reports/global-ev-outlook-2021`, year = 2021.

[35] Doseok Jang, Lucas Spangher, Tarang Srivistava, Manan Khattar, Utkarsha Agwan, Selvaprabu Nadarajah, and Costas Spanos. "Offline-online reinforcement learning for energy pricing in office demand response: lowering energy and data costs". In: *Proceedings of the 8th ACM International Conference on Systems for Energy-Efficient Buildings, Cities, and Transportation*. 2021, pp. 131–139.

[36] Liyan Jia, Qing Zhao, and Lang Tong. "Retail pricing for stochastic demand with unknown parameters: An online machine learning approach". In: *2013 51st Annual Allerton Conference on Communication, Control, and Computing (Allerton)*. IEEE. 2013, pp. 1353–1358.

[37] Dileep Kalathil, Chenye Wu, Kameshwar Poolla, and Pravin Varaiya. "The sharing economy for the electricity storage". In: *IEEE Transactions on Smart Grid* (2017).

[38] Seung-Jun Kim and Geogios B Giannakis. "An online convex optimization approach to real-time energy pricing for demand response". In: *IEEE Transactions on Smart Grid* 8.6 (2016), pp. 2784–2793.

[39] P. Kofinas, A.I. Dounis, and G.A. Vouros. "Fuzzy Q-Learning for multi-agent decentralized energy management in microgrids". In: *Applied Energy* 219 (2018), pp. 53–67. ISSN: 0306-2619. DOI: https://doi.org/10.1016/j.apenergy.2018.03.017. URL: https://www.sciencedirect.com/science/article/pii/S0306261918303465.

[40] Vijay R Konda and John N Tsitsiklis. "Actor-critic algorithms". In: *Advances in neural information processing systems*. Citeseer. 2000, pp. 1008–1014.

[41] National Renewable Energy Laboratory. *NREL PVWatts Calculator Tool*. URL: https://pvwatts.nrel.gov.

[42] Nian Liu, Xinghuo Yu, Cheng Wang, Chaojie Li, Li Ma, and Jinyong Lei. "Energy-sharing model with price-based demand response for microgrids of peer-to-peer prosumers". In: *IEEE Transactions on Power Systems* 32.5 (2017), pp. 3569–3583.

[43] Zhenhua Liu, Minghong Lin, Adam Wierman, Steven H. Low, and Lachlan L.H. Andrew. "Greening Geographical Load Balancing". In: *Proceedings of the ACM SIGMETRICS Joint International Conference on Measurement and Modeling of Computer Systems*. SIGMETRICS '11. San Jose, California, USA: Association for Computing Machinery, 2011, pp. 233–244. ISBN: 9781450308144. DOI: 10.1145/1993744.1993767. URL: https://doi.org/10.1145/1993744.1993767.

[44] Renzhi Lu, Seung Ho Hong, and Xiongfeng Zhang. "A dynamic pricing demand response algorithm for smart grid: reinforcement learning approach". In: *Applied Energy* 220 (2018), pp. 220–230.

[45] Brida V. Mbuwir, Frederik Ruelens, Fred Spiessens, and Geert Deconinck. "Battery Energy Management in a Microgrid Using Batch Reinforcement Learning". In: *Energies* 10.11 (2017). ISSN: 1996-1073. URL: https://www.mdpi.com/1996-1073/10/11/1846.

[46] Clayton Miller and Forrest Meggers. "The Building Data Genome Project: An open, public data set from non-residential building electrical meters". In: *Energy Procedia* 122 (2017), pp. 439–444.

[47] National Regulatory Research Institute. *Getting the signals straight: Modeling, planning, and implementing non-transmission alternatives*. https://pubs.naruc.org/pub/FA86CD02-A0F1-EADA-2240-D4932060892F. 2015.

[48] OpenEI. *Time of Use pricing*. 2017. URL: https://openei.org/apps/USURDB/rate/view/5cbf78b25457a34e40671081#3__Energy (visited on 05/02/2017).

[49] Anay Pattanaik, Zhenyi Tang, Shuijing Liu, Gautham Bommannan, and Girish Chowdhary. "Robust deep reinforcement learning with adversarial attacks". In: *arXiv preprint arXiv:1712.03632* (2017).

[50] Amol Phadke, Nikit Abhyankar, Jessica Kersey, Taylor McNair, Umed Paliwal, David Wooley, Olivia Ashmoore, Robbie Orvis, Michael O'Boyle, Ric O'Connell, Utkarsha Agwan, Priyanka Mohanty, Priya Sreedharan, and Deepak Rajagopal. *2035 Report 2.0: Plummeting Costs and Dramatic Improvements In Batteries Can Accelerate Our Clean Transportation Future*. Tech. rep. University of California, Berkeley, 2021. URL: https://www.2035report.com/transportation/.

[51] S Pineda, H Bylling, and JM Morales. "Efficiently solving linear bilevel programming problems using off-the-shelf optimization software". In: *Optimization and Engineering* 19.1 (2018), pp. 187–211.

[52] J. Qin, I. Yang, and R. Rajagopal. "Submodularity of Storage Placement Optimization in Power Networks". In: *IEEE Transactions on Automatic Control* 64.8 (2019), pp. 3268–3283. DOI: 10.1109/TAC.2018.2882489.

[53] Junjie Qin, Sen Li, Kameshwar Poolla, and Pravin Varaiya. "Distributed storage investment in power networks". In: *2019 American Control Conference (ACC)*. IEEE. 2019, pp. 1579–1586.

[54] Junjie Qin, Kameshwar Poolla, and Pravin Varaiya. "Mobile storage for demand charge reduction". In: *IEEE Transactions on Intelligent Transportation Systems* (2021).

[55] Mike Quashie, Chris Marnay, François Bouffard, and Géza Joós. "Optimal planning of microgrid power and operating reserve capacity". In: *Applied Energy* 210 (2018), pp. 1229–1236.

[56] M. Rosenstein and A. Barto. *Supervised Learning Combined with an Actor-Critic Architecture TITLE2:* tech. rep. USA, 2002.

[57] Federico Rossi, Ramon Iglesias, Mahnoosh Alizadeh, and Marco Pavone. "On the interaction between Autonomous Mobility-on-Demand systems and the power network: Models and coordination algorithms". In: *IEEE Transactions on Control of Network Systems* 7.1 (2019), pp. 384–397.

[58] Walid Saad, Zhu Han, and H Vincent Poor. "Coalitional game theory for cooperative micro-grid distribution networks". In: *2011 IEEE international conference on communications workshops (ICC)*. IEEE. 2011, pp. 1–5.

[59] Pedram Samadi, Hamed Mohsenian-Rad, Robert Schober, and Vincent WS Wong. "Advanced demand side management for the future smart grid using mechanism design". In: *IEEE Transactions on Smart Grid* 3.3 (2012), pp. 1170–1180.

[60] Andrew Sendy. *What is Virtual Net Metering and who is it for?* 2019. URL: https://www.solar-estimate.org/news/what-is-virtual-net-metering-and-who-is-it-for.

[61] Pierluigi Siano. "Demand response and smart grids—A survey". In: *Renewable and sustainable energy reviews* 30 (2014), pp. 461–478.

[62] Lucas Spangher, Utkarsha Agwan, William Arnold, and Tarang Srivastava. 2021. URL: https://github.com/utkarshapets/microgrid-RL.

[63] Lucas Spangher, Akash Gokul, Joseph Palakapilly, Utkarsha Agwan, Manan Khattar, Wann-Jiun Ma, and Costas Spanos. "OfficeLearn: An OpenAI Gym Environment for Reinforcement Learning on Occupant-Level Building's Energy Demand Response". In: *Tackling Climate Change with Artificial Intelligence Workshop at NeurIPS, 2020.* 2020.

[64] Christoph Steitz. *Nissan Leaf gets approval for vehicle-to-grid use in Germany.* https://www.reuters.com/article/us-autos-electricity-germany/nissan-leaf-gets-approval-for-vehicle-to-grid-use-in-germany-idUSKCN1MX1AH. 2018.

[65] P. Sterchele, A. Palzer, and H. Henning. "Electrify Everything?: Exploring the Role of the Electric Sector in a Nearly CO_2-Neutral National Energy System". In: *IEEE Power and Energy Magazine* 16.4 (2018), pp. 24–33. DOI: 10.1109/MPE.2018.2824100.

[66] Richard S Sutton and Andrew G Barto. *Reinforcement learning: An introduction.* MIT press, 2018.

[67] Richard S. Sutton. "Dyna, an Integrated Architecture for Learning, Planning, and Reacting". In: *SIGART Bull.* 2.4 (July 1991), pp. 160–163. ISSN: 0163-5719. DOI: 10.1145/122344.122377. URL: https://doi.org/10.1145/122344.122377.

[68] J. A. Taylor. "Financial Storage Rights". In: *IEEE Transactions on Power Systems* 30.2 (2015), pp. 997–1005.

[69] United States Environmental Protection Agency. *Inventory of U.S. Greenhouse Gas Emissions and Sinks.* Tech. rep. https://www.epa.gov/ghgemissions/inventory-us-greenhouse-gas-emissions-and-sinks. 2020.

[70] US Internal Revenue Service. *Standard Mileage Rates.*

[71] José R Vázquez-Canteli and Zoltan Nagy. "Reinforcement learning for demand response: A review of algorithms and modeling techniques". In: *Applied energy* 235 (2019), pp. 1072–1089.

[72] Hao Wang and Jianwei Huang. "Incentivizing energy trading for interconnected microgrids". In: *IEEE Transactions on Smart Grid* 9.4 (2016), pp. 2647–2657.

[73] Yu Wang, Shiwen Mao, and R Mark Nelms. "On hierarchical power scheduling for the macrogrid and cooperative microgrids". In: *IEEE Transactions on Industrial Informatics* 11.6 (2015), pp. 1574–1584.

[74] WattTime. *Marginal Emissions Modeling: WattTime's approach to modeling and validation.* Tech. rep. WattTime, 2022. URL: `https://www.watttime.org/app/uploads/2022/10/WattTime-MOER-modeling-20221004.pdf`.

[75] WattTime. *WattTime Core API.* 2023. URL: `https://www.watttime.org/api-documentation/`.

[76] Wood Mackenzie. *US energy storage market shatters records in Q3 2020.* `https://www.woodmac.com/press-releases/us-energy-storage-market-shatters-records-in-q3-2020/`. 2020.

[77] Di Wu, Xu Ma, Sen Huang, Tao Fu, and Patrick Balducci. "Stochastic optimal sizing of distributed energy resources for a cost-effective and resilient Microgrid". In: *Energy* 198 (2020), p. 117284.

[78] F. Wu, P. Varaiya, P. Spiller, and S. Oren. "Folk theorems on transmission access: Proofs and counterexamples". In: *Journal of Regulatory Economics* 10.1 (1996), pp. 5–23.

[79] Yahoo Finance. *Con Edison Storing the Future for Energy Customers.* `https://finance.yahoo.com/news/con-edison-storing-future-energy-161632992.html`. 2017.

[80] Yu Yang, Utkarsha Agwan, Guoqiang Hu, and Costas J Spanos. "Selling Renewable Utilization Service to Consumers via Cloud Energy Storage". In: *arXiv preprint arXiv:2012.14650* (2020).

[81] Dongwei Zhao, Hao Wang, Jianwei Huang, and Xiaojun Lin. "Virtual energy storage sharing and capacity allocation". In: *IEEE transactions on smart grid* 11.2 (2019), pp. 1112–1123.

[82] Joshua S Graff Zivin, Matthew J Kotchen, and Erin T Mansur. "Spatial and temporal heterogeneity of marginal emissions: Implications for electric cars and other electricity-shifting policies". In: *Journal of Economic Behavior & Organization* 107 (2014), pp. 248–268.

Appendix A

Examples and Proofs for Ch. 4

A.1 Numerical Examples for Section 4.4

Numerical case for Example 2 Consider a two-period economic dispatch problem for a three bus network, with nodes 1,2,3 as in Fig. 4.2. Assume the system is equipped with a stationary battery of capacity 0.5 at node 1, and a mobile battery of capacity 0.5 which is located at node 3 in the first period and at node 1 in the second period. Further, assume each node has power generation with a quadratic cost function $C_i(g_i(t)) = g_i(t)^2$, and each of the lines has an identical susceptance value and capacity of 0.5. The energy demand of this system is concentrated at node 1, with a demand of 5 in the first period, and 10 in the second period. In this situation, both line $2 \rightarrow 1$ and line $3 \rightarrow 1$ are congested in time period 1. The LMPs for the two periods are $\lambda_1(1) = 9, \lambda_3(1) = 2, \lambda_1(2) = 16$, which means that $\mathsf{MV}^{\mathrm{ms}}(1) = \lambda_1(2) - \lambda_3(1) = 14$, $\mathsf{MV}^{\mathrm{ss}}(1) = \lambda_1(2) - \lambda_1(1) = 7$. Meanwhile, $\mathsf{MV}^{\mathrm{w}}(1) = \beta_{3 \rightarrow 1}(1) = 6$, and $\mathsf{MV}^{\mathrm{w}}(1) + \mathsf{MV}^{\mathrm{ss}}(1) = 13 < \mathsf{MV}^{\mathrm{ms}}(1)$.

Numerical case for Example 3 Consider the same setup as in a) but with a different demand. The demand of the system in the first time period is 5 units each at node 1 and 2, and 10 units at node 1 in the second period. In this situation, both line $3 \rightarrow 1$ and line $3 \rightarrow 2$ are congested in time period 1. The LMPs for the two periods are $\lambda_1(1) = 10, \lambda_3(1) = 3, \lambda_1(2) = 16$, which means that $\mathsf{MV}^{\mathrm{ms}}(1) = \lambda_1(2) - \lambda_3(1) = 13$, $\mathsf{MV}^{\mathrm{ss}}(1) = \lambda_1(2) - \lambda_1(1) = 6$. Meanwhile, $\mathsf{MV}^{\mathrm{w}}(1) = \beta_{3 \rightarrow 1}(1) = 8$, and $\mathsf{MV}^{\mathrm{w}}(1) + \mathsf{MV}^{\mathrm{ss}}(1) = 14 > \mathsf{MV}^{\mathrm{ms}}(1)$.

A.2 Proofs for Section 4.4

Proof for Theorem 4 From the Lagrangian of the economic dispatch problem in (4.15), we get that $\mathsf{MV}_k^{\mathrm{ms}}(\mathfrak{E}, \overline{\mathbf{s}}) = \mathbf{1}^\top \boldsymbol{\mu}_k$. Further, from the stationarity KKT condition with respect to $u_k(t)$, we get

$$L_t^\top (\boldsymbol{\mu}_k - \boldsymbol{\nu}_k) = -\gamma(t) + E_k(t)^\top H^\top \boldsymbol{\beta}(t),$$

where $L_t^\top$ is the tth column of $L^\top$, and $E_k(t)$ is the kth column of $E(t)$. At any time, only one of the pair of constraints in (4.15d) will be binding. Hence, either $\mu_k(t) = 0$ or $\nu_k(t) = 0$. Using the definition of $\boldsymbol{\lambda}(t)$ from (4.17), we get the expression in (4.18).

Proof for Lemma 5   A radial power network can be represented as a tree, and there is a unique path between any two nodes. Consider two nodes i, j with a path $i \to k_1 \to k_2 \to ... k_p \to j$, where $k_1, ... k_p$ are nodes in the power network. The LMP difference across i, j at any time can be written as

$$\lambda_j - \lambda_i = (\lambda_j - \lambda_{k_p}) + ... + (\lambda_{k_2} - \lambda_{k_1}) + (\lambda_{k_1} - \lambda_i),$$

i.e. the sum of LMP differences across nodes in the path between i, j. For any edge in the power network, we will have two β values (one in each direction) out of which only one can be non-zero - the β value corresponding to the direction of power flow, since the line can only be congested in that direction. From [68] we have that $\beta_{i,j}(t) - \beta_{j,i}(t) = \lambda_j(t) - \lambda_i(t)$, and if the power flow is $i \to j$, then

$$\mathsf{MV}_{i \to j}^{\mathrm{w}}(t) = \beta_{i,j}(t) = \lambda_j(t) - \lambda_i(t) \geq 0.$$

The value of stationary storage located at j at time t is

$$\mathsf{MV}_j^{\mathrm{ss}}(t) = \Big(\lambda_j(t+1) - \lambda_j(t)\Big)_+,$$

where $\lambda_j(t+1) - \lambda_j(t) \geq 0$ since the stationary storage would only transfer energy across time if it had a positive value from doing so. The marginal value of mobile storage that moves from node i at time t to node j at time $t+1$ can be expressed as

$$\mathsf{MV}^{\mathrm{ms}} = \Big(\lambda_j(t+1) - \lambda_i(t)\Big)_+ \tag{A.1}$$

$$= \Big(\lambda_j(t+1) - \lambda_j(t) + \lambda_j(t) - \lambda_{k_p}(t) + \tag{A.2}$$

$$... + \lambda_{k_1}(t) - \lambda_i(t)\Big)_+ \tag{A.3}$$

$$= \mathsf{MV}_j^{\mathrm{ss}}(t) + \mathsf{MV}_{k_p \to j}^{\mathrm{w}} + ... + \mathsf{MV}_{i \to k_1}^{\mathrm{w}}. \tag{A.4}$$

A.3   Proofs for Section 4.5

Proof for Lemma 6

Consider the Lagrangian of the MPED-S problem, specifically the terms involving $\mathbf{u}_k$

$$\mathcal{L} = f(\mathbf{p}) + \sum_k \min_{\mathbf{u}_k} \sum_t \lambda_{i_k(t)}(t) u_k(t) + \boldsymbol{\mu}_k^\top (L\mathbf{u}_k - \bar{s}_k) \tag{A.5}$$

$$- \boldsymbol{\nu}_k^\top L\mathbf{u}_k + \boldsymbol{\omega}_k^\top (-\mathbf{u}_k - \overline{u}_k(\bar{s}_k)\boldsymbol{\Delta}_k^{\mathrm{S}}) \tag{A.6}$$

$$+ \boldsymbol{\phi}_k^\top (\mathbf{u}_k - \overline{u}_k(\bar{s}_k)\boldsymbol{\Delta}_k^{\mathrm{S}}). \tag{A.7}$$

The Lagrangian can be decomposed over $\mathbf{u}_k$, and each inner minimization problem over $\mathbf{u}_k$ is equivalent to the Lagrangian of (4.28), which proves that their optimal solutions will coincide.

Proof for Theorem 8

From the Lagrangian of the economic dispatch problem in (4.13), we get that $\mathsf{MV}_k^{\mathrm{ms}}(\mathfrak{E}, \bar{\mathbf{s}}) = \mathbf{1}^\top \boldsymbol{\mu}_k + \bar{u}_k'(\bar{s}_k)(\boldsymbol{\Delta}_k^{\mathsf{S}})^\top (\boldsymbol{\omega}_k + \boldsymbol{\phi}_k)$. Further, from the stationarity KKT condition with respect to $u_k(t)$, we get

$$L^\top (\boldsymbol{\mu}_k - \boldsymbol{\nu}_k) + \boldsymbol{\omega}_k - \boldsymbol{\phi}_k = -\boldsymbol{\lambda}_{i_k}.$$

Under Assumption 4, only one of the dual variables is non-zero at any given time. We can construct a dummy variable $\boldsymbol{z}_k = \boldsymbol{\mu}_k - \boldsymbol{\nu}_k + \boldsymbol{\omega}_k - \boldsymbol{\phi}_k$ and $T \times T$ dimensional diagonal matrices A, B such that $A\boldsymbol{z}_k = \boldsymbol{\mu}_k - \boldsymbol{\nu}_k; B\boldsymbol{z}_k = \boldsymbol{\omega}_k - \boldsymbol{\phi}_k$. Matrix A has diagonal entries equal to 1 corresponding to times when the capacity constraint is active, and 0 otherwise. Similarly, B has diagonal entries equal to 1 corresponding to times when the power constraint is active, and 0 otherwise, i.e., $A + B = I$. As defined previously, L is a lower triangular matrix defined as $L_{ij} = 1$ if $i \geq j$, and 0 otherwise. $L^\top$ then becomes an upper triangular matrix. The matrix $L^\top A$ has a 1 at indices (t_1, t_2) where $t_1 \leq t_2$ and $A_{t_2 t_2} = 1$, i.e., if the energy capacity constraint is active at time $t = t_2$. This ensures that $L^\top A$ has a rank equal to the rank of matrix A, since it has non-zero linearly independent rows for all times when the energy capacity constraint is active. Since B has linearly independent rows for power capacity constrained periods, we can see that $L^\top A + B$ is full rank with all the diagonal elements being 1, and the elements at (t_1, t_2) being 1 if $t_1 \leq t_2$ and $A_{t_2 t_2} = 1$. Then, we can obtain an expression for $\boldsymbol{z}_k$

$$\boldsymbol{z}_k = (L^\top A + B)^{-1}(-\boldsymbol{\lambda}_{i_k}).$$

It is easy to verify that the structure of matrix $(L^\top A + B)^{-1}$ is such that the t_p-th column (corresponding to a power constrained time) is an elementary vector $\boldsymbol{e}_{t_p}^\top$, and the t_e-th column (corresponding to an energy capacity constrained time) is $[-1, ..., -1, 1, 0, ..., 0]^\top$ where -1 appears $t_e - 1$ times, and the 1 is at the t_e-th location. We can use this equation to obtain expressions for $\boldsymbol{\mu}_k - \boldsymbol{\nu}_k, \boldsymbol{\omega}_k - \boldsymbol{\phi}_k$. Replacing these expressions into the marginal value formulation leads us to the result in Theorem 8.